The Pennsylvania State University
The Graduate School

PROBING THE DARK UNIVERSE WITH GRAVITATIONAL WAVES FROM SUBSOLAR MASS COMPACT OBJECTS

A Dissertation in
Physics
by
Ryan Magee

Submitted in Partial Fulfillment
of the Requirements
for the Degree of

Doctor of Philosophy

May 2021

The dissertation of Ryan Magee was reviewed and approved by the following:

Chad Hanna
Associate Professor of Physics & Astronomy and Astrophysics
Dissertation Advisor
Chair of Committee

Yuexing Li
Associate Professor of Astronomy

B.S. Sathyaprakash
Elsbach Professor of Physics & Professor of Astronomy and Astrophysics

Sarah Shandera
Associate Professor of Physics

Richard Robinett
Professor of Physics
Associate Head for Undergraduate and Graduate Studies

Abstract

The detection of gravitational waves by Advanced LIGO in 2015 marked the start of a new era in astrophysics. These small ripples in space-time - first predicted in the early 20th century by Albert Einstein - encode properties of the progenitor system and provide a powerful new way to probe distant and extreme astrophysical environments. My dissertation focuses on contributions I have made in facilitating the multi-messenger detection of electromagnetically bright sources and using LIGO's observations (or lack thereof) to constrain models of the dark matter. I describe the motivation for Advanced LIGO searches for sub-solar mass ultracompact binaries, as well as two recent searches I carried out with the LIGO-Virgo Scientific Collaboration. No confident detections were made in these searches, but the null result allowed us to place the tightest contraint to date on a particular model of the dark matter. I also discuss my contributions to efforts to detect binary neutron stars. Although the first BNS detection, GW170817, was a model multi-messenger discovery, there remains much to be learned about the extreme environment of the coalescence that can only be resolved by additional, prompt observations. I describe a subthreshold search for BNS that aims to increase our catalog of joint discoveries by facilitating searches for temporal or spatial coincidence, as well as recent attempts to detect BNS prior to merger to enable prompt electromagnetic followup.

Table of Contents

Bibliography 120

List of Figures

List of Tables

Acknowledgments

First, I have to thank my family for the tremendous amount of love and support they've provided me over the years. My mom and dad provided endless encouragement to pursue my interests. They humored my scientific escapades as a kid and eagerly read all of my published papers as an adult. My brother and sister, Sean and Katie, have also constantly supported me. Their chiding has been a source of much needed levity throughout too many years of schooling. I'm fortunate to have had the support of my extended family as well. Aunt, Grandpa, Nana and Popa, and the dozens of others I can't fit neatly in here: thank you all for always encouraging me.

My graduate career has been successful thanks to the patience and advice of my advisors. Working in the IGC has been a formational experience, and I am especially grateful for the guidance provided by Sarah and Sathya. Most of all, I am grateful for the patience, understanding, curiosity, and compassion of my advisor, Chad. Despite his incomprehensibly packed schedule, Chad always found time to guide my path through research, the LIGO collaboration, and academia in general. I will forever be grateful to have had him as my advisor.

Working in the Penn State LIGO group has been more fun than I could have imagined, and it is bittersweet to finish my time here. From the beginning, Alex Pace, Cody Messick, Duncan Meacher, Patrick Godwin, and Sydney Chamberlin made the group a fun place to work. It didn't take long for me to leave my official office behind in favor of the conference room. Becca, Debnandini, Divya, Javed, Rachael, and Surabhi all joined after me, but reinforced my love of this group.

Many students and post-docs have passed through the IGC while I was there, but I wanted to specifically acknowledge a few. Anne-Sylvie Deutsch was amazingly patient as I collaborated with her on what later turned into the first half of my thesis. Ssohrab Borhanian provided me with endless laughs and a more lighthearted take on what really matters (and, of course, for reminding me that chameleons are quite condescending). Cody Messick for introducing me to the quirks and 'features' of GstLAL and Surabhi Sachdev for being a constant encylopedia and sounding

board - I would not have graduated in twice the time if not for your unbelievable patience and willingness to help.

And last but certainly not least, I couldn't have done this without my significant other, Hallie. Thank you for listening to me practice countless talks and always lifting me up. I will always remember you watching my Zoom defense presentation from across the room while Poppy slept at my feet.

The material in this dissertation is based on work funded by the National Science Foundation under grants OAC-1841480 and PHY-1454389. Any opinions, findings, and conclusions or recommendations expressed in this material are those of the author(s) and do not necessarily reflect the views of the National Science Foundation.

The material in this dissertation is also based on work funded by the Charles E. Kaufman Foundation of the Pittsburgh Foundation under grant KA2016-85224. Any opinions, findings, and conclusions or recommendations expressed in this material are those of the author(s) and do not necessarily reflect the views of the Charles E. Kaufman Foundation.

Dedication

To Mom, Dad, Sean, Katie, and Hallie.

Chapter 1
Introduction

1.1 Gravitational waves and their detection

The theory of general relativity elegantly describes gravity as the coupled relationship between energy density and spacetime curvature. This relationship is neatly contained in *Einstein's equations*, which relate the curvature of spacetime encoded by the metric tensor, $g_{\mu\nu}$, with the distribution of energy as described by the stress-energy tensor, $T_{\mu\nu}$:

$$G_{\mu\nu} + \Lambda g_{\mu\nu} = \frac{8\pi G}{c^4} T_{\mu\nu} \tag{1.1}$$

where the Einstein tensor is defined as

$$G_{\mu\nu} = R_{\mu\nu} - \frac{1}{2} R g_{\mu\nu}. \tag{1.2}$$

and $R_{\mu\nu}$ and R denote the Ricci curvature tensor and Ricci scalar, respectively. The curvature of spacetime described by the left hand side of 1.1 controls how matter moves, while the stress-energy tensor on the right hand side describes how spacetime deforms in the presence of energy densities. This relationship is complex and inherently dynamic; as matter moves along paths guided by the spacetime curvature, the distribution of matter shifts and the curvature of space changes. Exact solutions to this set of equations are difficult or impossible to find in most scenarios.

Early on, Einstein realized that approximating $g_{\mu\nu}$ as the flat spacetime metric, $\eta_{\mu\nu}$, plus some small perturbation, $h_{\mu\nu}$, reduced the field equations to linear, second

order partial differential equations. Under appropriate gauge conditions, these linearized vacuum field equations reduce to a form that is exactly solvable by wave-like solutions:

$$\Box \bar{h}_{\mu\nu} = -\frac{16\pi G}{c^4} T_{\mu\nu} \tag{1.3}$$

Here, $\Box$ is the D'Alembertian operator and $\bar{h}_{\mu\nu}$ represents the trace reversed metric perturbation. Solutions to these wave equations are what we call *gravitational waves*; small perturbations in spacetime curvature that propagate at the speed of light.

The perturbative approach taken by linearized gravity ignores the inherently non-linear nature of general relativity, and though Einstein recognized that this approach yielded gravitational waves, it was not clear if they were simply a mathematical artifact of the approximation or a feature of the full theory. Einstein himself struggled with this[1], and the theoretical hurdles in the non-linear regime weren't overcome until after his death [33–36].

Nevertheless, far from gravitational-wave sources the full solution reduces to the linearized solution and in vacuum they become

$$\Box \bar{h}_{\mu\nu} = 0 \tag{1.4}$$

These equations admit a plane wave solution that propagates at the speed of light; for a plane wave traveling in the z direction the solution is

$$\bar{h}^{TT}_{\mu\nu} = Re(A_{\mu\nu} e^{ik_\lambda x^\lambda}) \tag{1.5}$$

where $A_{\mu\nu}$ is the amplitude

$$A_{\mu\nu} = \begin{pmatrix} 0 & 0 & 0 & 0 \\ 0 & h_+ & h_\times & 0 \\ 0 & h_\times & -h_+ & 0 \\ 0 & 0 & 0 & 0 \end{pmatrix}$$

and TT denotes our choice to exploit redundant degrees of freedom and express the perturbation in a *transverse and traceless* gauge such that $\bar{h}^{TT}_{\mu\nu} = h^{TT}_{\mu\nu}$. We refer

[1] His personal correspondence with Max Born showed that at times he believed he proved their non-existence [32].

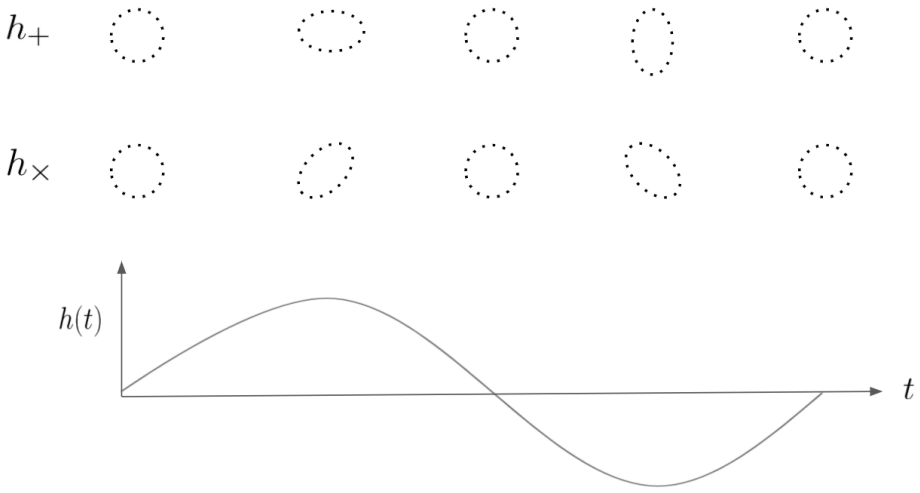

Figure 1.1: The impact of passing gravitational waves of + (top) and × (middle) polarization on a ring of freely falling test particles as time progresses. The bottom row shows how the strain changes in time, which is the quantity ground based interferometers aim to measure.

to h_+ and $h_\times$ as the two *polarizations* of the gravitational wave, and they are the only independent components of the metric perturbation. Although the wave is traveling in the z direction, the perturbations only act in the perpendicular x and y directions. For this reason, we call gravitational waves *transverse waves*. This propagating perturbation changes the distance between points in an oscillatory fashion, as shown in Fig 1.1. The + polarized component of the wave describes the increase (and subsequent decrease) in the distance between points in the x direction and the decrease (and subsequent increase) in the distance between points in the y direction. The × polarization describes similar behavior but along axes rotated 45 degrees. The amplitude of the perturbation is called the *strain*, and it describes the fractional change in distance caused by passing gravitational waves.

Despite the theoretical advances that proved that fully non-linear general relativity allowed for the existence of gravitational waves, their detection posed challenges as well since spacetime is extremely stiff and most processes don't appreciably change our local metric. Astrophysics probes some of the most extreme environments in our universe where violent processes are able to induce non-stationarities that persist to cosmic distances, but even the strongest gravitational

waves arriving on earth were/are expected to have strains less than $\mathcal{O}(10^{-20})$.

The first evidence for the existence of gravitational waves did not come from observing the effects of passing waves but from measurements of a distant pulsar. One of the key predictions of the theoretical work carried out in the 1950s was that gravitational waves carry energy, implying that systems that emit gravitational waves are losing energy. The discovery and subsequent observations of PSR B1913+16 by Russell Hulse and Joseph Taylor confirmed this prediction; in 1982, they showed that the rate of orbital decay of the pulsar closely matched the rate at which energy was expected to be lost via gravitational radiation [37]. This discovery ultimately earned them the Nobel Prize and provided incredibly strong evidence for the existence of gravitational waves.

The effects of passing gravitational waves were not directly observed until the detection of GW150914 by the Advanced LIGO interferometers [38], but not for lack of effort. Joseph Weber famously constructed Weber bars in the 1960s, devices that aimed to measure gravitational waves through excitations of vibrational modes in aluminum. Although he initially claimed to have detected gravitational waves [39–41], it was quickly realized that the observed event rate was much too high. By the late 1990s and early 2000s, gravitational wave detectors began to resemble their modern interferometric form [42, 43]. In particular, we highlight the Initial Laser Interferometer Gravitational Wave Observatory (LIGO) detectors, the precursor of the modern Advanced LIGO interferometers. Initial LIGO collected and analyzed data from 2002 to 2010, though no detections were made [44]. In 2010, the interferometers were shut down for a five year period of upgrades to their Advanced configuration [45]. These changes increased the reach of the detectors by a factor of $\sim$10.

Modern ground-based gravitational-wave detectors aim to measure perturbations in spacetime caused by passing gravitational waves and enable inferences about the distant processes that caused them. At present, the two Advanced LIGO interferometers remain the most sensitive gravitational-wave detectors. The LIGO interferometers rely on Michelson interferometry, and are capable of measuring strains $\mathcal{O}(10^{-23})$. Figure 1.2 contains a simple diagram of the interferometers at work. Light from a laser is separated by a beam splitter and sent down two orthogonal, 4km Fabry-Perot cavities. Each end of the cavities contains a freely falling test mass that reflects incident laser light and increases the effective length

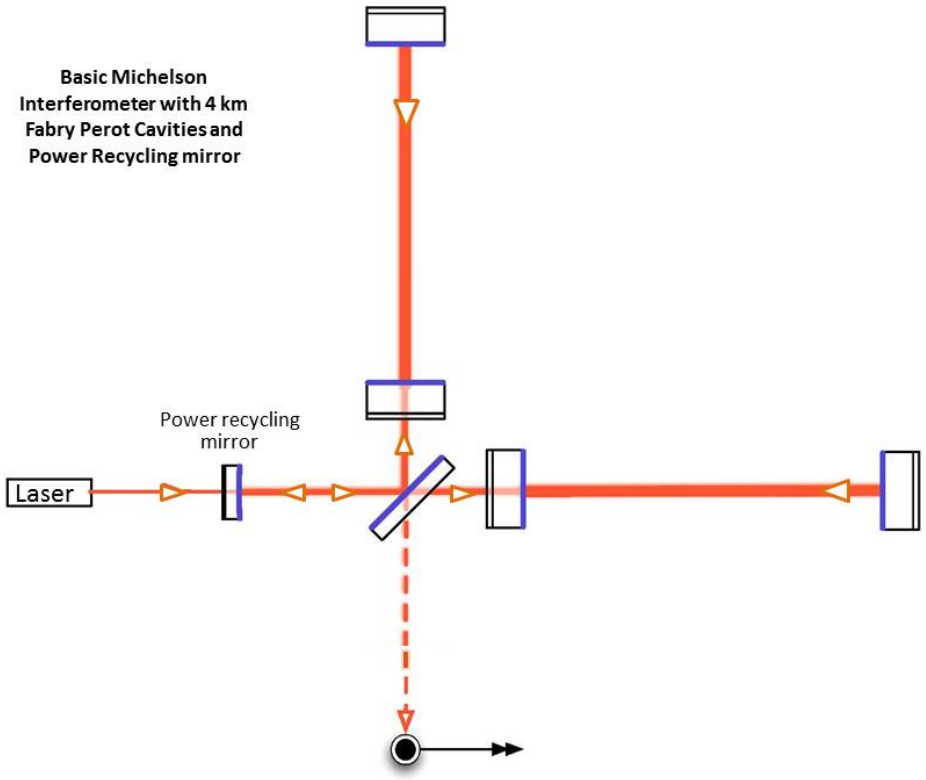

Figure 1.2: A simplified schematic of the LIGO interferometers. The detectors are based on Michelson interferometry and make use of Fabry-Perot cavities and power recycling mirrors to increase sensitivity. This figure is reproduced from [1].

of the arms to over 1000km. The laser light is eventually recombined at the beam splitter and output to a photodiode. When space is quiet and there are no gravitational waves passing earth, the recombined beams destructively interfere. If, however, gravitational waves are incident on the detector, the arms are squeezed and stretched slightly. This difference in the separation of the test masses manifests itself as an accumulated phase difference between the light stored in each arm. When the beams are recombined, they now constructively interfere and the intensity of light incident on the photodiode increases. The raw photodiode output is converted to strain data, which can then be analyzed by gravitational wave detection pipelines.

The strain measured by ground-based interferometers depends on how the detector responds to each gravitational-wave polarization; this is described by the detector response functions, F_+ and $F_\times$. In general, the amplitude of the strain

observed by LIGO is

$$h = F_+ h_+ + F_\times h_\times = \frac{\Delta L}{L} \tag{1.6}$$

where L is the length of one of the interferometer's arms and ΔL represents the change in length. For Advanced LIGO's 4km long arms, strains of $\mathcal{O}(10^{-23})$ represent changes in the detector arm length of $\mathcal{O}(\text{proton radius})$.

Remarkably, detection has become commonplace in the five years since the detection of GW150914. Advanced LIGO and Advanced Virgo [46] have announced 39 new gravitational-wave candidates from the first half of their recently concluded third observing run (O3) [2]; this is a marked increase over the 11 candidates observed across the first two observing runs. By the end of the decade, the Advanced LIGO and Advanced Virgo interferometers will reach their design sensitivities and observe a factor $\mathcal{O}(10)$ more events per year of observation [47].

Thanks to the ingenuity of Advanced LIGO-Virgo instrumentalists, we are rapidly leaving the era of gravitational-wave discovery and entering one of gravitational-wave facilitated science. In the coming sections, I will describe Advanced LIGO-Virgo's (presently) most promising gravitational-wave candidate class and touch on just a few of the prospects for broader astrophysics and cosmology enabled by compact binary observations.

1.2 Compact binaries

Broadly speaking, LIGO considers four classes of gravitational-waves: continuous gravitational waves, stochastic gravitational waves, burst gravitational waves, and gravitational waves from compact binary coalescences. Current (or in some cases, future) ground-based gravitational-wave detectors are sensitive to each type though the techniques used to extract the signals from the data are vastly different. My thesis has focused exclusively on detecting and interpreting gravitational-waves from compact binaries.

Binary stars are common in our Universe, though there is some disagreement on the exact fraction of stars in binaries. Most binary star systems are thought to form alongside the component stars themselves. Modern observations support that this likely occurs via fragmentation of their shared protostellar disk [48]. If both stars have masses above $\sim 8\,M_\odot$, then their evolutionary track culminates in the

formation of either a neutron star or a black hole [49]. Thus as binary stars burn through all of their fuel and die, binary neutron stars (BNS), binary black holes (BBH), and neutron star - black hole (NSBH) systems take their place. These three systems are what we typically refer to as *compact binaries*.

When two compact objects become gravitationally bound, they become trapped in a slow march towards their inevitable merger. As the objects orbit one another, they slowly lose energy via gravitational radiation. Their orbital radius contracts as energy is radiated away, and the orbital frequency increases. This is a runaway process; as more energy is emitted in the form of gravitational waves, the rate of emission also increases. This is known as the *inspiral* phase of the binary. The rate at which the gravitational wave signal evolves during this stage is set by a combination of the two component masses known as the chirp mass, $\mathcal{M}$:

$$\frac{df}{dt} = \frac{96\pi^{8/3}}{5}\left(\frac{G\mathcal{M}}{c^3}\right)^{5/3} f^{11/3} \tag{1.7}$$

$$\mathcal{M} = \frac{(m_1 + m_2)^{3/5}}{(m_1 m_2)^{1/5}} \tag{1.8}$$

More massive binaries thus evolve more quickly; while low mass BNS systems can endure in LIGO's sensitive band for hundreds or thousands of orbits at present sensitivites, BBHs are typically only observed for their final few cycles. The inspiral phase ends as the two compact objects begin to plunge into one another during the *merger* phase, which is where the gravitational-wave emission peaks. After the two objects have coalesced, the remnant compact object settles to its final state during the *ringdown*.

In order to reliably identify compact binaries in LIGO data, we require accurate models of the gravitational-wave emission predicted by general relativity. In general, the gravitational-wave emission from compact binaries is described by a set of fifteen parameters: eight intrinsic parameters describe the masses and spins of the components and seven extrinsic parameters describe the location, orientation, coalescence phase, and coalescence time of the binary. The intrinsic parameters determine the underlying dynamics of the system, while the extrinsic parameters modify the amplitude and phase of the signal incident on the interferometers.

The inspiral phase is well modeled by post-Newtonian and effective-one-body [50] approximation methods. For low-mass systems, waveform approximants that only

model the inspiral phase are an appropriate choice [51, 52]. For high-mass systems that only spend a few cycles observable in this phase, it is important to model the later emission as well. The merger phase cannot be modeled analytically, but advances in numerical relativity [53–55] have painted a more complete picture of the emission during this phase of binary evolution. Modern waveform approximants often combine approaches and use hybridized waveforms that match the analytic and semi-analytic methods with numerical and perturbative methods to model the inspiral, merger, and ringdown. The waveforms available are increasingly robust and now incorporate tidal effects, spin precession, and emission from higher order modes.

Accurate waveforms facilitate inferences of the progenitor's properties. On a system by system basis, these measurements can provide clues into how the binary formed. On an aggregate level, they can enable broader statistical statements on the populations of neutron stars and black holes that exist in our Universe. As a graduate student, I have contributed to the census of the stellar remnants in our Universe through my work with the GstLAL-based inspiral pipeline (henceforth GstLAL).

Compact binaries provide unique insight into the endpoints of stellar evolution for binary star systems, but they are also a tantalizing way to probe more unconventional physics. Could LIGO be observing some type of exotic star? Could LIGO's black holes be a signature of the dark matter? Are LIGO's low-mass compact objects neutron stars or black holes? The path to answer these questions starts with the identification of candidate compact binaries in LIGO's data.

1.3 Data analysis

Gravitational-wave detection pipelines aim to identify signals that match the expected gravitational-wave emission, $h(t)$, in the detector data, $d(t)$. This is complicated by the fact that LIGO data is subject to a wide array of noise sources across its sensitive band. The one-sided power spectral density (PSD), $S_n(f)$, describes how the noise changes in frequency:

$$\langle \tilde{n}(f)\tilde{n}(f')\rangle = \frac{1}{2}S_n(f)\delta(f-f'), f > 0 \tag{1.9}$$

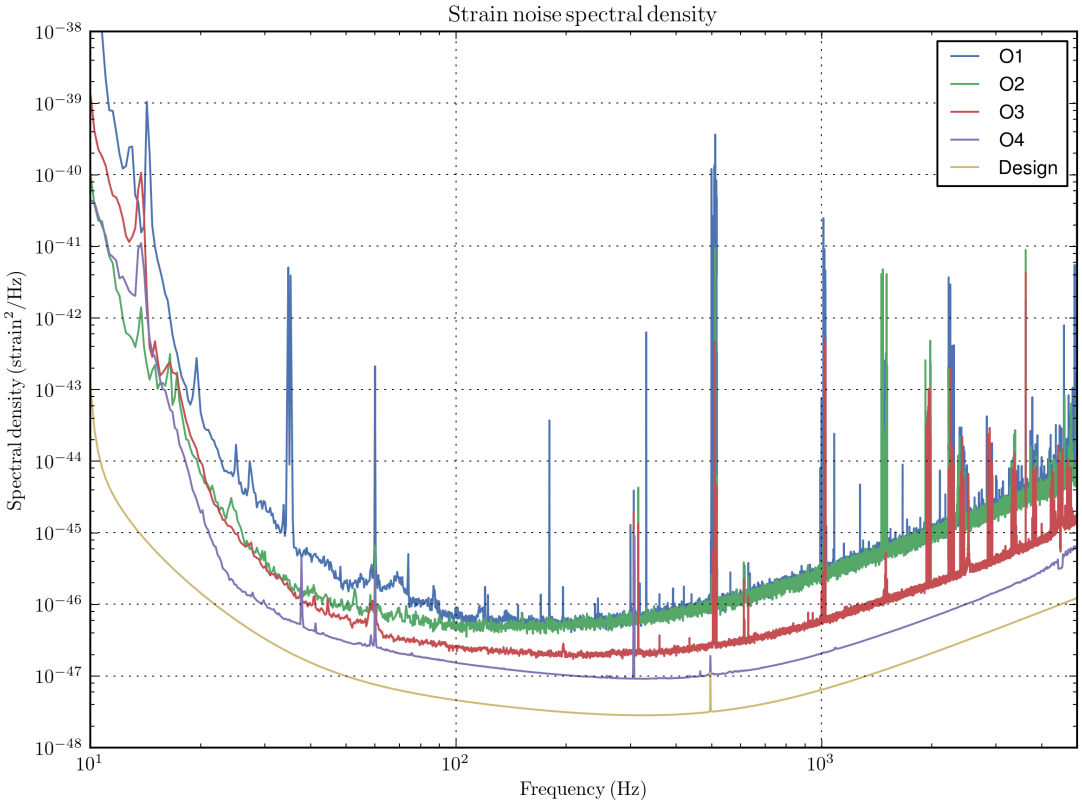

Figure 1.3: The past and expected evolution of the noise spectra in LIGO-Livingston. LIGO is presently most sensitive from $\sim 100 - 300$ Hz. Note in particular the expected improvements at frequencies $\lesssim 20$Hz. These are crucial to realize early warning detection with this generation of interferometers; see Chapter 7 for more discussion on future early warning prospects. The PSDs were obtained from the public LIGO DCC documents G1600151, G1801952, and T2000012.

where $\tilde{n}(f)$ is the Fourier transform of the noise time series $n(t)$.

$$\tilde{n}(f) = \int_{-\infty}^{\infty} n(t) e^{-2\pi i f t} dt \tag{1.10}$$

To account for the strong frequency dependence of the detector noise, the data are *whitened* before analysis. This is done by first Fourier transforming the data to the frequency domain, weighting by the power spectra, and Fourier transforming back to the time domain. Given a measured power spectrum, the whitened data

are then defined as:

$$\hat{d}(t) = \int_{-\infty}^{\infty} \frac{\tilde{d}(f)}{\sqrt{S_n(|f|)/2}} e^{2\pi i f t} df \tag{1.11}$$

This procedure weights the data such that the frequencies with lower noise are more heavily weighted. By definition, the whitened data is uncorrelated from (time) sample to sample and should have mean 0 and variance 1 for Gaussian noise. Because whitening changes the characteristics of the data, we also have to whiten any quantities that we wish to correlate with the data. This motivates us to define the noise-weighted inner product for two time-series $a(t)$ and $b(t)$ to be:

$$\begin{aligned} \langle a|b\rangle &= 2\int_{-\infty}^{\infty} \frac{\tilde{a}(f)\tilde{b}^*(f)}{S_n(|f|)} df \\ &= \int_{-\infty}^{\infty} \hat{a}(\tau)\hat{b}(\tau) d\tau \end{aligned} \tag{1.12}$$

where $\hat{a}(\tau)$ and $\hat{b}(\tau)$ denote the PSD whitened time series.

Detection pipelines can use *matched-filtering* to correlate the expected gravitational-wave emission for a system with the data to output the *signal-to-noise ratio* (SNR). The modeled emission is called the *template waveform*. For template waveforms, $h(t)$, normalized such that $\langle h|h\rangle = 1$, the SNR time series is

$$\rho(t) = \langle d|h\rangle = \int_{-\infty}^{\infty} \hat{h}(\tau)\hat{d}(\tau + t) d\tau \tag{1.13}$$

Of course, the properties of astrophysical binaries are not known in advance. After setting the desired recoverable parameter space for a search, we construct a discrete set of gravitational waveforms (varying only the intrinsic parameters) known as a *template bank* to cover the continuous parameter space. The discrete nature of the bank means that astrophysical signals with parameters not exactly matched by a template will suffer signal loss. Searches typically construct banks such that the minimum overlap between a template and *any* signal with parameters covered by the bank is 97%. This limits the SNR loss to 3%, ensuring that only $\sim 10\%$ of astrophysical signals are missed due to the discrete bank. As an example, the template bank used for the GstLAL search in Advanced LIGO's third observing run (O3) [2] is shown in Fig 6.1.

There are presently four matched-filter pipelines that contribute to Advanced

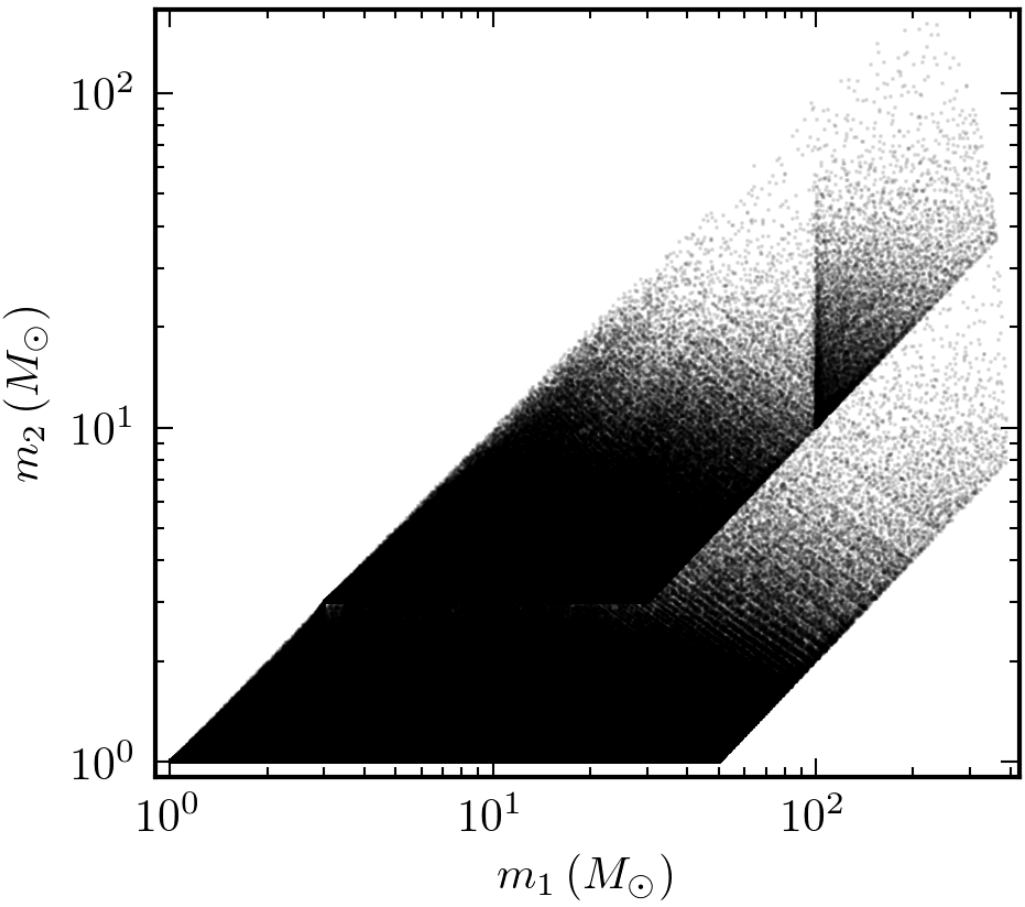

Figure 1.4: The template bank used by GstLAL in Advanced LIGO's third observing run. Each dot represents a single waveform in the m_1, m_2 plane. The bank is a 4-dimensional object. For computational considerations, we only search for binaries with aligned component spins. Any two waveforms represented by coordinates within the 4-volume are at least 97%, and often 99%, similar by construction. The bounds of the bank are complicated and described in Table II of [2].

LIGO-Virgo results: GstLAL [56–58], MBTA [59], PyCBC [60–64], and SPIIR [65]. The remainder of this section is specific to the detection pipeline I contributed to as a graduate student, GstLAL [56, 58][2]. GstLAL groups similar templates together in bins, $\bar{\theta}$. The type of grouping is a configuration option, but is typically done based on the value of the chirp mass, an effective spin parameter [66–69],

[2]Appendix A contains a description of the GstLAL library and the contributions it has made thus far in gravitational-wave astrophysics.

template duration, or template bandwidth. To reduce the cost of matched filtering, templates are decomposed via singular value decomposition (SVD) into a new set of orthonormal filters that can later be used to reconstruct the response of individual templates [70, 71].

The waveforms are correlated with the data and maximized over the (unknown) extrinsic parameters to produce a SNR time series. Local maxima in the time series are denoted as *triggers*. Typically, detection pipelines implement a threshold on SNR to reduce the trigger volume. Surviving triggers are analyzed for coincidence across interferometers (if possible) and then ranked by a detection statistic. Triggers that pass threshold but do not participate in coincidence are ranked as well.

In purely Gaussian, stationary noise, the SNR is the optimal ranking statistic; higher values of SNR correspond to higher probabilities that the data in question contains a signal matching the waveform in question. LIGO data, however, is subject to a wide array of noise sources across its sensitive band that are neither stationary nor Gaussian, and the SNR is consequently a poor detection statistic. These deviations from stationarity are called *glitches*. Gravitational-wave detection pipelines employ additional data conditioning methods and construct their own ranking statistics (of which the SNR of the candidate is just a component) to mitigate the impact of these transients.

GstLAL employs an automatic gate based on deviations in the whitened data. As previously mentioned, purely Gaussian data has mean 0, variance 1, and uncorrelated samples once whitened. Glitches often remain evident in the whitened data and can leave short time scale correlations. To combat their effect, GstLAL gates times where the whitened data stream momentarily exceeds a value greater than some fiducial number of standard deviations from the mean. The data at that time, as well as the surrounding 0.25 seconds of data on either side, are excised and replaced with zeros. Unfortunately, loud gravitational wave signals (especially those from BBHs) can also remain visible in the whitened data. To ensure that these candidates are not thrown away, a variable gating threshold is set that scales in chirp mass; this is set to scale from 15 to 100 standard deviations across the $0.8\,M_\odot - 45\,M_\odot$ range. Still, the risk remains that an extraordinarily loud signal might be missed due to this conditioning step.

The majority of non-astrophysical transients in the data are not removed via gating. To further distinguish signals from the noise, GstLAL employs an

autocorrelation-based signal consistency check, ξ^2. The ξ^2 value is a powerful way to measure the goodness of fit of a single template to the data. For a single template, $h_i(t)$, it is defined by:

$$\xi_i^2 \propto \int_{-\delta t}^{\delta t} |\rho_i(t) - \rho_i(0) R_i(t)|^2 dt \tag{1.14}$$

where $\rho_i(t), \rho_i(0)$ and $R_i(t)$ are the complex SNR at time t, the peak SNR, and the autocorrelation function, respectively, for template h_i. The value is normalized by the expectation value for this term in purely Gaussian noise.

The window of integration is small ($\sim ms$) and glitches can still appear to match single template waveforms well over this duration. To help combat this, I have recently worked to implement an additional chi-squared like statistic that measures the response of the template bank (or a region of it) to a candidate signal. The *bank chi-squared* test for template h_β is defined as

$$\Gamma_\beta \propto \sum_{\alpha=1}^{n} |\rho_\alpha - \frac{1}{C} \langle \mathbf{h}_\alpha | \mathbf{h}_\beta \rangle \rho_\beta|^2 \tag{1.15}$$

Once again, the normalization is set by the expectation value in Gaussian noise.

In addition to the SNR and ξ^2 values[3] in each detector, GstLAL records the coalescence phase and coalescence time measured in each detector for every candidate trigger. Together, these are used to construct the likelihood-ratio ranking statistic, $\mathcal{L}$. GstLAL's likelihood ratio is presently defined as,

$$\mathcal{L} = \frac{P(\vec{D}, \vec{O}, \vec{\rho}, \vec{\xi^2}, \vec{\phi}, \vec{t} | \mathrm{s})}{P(\vec{D}, \vec{O}, \vec{\rho}, \vec{\xi^2}, \vec{\phi}, \vec{t} | \mathrm{n})} \tag{1.16}$$

where $\vec{D}$ are the horizon distances of operating interferometers, $\vec{O}$ is the set of interferometers participating in the candidate, and $\vec{\rho}, \vec{\xi^2}, \vec{\phi}, \vec{t}$ are the SNR, autocorrelation-based signal consistency check value, coalescence phase, and coalescence time in each interferometer. For candidates appearing in two or more interferometers, the observed differences in amplitudes, coalescence times, and coalescence phases can be checked for consistency [57].

To estimate the background of the search, GstLAL collects triggers not found

[3]Full implementation of bank chi-squared test is an area of ongoing research

in coincidence across interferometers at times when the LIGO-Livingston and LIGO-Hanford interferometers are operating[4]. The background is collected on a bin by bin basis and used to estimate the likelihood that noise produces a trigger with similar ρ and ξ^2/ρ^2 values.

A $\mathcal{L}$ value is assigned to each candidate on a bin by bin basis[5]. Because real gravitational waves can ring up multiple templates in a bank, we cluster across all template groupings to pick out the maximum likelihood template. This is done in $+/-4$ second windows.

After all candidates have been assigned likelihoods, the pipeline produces a significance estimate. The background is sampled on a bin by bin basis to estimate the likelihood-ratio probability density functions for noise. We marginalize the PDF for each bin to produce a global estimate of the $\mathcal{L}$ distribution in noise, and use it as a mapping between $\mathcal{L}$ and false-alarm-rate (FAR). The FAR describes the rate at which we expect noise to produce a candidate with a likelihood-ratio value at least as high as the one observed. The FAR acts as a measure of our confidence in the astrophysical origin of a candidate, and is the quantity used to set detection thresholds for low-latency and archival analyses in the LVC.

1.4 Astrophysics and cosmology with gravitational waves

Gravitational waves are an entirely new lens with which to observe our Universe. They probe environments and processes unaccessible to other methods of observation and, because of this, they are an invaluable tool for advancing our knowledge of astrophysics and cosmology.

The LIGO-Virgo Collaboration (LVC) has already observed ~ 70 candidates signals. Individually, the inferred masses and spins provide clues on how each binary was born. Collectively, the distribution of masses and spins paints an increasingly detailed picture of the properties of compact objects in the stellar graveyard. Recent

[4]Historically, triggers not found in coincidence during coincident time were kept as background. The large difference in sensitivity between the LIGO interferometers and Virgo necessitated this stricter definition.

[5]For a more detailed discussion on the likelihood ratio and how the numerator and denominator are factored and evaluated, see [56, 58].

discoveries [72,73] remind us that this picture is incomplete, and force us to reassess conventional knowledge of stellar evolution [74].

As a member of the LVC, I am expected to contribute over half of my research efforts to core collaboration activities. Many of my contributions were through the development and use of the GstLAL-based inspiral pipeline [56,57,75]. I continue to act as one of the leads for ongoing development efforts of the GstLAL-based inspiral pipeline, and I most recently led GstLAL analysis efforts for GWTC-2 [2]. Our analysis was responsible for 11 unique candidates not observed by other detection pipelines. I was directly responsible for significance and sensitivity statements made by the LVC [2, 30, 72].

Searches for compact binaries can inform far more than our understanding of evolutionary models and compact object populations. One exciting possibility is gravitational wave contributions to our understanding of the dark sector. Indeed, Advanced LIGO observations have already led to independent measurements of the Hubble constant [76, 77], though these have not yet resolved the SH0ES/Planck discrepancy [78, 79]. As a first and second year graduate student, I led the LVC in searches for sub-solar mass compact objects. We were able to use these results to inform models of compact object (see Chapters 4 and 5) *and* particulate [80] dark matter. What is especially exciting is that these methods have arisen within just five years of the first detection of gravitational waves. As the field continues to mature, the potential for additional contributions to our understanding of the dark sector is immense.

Gravitational waves can also act as a probe of physics in matter containing systems. Although supernovae likely remain undetectable for the time being, probable binary neutron star and neutron star - black hole systems have already been detected. In the case of GW170817, this was accompanied by coincident observations across the electromagnetic spectrum. Future detectors will one day be sensitive enough to measure tidal deformability in neutron stars, but until then our fastest path towards understanding the extreme physics within is multi-messenger astronomy. GW170817 remains the only multi-messenger discovery made with gravitational waves, yet it has already revealed so much about the processes that take place near merger.

My dissertation describes a portion of my efforts to further the physics done with gravitational waves. Chapters 2, 3, 4, and 5 describe the motivations, methods, and

results in LIGO-Virgo Collaboration searches for subsolar-mass compact objects. They discuss possible connections between these objects and the dark matter, and constrain their abundance. Chapters 6 and 7 discuss a search for subthreshold binary neutron stars and the development of an early warning system for electromagnetically bright compact binaries. The works described in each chapter aim, in their own way, to increase the number of multimessenger discoveries with gravitational waves.

Chapter 2
Disentangling the potential dark matter origin of LIGO's black holes

2.1 Motivation

GWs are a novel way to observe the dark Universe, and I am particularly interested in connecting LIGO's detections with the *dark matter* and *dark energy*. Although dark matter and dark energy comprise $\sim 27\%$ and $\sim 68\%$ of our Universe's energy density, respectively, the specifics of their nature remain largely unknown. Broadly speaking, cold dark matter candidates fall into two distinct classes: particulate and compact object. Searches for particulate dark matter have continued to return null results [81, 82], despite isolated observations that have hinted at detection [83–86]. Similarly, attempts to measure microlensing signatures of compact objects in the galactic halo revealed a dearth of events and led to tight constraints on compact object abundance and waning interest in this candidate class by the mid-2000s [17].

Renewed critiques of microlensing methods [87] and the detection of GW150914 reinvigorated interest in the connection between compact objects and the dark matter [88] and inspired a flurry of dark matter models that produce black holes at masses accessible to ground based interferometers.

The cleanest way to distinguish black holes born via stellar evolution from those formed by other mechanisms is through the mass. The detection of a compact binary with a component below $1M_\odot$ [89], between $2M_\odot$ and $5M_\odot$ (the lower mass gap) [90–93], or above $\sim 50M_\odot$ (the upper mass gap) [94] would be a strong indication of new physics since these masses are generally considered unaccessible to conventional astrophysical channels. There are several candidates in Advanced LIGO's third observing run that already imply a $2-5M_\odot$ component [72] (as well as recent electromagnetic candidates [95]), and we know of at least one compact object in this range - the remnant of GW170817. Similarly, we know of multiple LIGO BBH merger remnants above $\sim 50M_\odot$. Hierarchical mergers thus contaminate both mass gaps, meaning that in practice it is nearly impossible to distinguish first generation mergers with unknown formation channels from second generation mergers of BNS and BBH remnants.

The subsolar mass space, however, is entirely disjoint from known astrophysical populations of LIGO sources since compact objects below $1M_\odot$ are not expected as an end product of stellar evolution. The detection of a binary with a component below $1M_\odot$ would therefore provide a clean signature of alternative formation mechanisms. As a graduate student I led the LIGO Scientific Collaboration in two *Physical Review Letter* publications on searches for subsolar mass compact objects [28, 96, 97]. Although no unambiguous detections were made, the null result allowed us to place the tightest limits to date on a primordial black hole model of the dark matter.

Chapter 2 contains the work that led us to search for subsolar-mass binaries. It contains a brief summary of the rise, fall, and renewed interest in compact objects as a component of the dark matter, and describes a primordial black hole model of the dark matter that matched Advanced LIGO's observations as well as existing constraints.

Chapter 3 describes studies done in advance of the collaboration's subsolar-mass searches to justify design decisions. It also describes how the lack of a detection can be used to generate a constraint on binary merger rate and on a specific

primordial black hole model. Chapters 4 and 5 contains the published results of the two Advanced LIGO-Virgo searches for subsolar-mass objects. Although no detections were made in either case, they describe increasingly stringent constraints on primordial black holes below$\sim 1\,M_{\odot}$.

2.2 Abstract

The nature of dark matter (DM) remains one of the biggest open questions in physics. One intriguing dark matter candidate, primordial black holes (PBHs), has faced renewed interest following LIGO's detection of gravitational waves from merging stellar mass black holes. While subsequent work has ruled out the possibility that dark matter could consist solely of black holes similar to those that LIGO has detected with masses above $10M_{\odot}$, LIGO's connection to dark matter remains unknown. In this work we consider a distribution of primordial black holes that accounts for all of the dark matter, is consistent with all of LIGO's observations arising from primordial black hole binaries, and resolves tension in previous surveys of microlensing events in the Milky Way halo. The primordial black hole mass distribution that we consider offers an important prediction–LIGO may detect black holes smaller than have ever been observed with $\sim 1\%$ of the black holes it detects having a mass less than the mass of our Sun and $\sim 10\%$ with masses in the mass-gap. Approximately one year of operating advanced LIGO at design sensitivity should be adequate to begin to see a hint of a primordial black hole mass distribution. Detecting primordial black hole binaries below a solar mass will be readily distinguishable from other known compact binary systems, thereby providing an unambiguous observational window for advanced LIGO to pin down the nature of dark matter.

2.3 Introduction

Advanced LIGO's first observing run detected gravitational waves from the mergers of two separate binary black hole systems (BBHs), GW150914 [38] and GW151226 [98]. A third candidate event, LVT151012 [99], was also observed. The second observing run is currently underway and at least one more merger has been confirmed, GW170104 [100]. These detections prove the existence of compact

binary systems with component masses between $7 - 35M_\odot$ and demonstrate not only that they merge over a timescale less than the age of the universe, but also that BBHs are relatively common and LIGO should expect to continue to detect their coalescences [101]. LIGO's detections are all consistent with relatively low spin black holes, and together they are in agreement with a power-law spectrum for the number density per unit mass of black holes, $dN/dM \propto M^{-\alpha}$, with a 90% credible interval $\alpha = 2.3^{+1.3}_{-1.4}$ [100, 102]. LIGO is or will be sensitive to binary black holes between $\sim .01 - 100M_\odot$ at extra-galactic distances, and while the mass distribution was calculated assuming a minimum black hole mass of $5M_\odot$, it remains unknown over what mass range the presently observed power law will hold.

The notion that LIGO could detect gravitational waves from the merger of two primordial black holes has existed for nearly two decades [103], though interest in PBHs has been around for much longer [104]. Until 2004, the LIGO Scientific Collaboration actively searched for BBHs with component masses below $1M_\odot$ [105, 106]. The average range to a binary with component masses $(0.35, 0.35)M_\odot$ was approximately 3 Mpc [106], though advanced LIGO should already be able to improve on that range by a factor of ten [107]. The PBH theory of dark matter fell out of favor with stronger constraints from microlensing searches placing strict limits on primordial black holes below a solar mass [3, 5, 108], though the idea recently resurfaced with the first model suggesting that all dark matter consisted of PBH with a nearly monochromatic distribution around $\sim 30M_\odot$ [109, 110]. It has since been pointed out that the monochromatic scenario has two problems. First, constraints from dwarf galaxy dynamics and radio wave observations imply that not all of dark matter can be explained by $\sim 30M_\odot$ black holes [6, 7, 111]. Second, the expected merger rate predicted by this model would be above the inferred merger rate provided by LIGO [100, 112, 113]. These concerns suggest that if LIGO is probing a population of PBHs with its current detections, PBHs might only make up a small fraction of the dark matter in the universe. We address both concerns in this letter.

2.4 An overview of constraints on primordial black hole dark matter

For a given PBH distribution, $n(M)$, we can define the cumulative mass density as,

$$\rho(M_1, M_2) = \int_{M_1}^{M_2} M n(M) dM. \tag{2.1}$$

We can then write the fraction of DM made up of PBHs in some mass range as

$$f(M_1, M_2) = \frac{\rho(M_1, M_2)}{\rho_{CDM}} \tag{2.2}$$

where ρ_{CDM} is the presently observed cold dark matter density and $f \leq 1$. Constraints on PBH dark matter are typically presented assuming a monochromatic spectrum, but the consistency of LIGO's detections with a power law distribution raises the question: is it possible for an extended PBH distribution compatible with LIGO's observations to account for 100% of the dark matter? Contraints on monochromatic distributions can still provide meaningful limits on extended spectra such as the one we later consider. The constraint curves (shown in Fig. 2.1 for the LIGO region) bound df/dM, though [8] points out that this is not enough to guarantee the compliance of a given extended mass function with the constraints. In general, this is a difficult task and the most rigorous test is to explicitly recalculate every constraint for a given distribution, which several groups have already examined for various functional forms. The primary constraints that we consider in this work are already in a cumulative form that limits the fraction of dark matter that can be composed of primordial black holes above a given mass.

Quasi log-normal forms have been extensively analyzed by [114] and [115], with the former ruling out this family of mass functions as a source of all DM for $10^{-7} M_\odot < M < 10^5 M_\odot$ while the latter showed that for a narrow window where $10^{-10} M_\odot < M < 10^{-8} M_\odot$ this remains a possibility. These results all assume some of the strictest interpretations of the microlensing constraints.

In the LIGO region, microlensing [3–5, 108, 116, 117] and star cluster dynamics in the Eridanus II [7] and Segue 1 dwarf galaxies [6] place the tightest constraints on PBH dark matter (Fig. 2.1). If the latter constraints are relaxed, power-law,

log-normal, and critical collapse mass functions could allow for 100% PBH dark matter for two small windows surrounding $5 \times 10^{-16} M_\odot$ and $2 \times 10^{-14} M_\odot$ as well as for $25 - 100 M_\odot$, though Carr finds that no more than 10% can be accounted for by these mass functions when the dwarf galaxy constraints are considered [118]. The first two windows (as well as the one [115] describe) are unreachable by LIGO, and the $\sim 25 - 100 M_\odot$ interval could yield LIGO detection rates inconsistent with the works of [112] and [113]. Additionally, new constraints by [111] place similar limits to Eri II and Segue I on PBH DM in the window $25 - 100 M_\odot$ using observations with independent systematics, making this window less likely to contain all of the dark matter.

We explore an extended PBH mass function with the following properties. First, it will be single-peaked. Second, it will have a functional form and predicted rate consistent with LIGO observations to date. Third, it will not violate the tightest constraints on primordial black hole binaries in the mass range already observed by LIGO [6, 7] or the microlensing constraints set by [3], but it will violate those set by the EROS2 collaboration [5]. We note, however, that the microlensing constraints have recently been called into question since there are several possibilities for systematic errors that would make them far less constraining in the region of interest for this work [119]. Finally, our proposed mass function will account for 100% of the dark matter. While we do not explicitly recalculate the constraints for our test function, we use our results to generate predictions that will be directly testable by LIGO within the next few years.

2.5 Tension in the microlensing regime

[120] first proposed that massive compact halo objects (MACHOs) could be detected by searching for evidence of stellar microlensing in the Large Magellanic Cloud (LMC). Since then, the MACHO, EROS, and OGLE collaborations have all sought to identify microlensing candidates within the galaxy through multi-year observations of millions of stars. These collaborations were able to place tight constraints on the amount of compact object dark matter for $10^{-7} M_\odot < M < 10 M_\odot$, though the limits depend strongly on galactic halo models, as pointed out by [119]. These parameters that these models depend on, however, are subject to change; current observations suggest slower rotation speeds than were assumed at the time

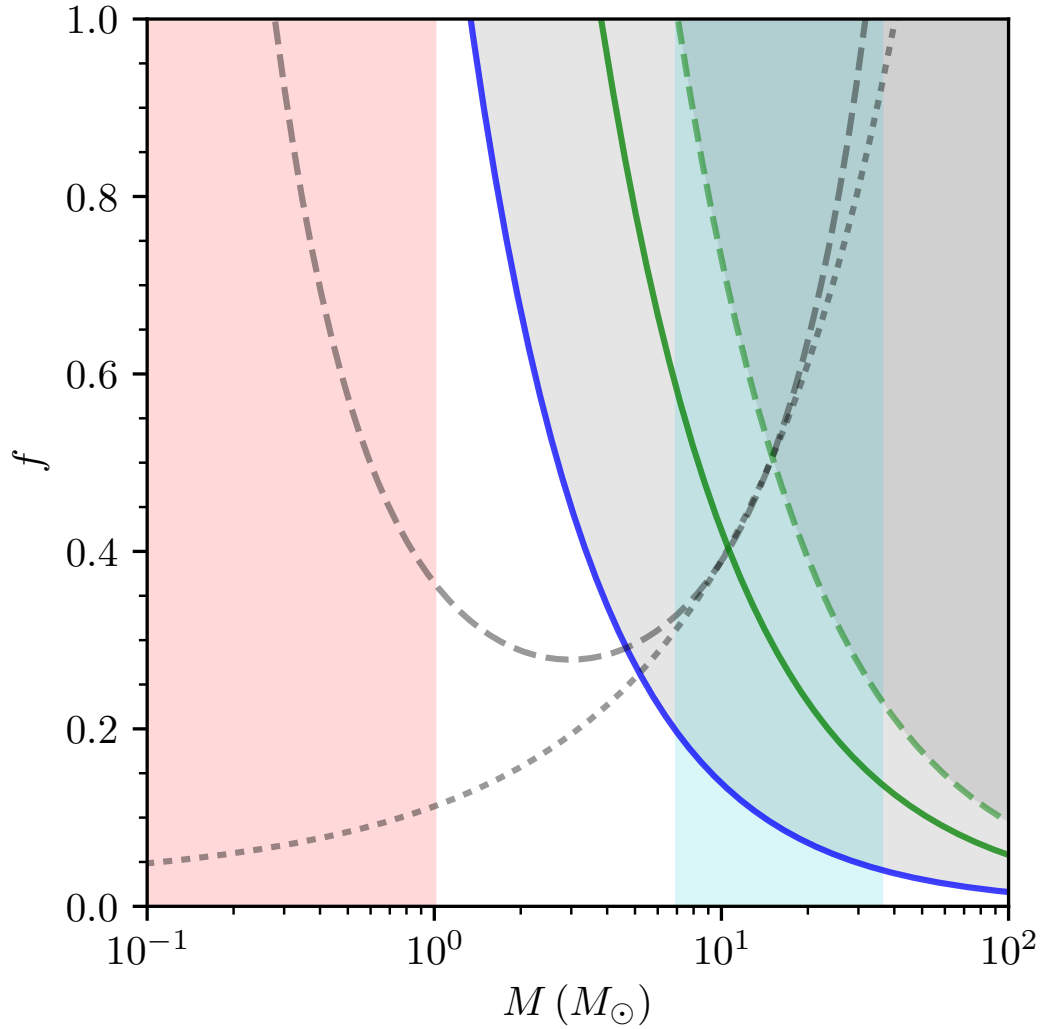

Figure 2.1: Several of the constraints on monochromatic PBH DM in the mass range detectable by LIGO. The red shows the range of most likely MACHO masses [3], while the light blue shows the range of component masses found by LIGO. The long and short dashed lines show the MACHO [4] and EROS2 [5] collaboration constraints on compact objects for the standard halo. The blue line shows a 99.9% confidence limit derived from mass segregation in Segue I [6] while the green lines are derived from the survival of a star cluster in Eridanus II [7,8] for velocity dispersions and dark-matter densities at the galactic center of $\sigma = 5, 10$ km s^{-1} respectively and $\rho = .1 M_\odot \text{pc}^{-3}$. The shaded regions are excluded by these constraints. Our mass function is designed to satisfy the constraints set by the blue curve for $M > 1 M_\odot$. We allow it to break the constraint set by the lower dotted line (EROS2) while satisfying those set by the MACHO collaboration since MACHO claimed multiple detections of compact objects while EROS2 had a single candidate event.

of the microlensing surveys [121, 122], stellar velocity dispersion observations no longer show flat rotation curves [123], and [124] showed that placing limits on the mass of the Milky Way is strongly dependent on the assumed galaxy model. These studies show that accepted values of astrophysical parameters have changed and that these variations can affect predictions for other halo parameters. Any deviation from the standard model has profound impacts on the dark matter constraints, which is abundantly clear from the MACHO first year [116] and 5.7 year results [3], which were unable to rule out a 100% compact object halo at 90% confidence for certain models. [119] acknowledges that the models that did allow for 100% MACHO dark matter may not be an accurate depiction of the Milky Way, but suggests that ruling out MACHO dark matter is premature. [125] also explicitly explored this model dependency for the tighter EROS2 constraints and tracked changes resulting from the variation of several parameters, confirming Hawkins' claim that current constraints are extremely model dependent.

As pointed out by [110], microlensing surveys would also be far less constraining if PBHs clustered into sub-halos. There may already be evidence for this; the MACHO collaboration identified several candidate binary microlensing events with mostly sub-solar lens masses [126, 127].

The MACHO collaboration claimed positive detections of compact halo objects with most likely masses of $.15 - .9 M_{\odot}$ [3], and recent microlensing surveys have hinted at similar results [128]. If we interpret even one detection as a possible dark matter candidate, then we need a distribution that spans the MACHO and LIGO mass ranges. LIGO will be sensitive to binaries in the MACHO range, and will provide a way of making a definitive detection or establishing constraints with completely independent systematics from those used to derive current limits on PBH DM.

2.6 An extended primordial black hole mass function

Motivated by the LIGO and MACHO observations, we consider a modified Schecter function for the PBH mass distribution given by,

$$n(M) = C\left(\frac{M^*}{M}\right)^{\alpha} e^{-\frac{M^*}{M}}, \tag{2.3}$$

where the constant C has units of $\text{vol}^{-1}\text{mass}^{-1}$.

This implies that the differential mass fraction can be written as,

$$\frac{df}{dM} = \frac{M}{\rho_{\text{CDM}}} n(M) \qquad = \frac{CM^*}{\rho_{\text{CDM}}}\left(\frac{M^*}{M}\right)^{\alpha-1} e^{-\frac{M^*}{M}}, \tag{2.4}$$

which is also a modified Schecter function. We stress that we are not suggesting any connection to the Press-Schecter formalism with our choice of this functional form.

We choose this distribution because it has a power-law tail that fits LIGO observations and exhibits a natural exponential cutoff at mass M^*. This allows us to place the mass function's peak within the bounds set by the MACHO collaboration. The only additional free parameter is the overall normalization, which we constrain by considering normalizations which integrate to the overall mass density of dark matter so that we might account for all of dark matter with this population of black holes.

In Fig. 2.2 we show the M^* and α values that are consistent with LIGO observations and the dwarf galaxy constraints[1], as well as an interpretation of the MACHO results which allows for a peak in the mass function with objects of masses between 0.06–1$M_\odot$[2]. Among the regions permitted by these constraints we favor those with the lowest α to be consistent with the present most likely LIGO estimate of $\alpha = 2.3$, though we note that all α in Fig. 2.2 are within LIGO's 90% confidence interval estimate. From the highest α contour, we examine the two end points

[1]Strictly speaking, we only mandate consistency up to $100M_\odot$. Though our distributions violate these constraints at higher masses, the excess is so small ($\sim 1\%$) that uncertainties in the dark matter density itself would need to be taken into account.

[2]We use the fact that the function defined in (2.4) peaks at $M^*/(\alpha - 1)$

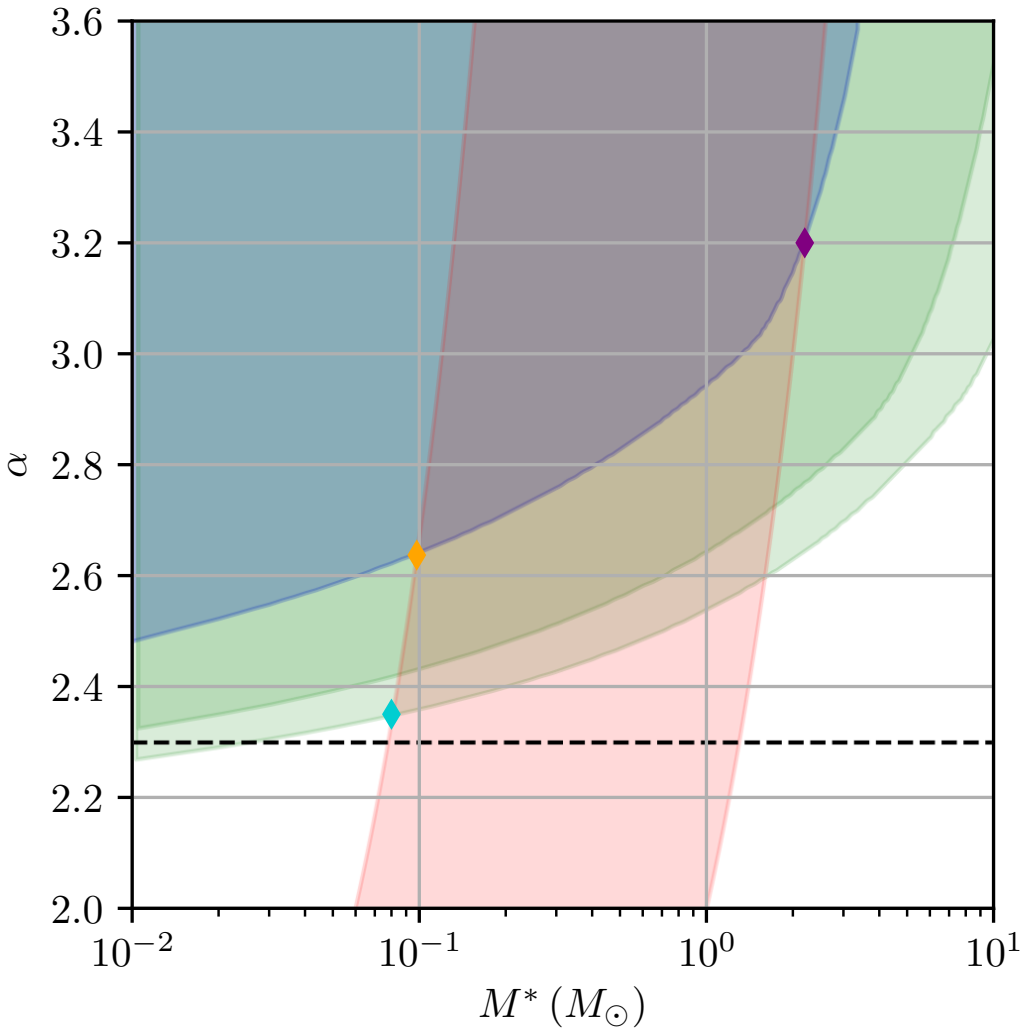

Figure 2.2: Allowed values of α and M^* for the PBH distribution (2.4). Within the LIGO allowed values of α, we consider the tightest constraints on LIGO binaries comprised of PBHs given by [6], which defines the blue region. The green regions show the Eridanus II constraints for the dispersions and density referenced in Fig. 2.1. The red region shows which values of α and M^* correspond to a mass function that peaks inside the 90% confidence region of the MACHO collaboration's detections across several different models at masses of $\sim 0.06 - 1.0 M_\odot$. The purple and orange diamonds indicate two test points, $M^* = 0.10, 2.25$ and $\alpha = 2.65, 3.25$ on which we evaluate the PBH mass function to determine the dark matter distribution and the expected LIGO rate shown in Table 2.1. Finally, the dotted line shows the value of α expected by LIGO, and we include an additional test point (turquoise diamond) at $M^* = .08 M_\odot$ and $\alpha = 2.35$ because it is both minimally consistent with the Eri II constraints and lies closest to LIGO's most probable value for α.

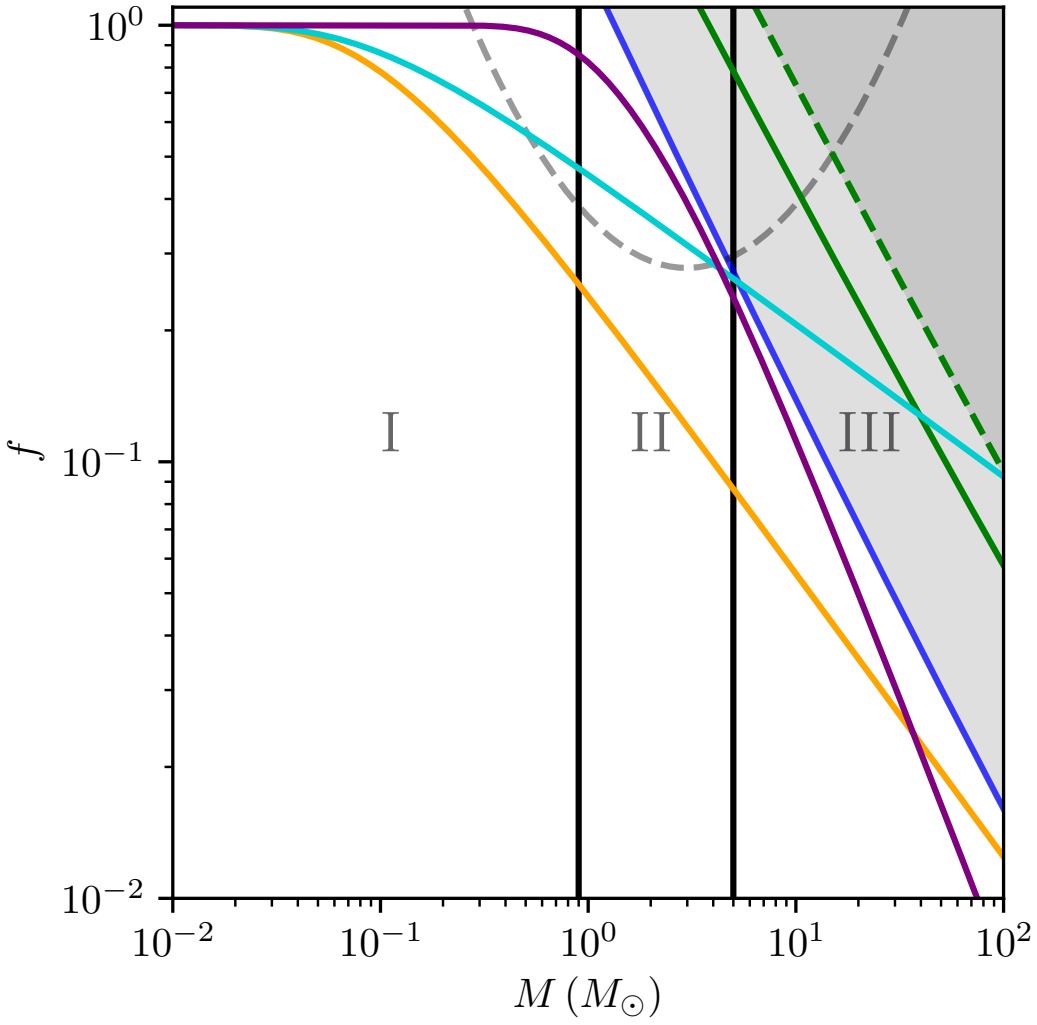

Figure 2.3: Satisfying constraints in the LIGO region. The blue, green, and gray lines show the Segue I, Eridanus II, and MACHO constraints once more. The shaded regions are those excluded by dwarf galaxy constraints. The purple, turquoise, and orange lines correspond to the diamonds of the same color in Fig. 2.2 and show the cumulative fraction of dark matter from the right. The vertical lines separate three regions of interest: sub-solar (I), BNS and mass gap (II), and BBH region (III). Of these observational windows, the sub-solar region would provide the most compelling evidence for PBH given the lack of alternative theories that could produce binary black holes at this mass. The sub-solar mass detection rate might be $\sim .3 - 1\%$ of the present LIGO BBH rate providing a definitive test for the PBH dark matter hypothesis.

$M^* = .10, 2.25 M_\odot$ and $\alpha = 2.65, 3.25$ as well as the point $M^* = .08, \alpha = 2.35$, which is the lowest value consistent with one version of the Eridanus II constraints. With these parameters, we consider three observational windows defined in Table 2.1. Region I includes masses up to $.9 M_\odot$, which is the lower limit on measured neutron star masses [129]. Region II contains binaries that could plausibly be neutron stars or black holes in the mass gap, and region III defines black holes consistent with current LIGO observations. The average masses, fraction of dark matter, and relative rates of detection by LIGO for these windows and values of M^* and α are shown in Table 2.1. The first two models allow for $\sim 99\%$ of the dark matter to be concentrated below $100 M_\odot$, while the last model accounts for $\sim 90\%$. In both cases, the remaining dark matter is accounted for by contributions above $100 M_\odot$.

2.7 LIGO primordial black hole merger rates

Region	Avg. Mass ($M_\odot$)	f	Relative rate
I	.1, .6, .1	.75, .12, .53	.01, .01, .003
II	1.7, 1.9, 1.8	.17, .62, .21	.13, .22, .06
III	11, 9.3, 12.8	.07, .25, .17	1, 1, 1

Table 2.1: The average mass, dark matter fraction, and relative rates of detection for LIGO in three regions of interest: I $[0, .9 M_\odot)$, II $[.9 M_\odot, 5 M_\odot)$, and III $[5 M_\odot, 100 M_\odot)$. These are arranged from left to right for the models color coded in Fig. 2.2 and Fig. 2.3 as the orange ($M^* = .1, \alpha = 2.65$), purple ($M^* = 2.25, \alpha = 3.25$), and turquoise ($M^* = .08, \alpha = 2.35$) diamonds and lines, respectively. For each model, the relative rate of detection by LIGO is set to 1 for region III and calculated for the other regions by (2.5).

The space-time volume that LIGO is sensitive to scales approximately as $M^{15/6}$, assuming equal mass binary systems with an average mass below $\sim 10 M_\odot$. Therefore, the relative LIGO detection fraction r can be approximated as

$$r = \left(\frac{\overline{M_2}}{\overline{M_1}} \right)^{15/6} \times \frac{N(\overline{M_2})}{N(\overline{M_1})} \tag{2.5}$$

Using the average mass for each region of interest in Fig. 2.3, this suggests relative rates of $\mathcal{O}(1\%)$ and $\mathcal{O}(10\%)$ for the sub-solar and BNS plus mass gap regions, respectively. Our calculations implicitly assume that the binary black hole population

is identical to the isolated population.

Several groups have already considered the formation of PBH binary systems and predicted detection rates for LIGO. Though most assume a monochromatic, $30M_\odot$ mass spectrum, our distribution should yield similar results for the surrounding mass range, $20 - 40M_\odot$. These groups have found that LIGO's observed rates are consistent with their results only if the fraction of dark matter is small, $\sim .002 < f < .02$ [112, 113]. Both mass functions consistent with the Segue I constraints predict a comparable fraction of $\sim .01 - .03$ for this window, with a total fraction of $\sim .02 - .04$ above $30M_\odot$. Performing this same analysis using the looser Eridanus II constraints at $\alpha = 2.35$, however, yields fractions in tension with these estimates with $\sim .03 - .04$ for $20M_\odot < M < 40M_\odot$ and $\sim .14$ above $30M_\odot$. Thus while LIGO's most probable α is marginally consistent with the Eridanus II constraints for our distribution, it appears to violate theoretical formation and merger rate calculations. Consequently we favor the $M^* = .1$, $\alpha = 2.65$ distribution since it has the lowest value of α that satisfies the Segue I constraints and contains the smallest fraction at or above $30M_\odot$.

Directly applying the restrictions set by [113] and [112] yields comparable results. Mandating that no more than 2% of the DM can exist at and above $30M_\odot$ predicts $\alpha \in [2.7, 3.4]$; this does not substantially change our rate predictions. If we instead demand that no more than $\sim .002$ exist above $30M_\odot$, our model predicts $\alpha \simeq 3.75$. This falls outside of the LIGO 90% confidence region for α and introduces an additional source of tension, suggesting that a distribution of that form would be extremely unlikely.

At the end of its first observing run, advanced LIGO predicted a BBH merger rate of $9 - 240\,\mathrm{Gpc}^{-1}\mathrm{yr}^{-1}$ [102]. This implies that once LIGO has surveyed 40 times the space-time volume of its first observing run there will be a $\sim 50\%$ chance of detecting 100 binary black hole mergers. Advanced LIGO hopes to improve its reach by a factor of three, leading to 27 times the volume accumulated per unit time. That suggests that a year long observing run with advanced LIGO at design sensitivity could detect a sub-solar mass binary black hole and provide smoking gun evidence for the primordial black hole dark matter hypothesis.

In principle, LIGO should detect a binary within the mass gap prior to the sub-solar regime which might already hint at the origin of dark matter. Work done by [130], however, shows that few detection scenarios provide certainty that

a detected binary existed within the mass-gap. They found that to confidently identify component masses between $2 - 5M_{\odot}$, hundreds of detections could be needed. Even then, it may be difficult to conclude that the black holes detected had primordial origins. A sub-solar detection, however, would unambiguously provide evidence for black holes created by non-stellar processes. We recommend a binary search in that mass range to better study primordial black hole dark matter by systematics indepedent of those used by microlensing surveys.

2.8 Discussion

Though there are many constraints on a primordial black hole model of dark matter, there is tension in the microlensing region. We find that a modified Schecter functional form for the differential number density can satisfy constraints above $\sim 1M_{\odot}$, remain consistent with both the 90% likely region for several MACHO models and LIGO observations, and explain all of dark matter. This distribution matches calculations made for the merger rate of binary PBHs at $\sim 30M_{\odot}$, and predicts a sizeable number of LIGO detections for both the subsolar and mass gap regions. In future work, it may be worth considering the spin distribution of primordial black hole populations. A recent study by [131] suggests that PBHs may be predominately slowly spinning. As more research is done into models of PBH spin distributions and as LIGO continues to refine its measurements, PBH spin analysis will become another strong channel for testing this model. LIGO has the unique opportunity to place its own constraints on PBH DM abundance while also testing for interesting new physics and we recommend searching for binary systems below one Solar mass with LIGO in order to provide the most definitive evidence for the PBH dark matter hypothesis.

2.9 Acknowledgements

We thank Sarah Shandera for useful discussions. We also thank the LIGO Scientific Collaboration and the VIRGO Collaboration, especially the Compact Binary Coalescence working groups for their many helpful comments and suggestions. This research was supported by the National Science Foundation through PHY-1454389. Funding for this project was provided by the Charles E. Kaufman Foundation of

The Pittsburgh Foundation.

Chapter 3
Methods for the detection of gravitational waves from sub-solar mass ultracompact binaries

3.1 Abstract

We describe detection methods for extensions of gravitational wave searches to sub-solar mass ultracompact binaries. Sub-solar mass searches were previously carried out during the Initial LIGO era, and Advanced LIGO boasts a detection volume approximately 1000 times larger than Initial LIGO at design sensitivity. Low mass compact binary searches present computational challenges, and we suggest a way to mitigate the increased computational cost while retaining a sensitivity much greater than previous searches. Sub-solar mass compact objects are of particular interest because they are not expected to form astrophysically. If detected they could be evidence of primordial black holes (PBH) or some other yet unknown

formation mechanism. We consider a particular model of PBH binary formation that would allow LIGO/Virgo to place constraints on this population within the context of dark matter, and we demonstrate how to obtain conservative bounds for the upper limit on the dark matter fraction.

3.2 Introduction

Advanced LIGO [132] and Advanced Virgo's [133] detections of gravitational waves from compact binary coalescences (CBC) have ushered in the dawn of gravitational wave astronomy. To date, there have been 5 detections of binary black hole mergers [134–137] and 1 detection of a binary neutron star system [9], each of which has expanded our knowledge of the properties and populations of compact objects in our universe. Advanced LIGO and Advanced Virgo's success in detecting traditional sources of gravitational waves suggest that ground based interferometers could be powerful new tools in observing the dark universe. We describe considerations for extensions of traditional compact binary searches to the sub-solar mass regime, and provide motivation for these searches in the context of dark matter. In particular, we consider a model where a uniform, monochromatic (equal mass) distribution of primordial black holes (PBH) make up a fraction of the dark matter. We examine the model's robustness and demonstrate how it can place constraints on the abundance of PBHs for different sub-solar mass populations.

3.3 Analysis Techniques

Advanced LIGO compact binary searches rely on matched filtering to extract candidate signals from the noise by correlating known gravitational waveforms with the data. Compact binary searches currently require $\mathcal{O}(10^5) - \mathcal{O}(10^6)$ templates to adequately recover arbitrary signals placed in the parameter spaces considered thus far (binary systems with a total mass of $2M_\odot - 600M_\odot$ [138, 139]). The addition of fully precessing waveforms in future observing runs could increase this by yet another factor of 10, though for now this remains computationally infeasible.

The difficulty of CBC searches scales with both the number and length of the waveforms used as matched filter templates, which could present a problem for sub-solar mass searches. Here we focus on the effect of the number of templates in

the template bank which is expected to scale (roughly) as:

$$N \propto m_{\rm min}^{-8/3} f_{\rm min}^{-8/3} \tag{3.1}$$

where $m_{\rm min}$ is the minimum mass included in the search and $f_{\rm min}$ denotes the starting frequency of the template waveforms [140]. Previous Advanced LIGO searches have searched for binaries with components as light as $1 M_\odot$ [138, 141]; extending these searches to lower masses could easily lead to a $10-100$ time increase in difficulty compared to offline analyses in Advanced LIGO's first observing run. Below we propose increasing $f_{\rm min}$ to mitigate the increased computational costs associated with low mass extensions of compact binary searches, and we calculate the expected loss in sensitivity that this brings.

3.3.1 Estimates of sensitivity

Second-generation ground-based gravitational wave detectors such as Advanced LIGO and Advanced Virgo are sensitive over a broad range of frequencies ($\sim 10 - 10\,000\,\mathrm{Hz}$) but they are most sensitive near 100 Hz [16]. Compact binary pipelines exploit this sensitivity and typically analyze a subset of the total bandwidth. In Advanced LIGO's first observing run, frequencies spanning $10 - 2048\,\mathrm{Hz}$ were analyzed [58]. This is an excellent approximation for standard CBC searches; the majority of the signal-to-noise ratio (SNR) is accumulated at lower frequencies and very little sensitivity is lost by cutting the analysis at 2048Hz. This is an even better approximation for sub-solar mass compact binaries since the frequency evolution of a binary goes as [142]:

$$\dot{f} \propto \mathcal{M}^{5/3} f^{11/3} \tag{3.2}$$

where

$$\mathcal{M} = \frac{(m_1 m_2)^{3/5}}{(m_1 + m_2)^{1/5}} \tag{3.3}$$

is the chirp mass of the system. Sub-solar mass systems therefore are not only long lived, but also spend a long time in LIGO's most sensitive band compared to heavier binaries. This suggests that it may be possible to analyze an even more

reduced frequency band than previous searches while retaining a significant amount of SNR.

Since orbital decay is slow for sub-solar mass ultracompact binaries, inspiral only waveforms appropriately approximate the signal received on earth. The amplitude of the waveform can be written as [22]:

$$\left|\tilde{h}(f)\right| = \frac{1}{D}\left(\frac{5\pi}{24c^3}\right)^{1/2}(G\mathcal{M})^{5/6}(\pi f)^{-7/6} \tag{3.4}$$

and the average recovered signal to noise ratio is given by:

$$\langle\rho\rangle = \sqrt{4\int_{f_{\min}}^{f_{\max}} \frac{\left|\tilde{h}(f)\right|^2}{S_n(f)}df} \tag{3.5}$$

where $S_n(f)$ denotes the single sided power spectral density, informally referred to as the "noise curve". $f_{\min}$ is determined by either the low frequency noise floor or the starting frequency of the template waveform (whichever is greater) and $f_{\max}$ is determined by the frequency of the innermost stable circular orbit ($f_{\rm ISCO}$) or the ending frequency of the template waveform (whichever is less) where $f_{\rm ISCO}$ is defined as:

$$f_{\rm ISCO} = \frac{c^3}{6\sqrt{6}\pi G M_{\rm total}} \tag{3.6}$$

For a $1M_\odot - 1M_\odot$ binary, $f_{\rm ISCO} \approx 2200\,\mathrm{Hz}$. The frequency monotonically increases for lighter total mass systems; for a sub-solar mass search, $f_{\max}$ is therefore determined by the bandwidth of the template waveforms.

We can substitute the waveform amplitude into the equation for SNR and rearrange to find the horizon distance for a given $\langle\rho\rangle$ (or equivalently, the SNR recovered at some fiducial distance):

$$D_{max} \propto \frac{1}{\langle\rho\rangle}\mathcal{M}^{5/6}\sqrt{4\int_{f_{\min}}^{f_{\max}} \frac{f^{-7/3}}{S_n(f)}df} \tag{3.7}$$

which is dependent on the noise curves, the chirp mass of the binary, and the frequency band of the analysis. This allows us to compare LIGO's sensitivity for frequency bands that do not encompass the full sensitive range. We choose the

$f \in$ (10Hz, 2048Hz) band as a point of comparison. The fraction of SNR retained is then:

$$f_{\rm SNR} = \frac{D(f_{\rm min},\, f_{\rm max})}{D(10\,{\rm Hz},\, 2048\,{\rm Hz})} \tag{3.8}$$

Note that this fractional reduction is independent of the mass of the binary. This presents an important trade off in sub-solar mass searches: increasing $f_{\rm min}$ drives the difficulty of a search down, but it also causes the search to lose sensitivity. This drop in SNR is equivalent to a fractional decrease in LIGO's average range, which means that the observed volume (and therefore the expected number of detections at a given chirp mass) is smaller by a factor of $f_{\rm SNR}^3$. Thus even a 3% loss in SNR would represent a detection volume nearly 10% smaller. The sensitive volume retained as a function of $f_{\rm min}$ and $f_{\rm max}$ is shown in Fig. 3.1.

3.3.2 Sensitive distance

Initial LIGO previously carried out searches for compact binaries with components as light as $0.2M_\odot$ [24]. Using the relations outlined above and the fact that current Advanced LIGO searches extend to $1M_\odot$ and $f_{\rm min} = 10\,{\rm Hz}$, we can estimate the reduction in frequency band and sensitivity required to keep the cost of a sub-solar mass search comparable to current Advanced LIGO searches. Equation 3.1 shows that we expect similar scalings in both $m_{\rm min}$ and $f_{\rm min}$. Thus if we decrease the lower mass bound of previous Advanced LIGO searches by a factor of 5, we need to *increase* $f_{\rm min}$ by a factor of 5 as well to keep the number of templates approximately constant. We estimate that in order to modify current searches to extend down to this mass we would need to increase $f_{\rm min}$ to $\sim$ 50Hz. This amounts to a loss of 10% in SNR and range, and therefore a loss of $\sim 30\%$ in volume and detection rate. The Initial LIGO sub-solar mass searches also made use of a reduced frequency band. The lowest mass binary considered in those searches remained visible at a range of $\sim 4\,{\rm Mpc}$ [25]. We estimate that for the same mass and for the frequency band suggested above, Advanced LIGO has a range of $\sim 58\,{\rm Mpc}$ which corresponds to a sensitive volume three orders of magnitude greater.

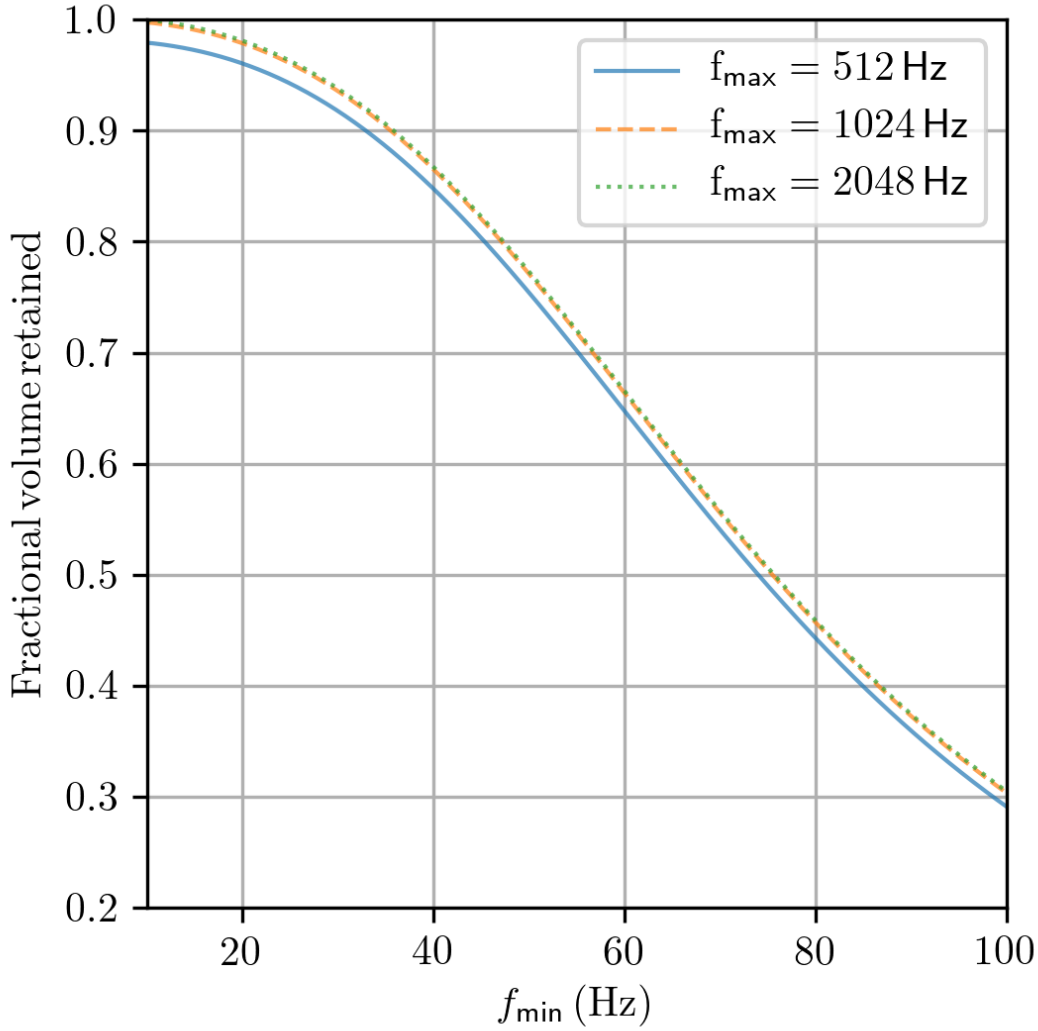

Figure 3.1: The fractional volume retained for various values of f_{max} and as a function of f_{min}. The dotted, dashed, and solid lines correspond to upper cut-off frequencies of 2048, 1024, and 512 Hz respectively. Note that there is very little difference between the various f_{max} values; this is because there is more than an order of magnitude more noise at these frequencies than the $\sim 100\,\mathrm{Hz}$ region and very little SNR is accumulated there. All values are measured relative to the band $f \in (10\,\mathrm{Hz}, 2048\,\mathrm{Hz})$.

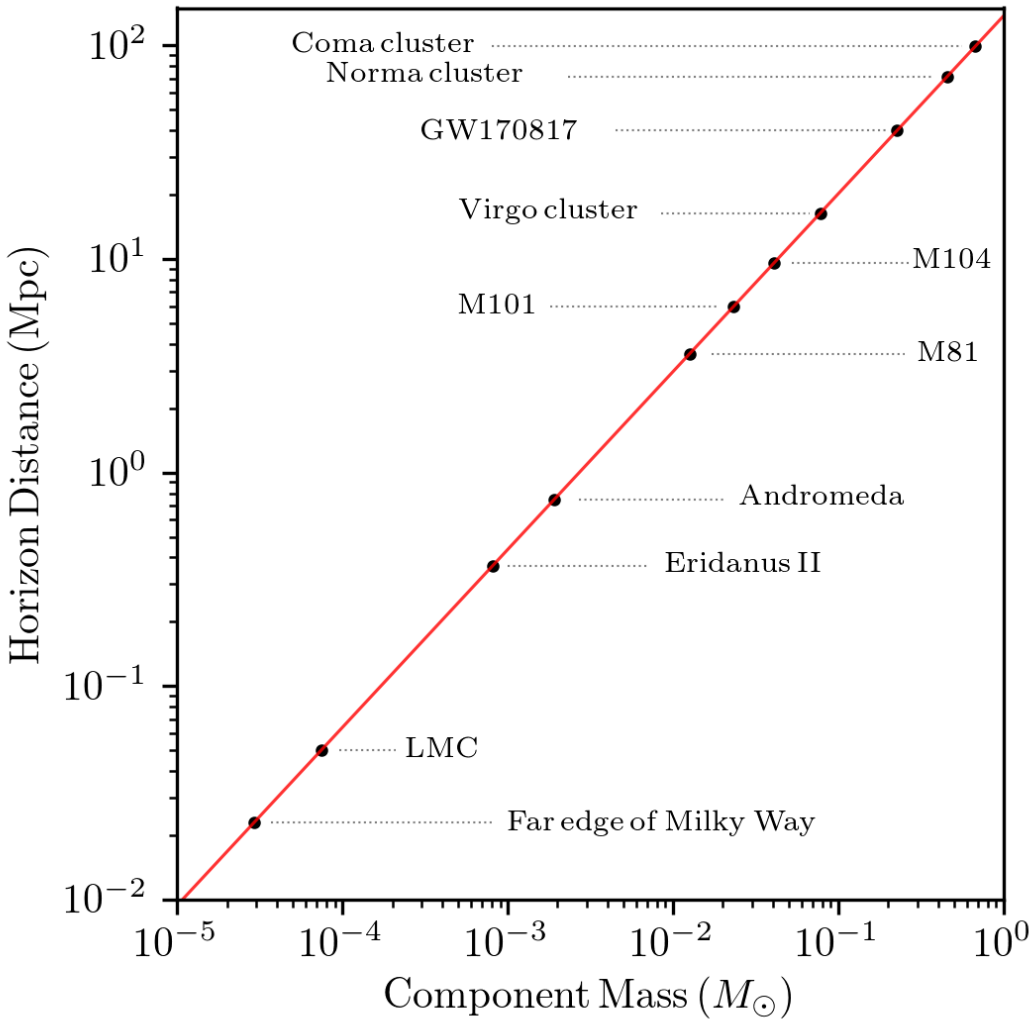

Figure 3.2: The distance to an optimally oriented, equal mass binary shown as a function of the component mass. LIGO remains sensitive to $\mathcal{O}(10^{-5}M_\odot - 10^{-5}M_\odot)$ binaries at extra-galactic distances. This plot assumes $f_{\rm min} = 10\,{\rm Hz}$ and $f_{\rm max} = 2048\,{\rm Hz}$ and therefore represents an optimistic view of horizon distance and ignores search difficulty. Nevertheless, this demonstrates that LIGO is capable of detecting extremely low mass ultracompact binaries at extra-galactic distances; understanding the scaling of sub-solar mass searches is crucial if we wish to probe that mass range. Astrophysical galaxies, groups, and clusters are included as a reference for cosmological distances. Several objects previously considered as observational candidates for the abundance of dark matter (Eridanus II, LMC/SMC, Segue I) are well within LIGO's range at low masses. Approximate distances taken from [9–15]. The noise curve used to approximate O1 sensitivity is "Early high/Mid low" from [16].

3.3.3 Approximation of the merger rate for null-results

We can estimate the upper limit on the merger rate in the event of a null-result using a combination of the methods outlined above. In Equation 3.7 we defined the horizon distance of the detector. This represents the maximum distance for which an optimally located and oriented source would be recovered with some $\langle\rho\rangle$. In general, however, detectors will measure a weaker response to a gravitational wave depending on the location and orientation of the binary. This reduction is described by the antenna patterns, F_+ and $F_\times$, which always take values less than or equal to 1 and are related to the signal observed on earth through:

$$h = F_+ h_+ + F_\times h_\times \tag{3.9}$$

Averaging the detector response over both location and orientation of the binary reduces the the strain recovered (and therefore the distance to a binary with some fiducial $\langle\rho\rangle$) by a factor of 2.26 [143–145]. This can be used to define the average range of the detector as

$$D_{avg} = \frac{D_{max}}{2.26} \tag{3.10}$$

The average sensitive distance allows us to approximate limits on the coalescence rate from null results for a general gravitational wave search. The loudest event statistic formalism [23] states that we can constrain the binary merger rate for a specific mass bin, i, to 90% confidence with:

$$\mathcal{R}_{90,i} = \frac{2.3}{\langle VT\rangle_i} \tag{3.11}$$

We can estimate the sensitive volume-time for a particular observing run using the earlier range approximation.

$$\langle VT\rangle_i = \tfrac{4}{3}\pi D^3_{avg,i} T \tag{3.12}$$

where T is the analyzable live-time of the two detectors. This method provides an excellent approximation of the sensitive 4-volume. The remaining plots in this paper use this procedure to estimate LIGO rates and LIGO sensitivity in the sub-solar

mass region.

3.3.4 Non-spinning waveforms

While reducing the frequency band is one way to mitigate the increased computational cost of sub-solar mass searches, non-spinning waveforms also offer an easy way to reduce the difficulty by potentially $1-2$ orders of magnitude. There are some theoretical justifications for non-spinning searches: some models predict sub-solar mass black holes to be predominately slowly spinning [146], and LIGO's previous detections have been consistent with low $\chi_{\rm eff}$ binaries. Regardless, a completely non-spinning binary is clearly a non-physical assumption. The efficacy of using non-spinning waveforms to recover spinning waveforms has been examined before [62, 147, 148]. In particular, [147] examined neutron star systems and found that non-spinning templates recovered aligned spin binary neutron stars to the desired level only for $-0.2 \lesssim \chi_{\rm eff} \lesssim 0$.

We performed a similar test on a population of $.5M_\odot - .5M_\odot$ binary black holes. We created a non-spinning template bank covering component masses $m_i \in (0.3M_\odot, 0.7M_\odot)$ using TaylorF2 waveforms [148, 149]. We then injected 10 000 spinning signals into fake data; each signal had spins that were purely aligned or anti-aligned with the orbital angular momentum and had dimensionless spin values of $|\chi_i| < 0.5$. We then calculated the overlap between our non-spinning template waveforms and the spinning signals. We find results similar to those of [147]; at low spin, there is a large overlap between the template waveforms and the injected, spinning signals. At higher spins, however, the maximum overlap rapidly falls off, implying that LIGO would miss a significant fraction of the signals with appreciable spin. In fact, we find that the non-spinning bank used here recovers signals well provided $\chi_{\rm eff} > -.08$ or $\chi_{\rm eff} < .02$. As $\chi_{\rm eff}$ deviates from these values, the fraction of signals missed grows rapidly. A spinning template bank is therefore necessary if sub-solar mass ultracompact binaries are either born with appreciable spin components or accrete enough matter to develop substantial spin. We are currently examining the effects of spin on the computational cost of sub-solar mass CBC searches, as well as other possible ways to mitigate the increased difficulty of a spinning search.

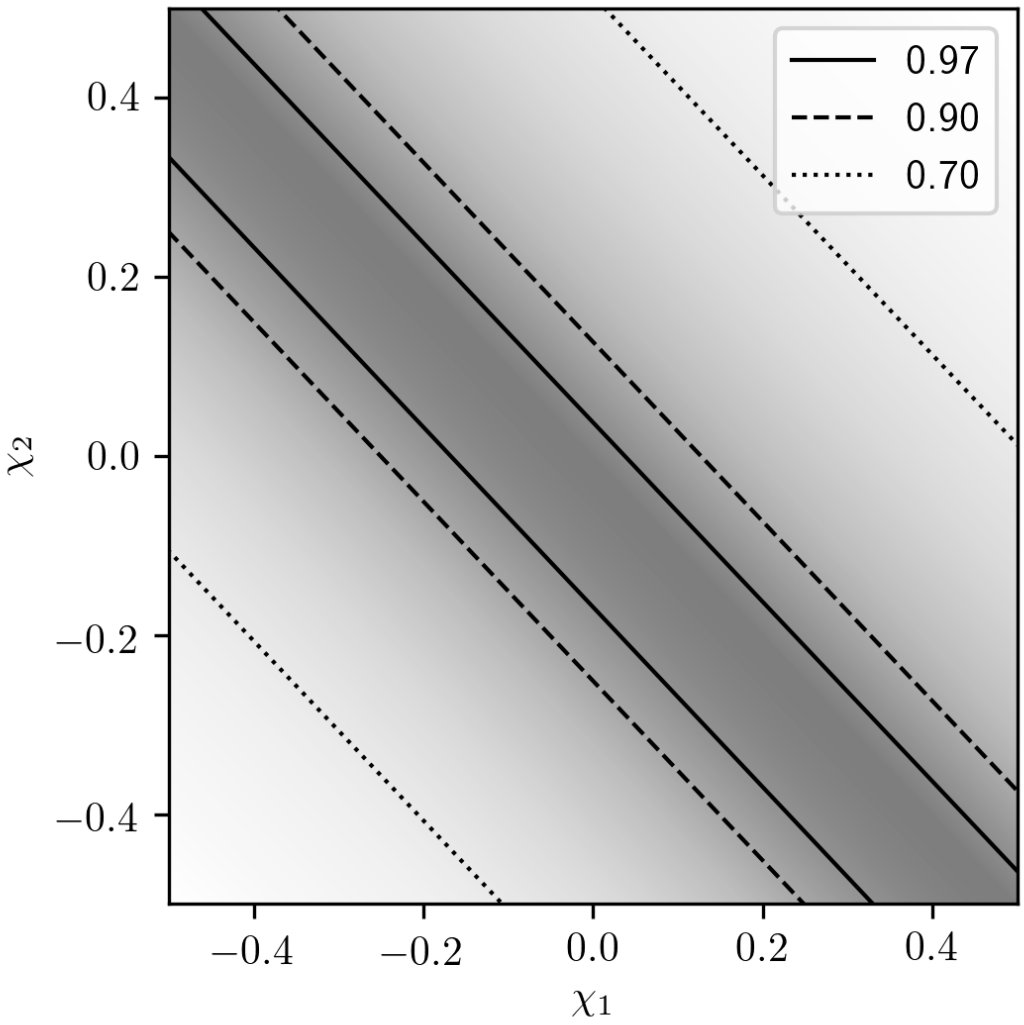

Figure 3.3: Recovery of spinning signals with a family of non-spinning template waveforms. Shown in black are lines of constant fitting factor (i.e. the maximum overlap between template waveforms and the injected signals) with the value specified by the line type. The shading shows how the fitting factor changes with the spin of the components in regions between the contours. While systems with $-.084 < \chi_{\rm eff} < .019$ are recovered well, the match between the two waveforms drops rapidly for $\chi_{\rm eff}$ outside this range. The SNR is proportional to the fitting factor, so the loss in SNR grows rapidly with total spin.

3.4 Potential constraints on primordial black hole abundance

While there is a large population of compact objects below one solar mass, the only objects compact enough for detection by LIGO are black holes and neutron stars. Other compact objects begin to coalesce at too low of an orbital frequency to produce gravitational waves in the sensitive band of ground-based interferometers. Neither black holes nor neutron stars are expected to form below one solar mass via known astrophysical mechanisms, though there are models that propose alternative ways to form black holes at this mass [150, 151]. It is interesting to consider the possibility that sub-solar mass black holes are formed via primordial processes and could be a component of the dark matter. In the event of either a detection or null-result LIGO can provide estimates on the merger rate, so it is therefore necessary to model the binary formation rate for primordial black holes in order to connect LIGO with primordial populations. Here we describe the sensitivity of one particular model to changes in input parameters, as well as the response of constraints on the dark matter fraction, $f_{\rm PBH} \equiv \Omega_{\rm PBH}/\Omega_{\rm DM}$, to changes in merger rate constraints that could be provided by LIGO. We motivate this model as a way to provide a conservative limit on $f_{\rm PBH}$.

We consider a model of (initially) uniformly distributed, monochromatic black holes formed in the early universe. A pair of nearest neighbor black holes will start to decouple from the background cosmological expansion and form a binary when the mean energy density in a volume encompassing the two exceeds the background energy density. A third, closest black hole to the binary injects angular momentum in the system by applying tidal forces, which ensures that the two black holes will orbit rather than collide head-on. The resulting expression for the merger rate of primordial black hole binaries in the local universe is given by:

$$\text{event rate} = n_{\rm PBH} \left.\frac{dP}{dt}\right|_{t=t_0} . \tag{3.13}$$

where dP is given by:

$$dP = \begin{cases} \frac{3\, f_{\rm PBH}^{\frac{37}{8}}}{58} \left[f_{\rm PBH}^{-\frac{29}{8}} \left(\frac{t}{t_c}\right)^{\frac{3}{37}} - \left(\frac{t}{t_c}\right)^{\frac{3}{8}} \right] \frac{dt}{t}, & t < t_c \\ \frac{3\, f_{\rm PBH}^{\frac{37}{8}}}{58} \left[f_{\rm PBH}^{-\frac{29}{8}} \left(\frac{t}{t_c}\right)^{-\frac{1}{7}} - \left(\frac{t}{t_c}\right)^{\frac{3}{8}} \right] \frac{dt}{t}, & t \geq t_c \end{cases} \tag{3.14}$$

and $n_{\rm PBH}$ by:

$$n_{\rm PBH} = \frac{3H_0^2}{8\pi G} \frac{\Omega_{\rm PBH}}{M_{\rm PBH}} \tag{3.15}$$

where

$$t_c = Q\alpha^4 \beta^7 \bar{x}^4 f^{25/3} \tag{3.16}$$

and

$$\bar{x} = \frac{1}{(1+z_{\rm eq})} \left(n_{\rm PBH}\right)^{-1/3} \tag{3.17}$$

with $Q = 3/170\, (GM_{\rm PBH})^{-3}$, G the gravitational constant, $z_{\rm eq}$ the redshift at matter-radiation equality, and $M_{\rm PBH}$ the mass of each individual black hole in this population. α and β are constants of $\mathcal{O}(1)$ that depend on the dynamics of binary formation and are typically set to 1. This model has been extensively studied [152–156].

This model provides a direct connection between LIGO and PBHs via an expected merger rate which is solely a function of the age of the universe, t_0, given some $M_{\rm BH}$ and $f_{\rm PBH}$. The merger rate is not analytically invertible, but if gravitational wave observations provide a constraint on the merger rate for black holes of a particular mass, then it can be numerically solved to obtain an upper limit on $f_{\rm PBH}$ for that mass bin. Similar procedures have been considered before [154, 156].

It is important to consider the robustness of this model and the relative strictness of the constraints it provides. First, consider the effects of varying α and β. Numerical simulations suggest that realistic values are $\alpha = 0.4$, $\beta = 0.8$ [152]. Though not immediately evident from the above equation, smaller values of α and β lead to larger *expected* rates and therefore more stringent estimates of the upper limit of $f_{\rm PBH}$. The dependence of the expected rate on α and β is shown explicitly in Figure 5.1. As α and β dip below 1, the expected merger rate increases. It

is a simple extension to approximate how the constraints on $f_{\rm PBH}$ are affected by variations of α and β. We can use the procedure outlined in 3.3.3 to approximate the upper limit on the merger rate, which we then invert to find limits on $f_{\rm PBH}$. We present bounds under this approximation for $\alpha = \beta = 1$ and $\alpha = 0.4$, $\beta = 0.8$ in Figure 3.5a. This figure shows a general feature of the model: as either α or β is decreased, the constraint on $f_{\rm PBH}$ for a given upper bound on the merger rate becomes tighter. Thus $\alpha = \beta = 1$ provides a more conservative limit on $f_{\rm PBH}$.

Of course, allowing α, β to increase beyond 1 yields looser constraints. At the time that two PBHs become gravitationally bound to one another, α describes the ratio between the semi-major axis of the binary and the initial physical separation of the two PBHs at the moment they become bound. It is therefore unphysical to expect $\alpha > 1$. β helps to determine the minimum ellipticity of the binary; for $\beta > 1$, the ellipticity becomes imaginary. $\alpha = \beta = 1$ therefore provides the *most* conservative rate estimate for this model.

Another important consideration is the sensitivity of this model to errors in observational measurements of the merger rate. We can propagate errors in rates measurements through to the dark matter fraction. From our upper limit on the merger rate estimate, we find that $f_{\rm PBH} \approx .28$ at $0.2M_\odot$ and $f_{\rm PBH} \approx .04$ at $1.0M_\odot$. If we allow for a 50% error in the merger rate estimate that this procedure provides we still find $f \in (.17, .37)$ and $f \in (.03, .06)$ for the respective mass bins, thus demonstrating that the constraints are relatively insensitive to even large errors in the upper bound on the merger rate.

There are several other assumptions made in this model that we do *not* attempt to quantify, but instead provide a brief qualitative argument on their effects. First, we have assumed that primordial black holes are uniformly distributed in space. In reality, we expect PBHs to cluster to some extent which would change the expected event rate for PBH binary mergers. Clustering would tend to increase the amount of binary coalescences, however, so the *expected* event rate would rise and therefore the maximum permissible fraction, $f_{\rm PBH}$, would decrease. Therefore a spatially uniform distribution of PBHs provides a conservative bound on $f_{\rm PBH}$. We also ignore the binary's evolution between formation and coalescence, as well as the possibility of late-universe binary formation. For a discussion of these effects, which appear to be sub-dominant (though they also drive the expected rate up), see [157]. A potentially larger effect comes from the assumption of a purely monochromatic

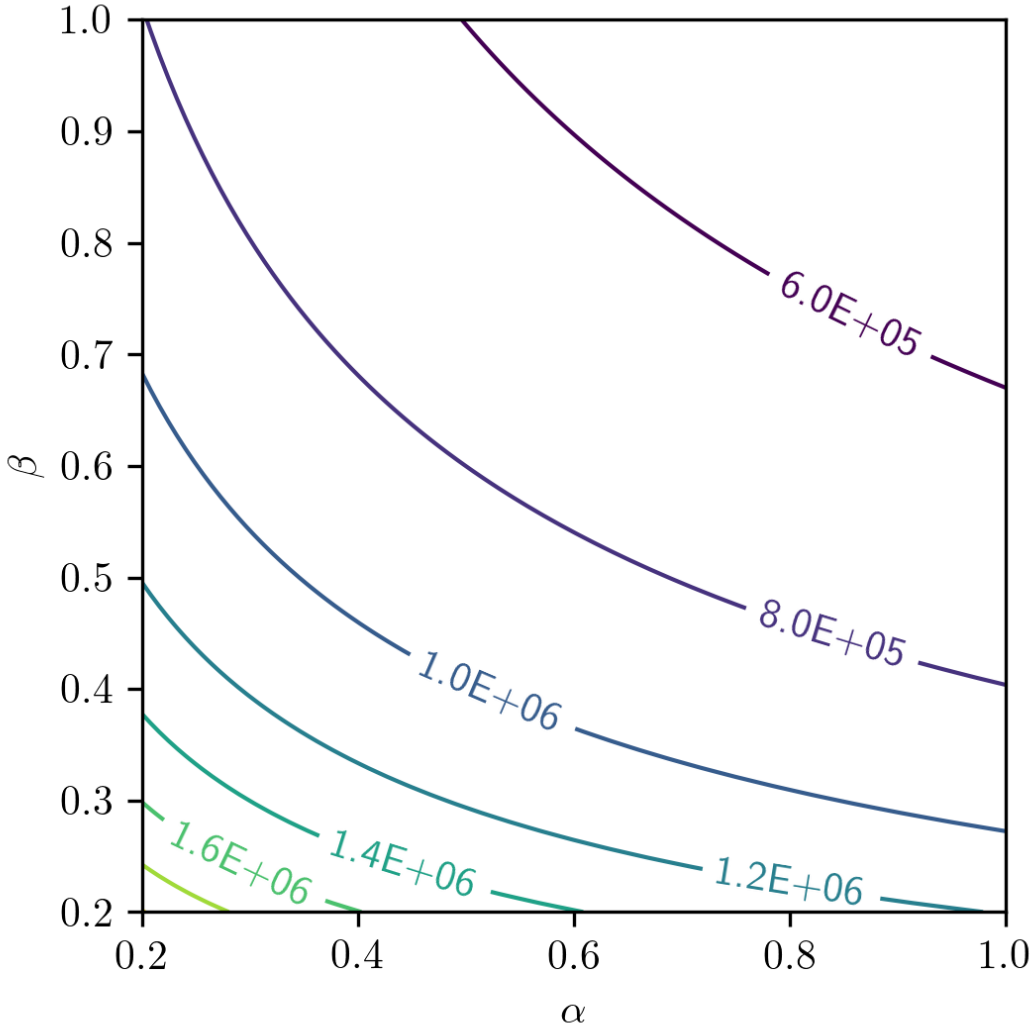

Figure 3.4: Merger rate dependence on α and β for a fixed dark matter fraction ($f = 0.5$) and primordial black hole mass ($M_{\rm BH} = 1.0 M_\odot$), shown in units of $\mathrm{Gpc}^{-3}\mathrm{yr}^{-1}$. The expected merger rate strictly increases as either α or β are changed from 1.0. Similar behavior is observed independent of the black hole mass or dark matter fraction. This implies that the constraints on the dark matter fraction that are typically published assuming $\alpha = \beta = 1$ are conservative for this model.

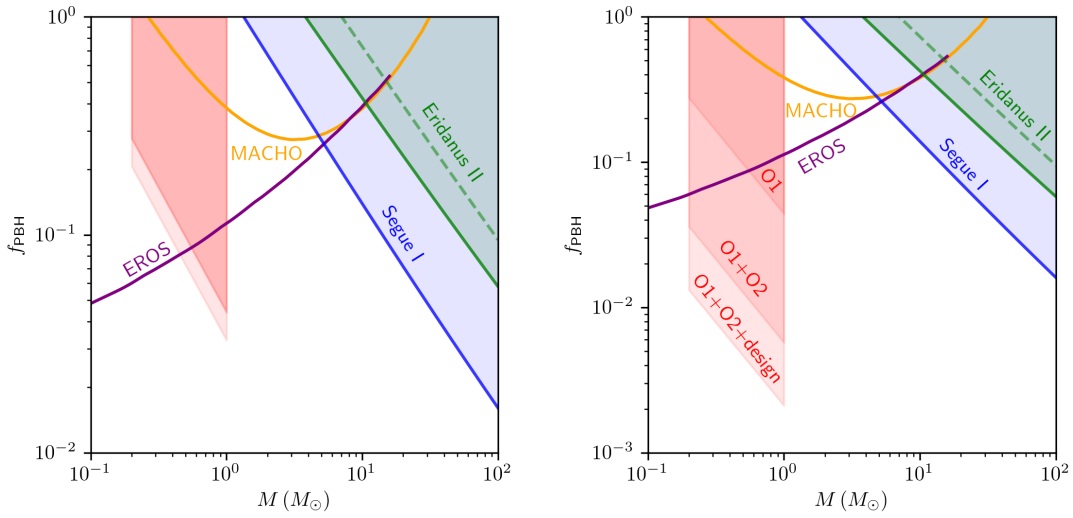

(a) Dark matter constraint dependence on α and β

(b) Future outlook for LIGO bounds on PBH dark matter

Figure 3.5: 3.5a Limits on the fraction of dark matter composed of primordial black holes in a monochromatic distribution. Shown in purple, yellow, blue, and green are reproductions of the constraints found in [17–20], respectively. Unlike in [21], the LIGO limits presented here are based on horizon distance estimates using the power spectra and the loudest event statistic [22, 23]. This method is described in the text. Potential LIGO results shown in red emphasize the small effect α and β have on the constraints. The bottom line shows the limit for $\alpha = 0.4$, $\beta = 0.8$, while the upper line shows $\alpha = \beta = 1$. 3.5b A possible outlook to the future. Shown here are constraints derived from the same formalism (and assuming continued null results). We follow the procedure mentioned in the text to approximate the rates constraints. Here we assume year long runs operating at 40% efficiency for the O2 and design contributions. LIGO will be able to place percent level limits on the fraction of dark matter in PBHs after a year of operating at design sensitivity. The noise curves used for this plot come from the data release associated with [16], specifically the "Early high/Mid low" column for O1, "Mid high/Late low" for O2, and "Design" for design.

distribution of black holes. Though the framework for this formation model has been extended to the unequal mass case in [152], we have not considered those effects here. Finally, we also ignore the effects of spin on binary formation.

3.5 Future prospects and discussion

As Advanced LIGO approaches design sensitivity, its horizon distance should increase by a factor of $2-3$ [47]. This, coupled with the more observation, means that LIGO could conceivably have a (cumulative) sensitive $\langle VT \rangle$ $\mathcal{O}(10)$ times larger than was observed in [21]. Figure 3.5b shows projections for how continued null results could contribute to constraints on $f_{\rm PBH}$ for this mass range. Ground based interferometers have the unique ability to strengthen bounds in the sub-solar mass regime by systematics independent of previous microlensing observations [17,18,158]. This is especially important in light of recent criticisms [87] and studies of the model dependencies of these surveys [159].

There are many areas in which sub-solar mass searches can improve on the suggestions outlined here. The most obvious are extensions to lower masses and spinning binaries, each of which presents its own challenges. Lower masses require denser template banks and they persist in LIGO's sensitive band longer. One possible solution could be to alter the width of the frequency band considered for different mass bins, thus stitching together a suitable template bank. Spin is more difficult to incorporate; early tests seem to imply at least a factor of 10 more templates would be required for fully spinning binaries. Examining smaller component spins, such as $\chi_i < 0.3$, could remain computationally feasible and help to mitigate the rapid fall off in sensitivity that non-spinning banks currently experience for moderate to high spin systems. We are actively pursuing extensions in these areas.

More careful PBH population modeling is also a necessity. In particular, a careful consideration of extended PBH distributions will offer more accurate and general merger rate predictions. Not only will this allow for more precise constraints, but it will also be useful in examining the feasibility of detecting preferred PBH distributions peaked in this mass range. While this paper has demonstrated that the model considered typically provides a conservative estimate of the bounds on $f_{\rm PBH}$, a more general formalism will allow testing of different inflationary models.

3.6 Acknowledgments

Funding for this project was provided by the Charles E. Kaufman Foundation of The Pittsburgh Foundation. Computing resources and personnel for this project were provided by the Pennsylvania State University. We thank the LIGO CBC working group and John Whelan, Nelson Christensen, and Graham Woan for many useful questions and comments. We thank Kipp Cannon for suggesting we consider non-spinning searches in the mass range considered. This document has been assigned the document number LIGO-P1800231-v3.

Chapter 4
Search for sub-solar mass ultracompact binaries in Advanced LIGO's first observing run

We present the first Advanced LIGO and Advanced Virgo search for ultracompact binary systems with component masses between 0.2 $M_\odot$ – 1.0 $M_\odot$ using data taken between September 12, 2015 and January 19, 2016. We find no viable gravitational wave candidates. Our null result constrains the coalescence rate of monochromatic (delta function) distributions of non-spinning (0.2 $M_\odot$, 0.2 $M_\odot$) ultracompact binaries to be less than $1.0 \times 10^6\,\mathrm{Gpc}^{-3}\mathrm{yr}^{-1}$ and the coalescence rate of a similar distribution of (1.0 $M_\odot$, 1.0 $M_\odot$) ultracompact binaries to be less than $1.9 \times 10^4\,\mathrm{Gpc}^{-3}\mathrm{yr}^{-1}$ (at 90% confidence). Neither black holes nor neutron stars are expected to form below $\sim 1M_\odot$ through conventional stellar evolution, though it has been proposed that similarly low mass black holes could be formed primordially through density fluctuations in the early universe and contribute to the dark matter density. The interpretation of our constraints in the primordial black hole dark matter paradigm is highly model dependent, however, under a particular primordial black hole binary formation scenario we constrain monochromatic primordial black

hole populations of 0.2 $M_\odot$ to be less than 33% of the total dark matter density and monochromatic populations of 1.0 $M_\odot$ to be less than 5% of the dark matter density. The latter strengthens the presently placed bounds from micro-lensing surveys of MAssive Compact Halo Objects (MACHOs) provided by the MACHO and EROS collaborations.

4.1 Introduction

The era of gravitational wave astronomy began with the observation of the binary black hole merger GW150914 [160]. Since then, four additional binary black hole mergers [134–137] and one binary neutron star merger [9] have been announced as of November 2017. Thus far, Advanced LIGO and Advanced Virgo searches have targeted binary systems with total masses from 2–600 $M_\odot$ [138, 139], but the LIGO and Virgo detectors are also sensitive to ultracompact binaries with components below 1 $M_\odot$ if the compactness (mass to radius ratio) is close to that of a black hole. White dwarf binaries, while often formed with components below one solar mass, are not sufficiently compact to be a LIGO/Virgo gravitational wave source. Neutron stars or black holes are sufficiently compact as would be other exotic compact objects. Previous gravitational wave searches for sub-solar mass ultracompact binaries used data from initial LIGO observations from Feb 14, 2003 – March 24, 2005 [24, 25]. Advanced LIGO [45] presently surveys a volume of space approximately 1000 times larger than the previous search for sub-solar mass ultracompact objects therefore improving the chances of detecting such a binary 1000-fold.

In conventional stellar evolution models, the lightest ultracompact objects are formed when stellar remnants exceed $\sim 1.4M_\odot$, the Chandrasekhar mass limit [161,162]. Beyond the Chandrasekhar mass limit, electron degeneracy pressure can no longer prevent the gravitational collapse of a white dwarf. The lightest remnants that exceed the Chandrasekhar mass limit form neutron stars [163]. When even the neutron degeneracy pressure cannot prevent collapse, heavier stellar remnants will collapse to black holes. Some equations of state predict that neutron stars remain stable down to $\sim 0.1M_\odot$ [164]; there is no widely accepted model for forming neutron stars below $\sim 1M_\odot$, though a recent measurement does not exclude the possibility of $0.92M_\odot$ neutron star [165]. This result may be due to the

low inclination of the system. The lowest precisely measured neutron star mass is $1.174 M_\odot$ [166]. Observationally, black holes appear to have a minimum mass of $\sim 5 M_\odot$ with a gap between the heaviest observed neutron star ($\sim 2 M_\odot$) and black hole masses [91, 92, 167, 168]. Detecting ultracompact objects below one solar mass could challenge our ideas about stellar evolution or possibly hint at new, unconventional formation scenarios.

Beyond conventional stellar evolution, one of the most prolific black hole formation models posits that primordial black holes (PBHs) could have formed in the early universe through the collapse of highly over-dense regions [104, 169–172]. It has been suggested that PBHs could constitute a fraction of the missing dark matter [169, 172], though this scenario has been constrained [8]. LIGO's detections have revived interest in black hole formation mechanisms and, in particular, the formation of primordial black holes (PBHs) [88, 154, 173]. Though there are proposals on how to distinguish a primordial black hole distribution from an astrophysical one [174–179], disentangling them is challenging when the populations overlap in mass. Hence, detection of sub-solar mass ultracompact objects would provide the cleanest signature for determining primordial formation. Still, recent proposals for non-baryonic dark matter models can produce sub-solar mass black holes either by allowing a lower Chandrasekhar mass in the dark sector [150], or by triggering neutron stars to collapse into $\sim 1 M_\odot$ black holes [151].

This letter describes a gravitational wave search for ultracompact binary systems with component masses between 0.2 $M_\odot$ and 1.0 $M_\odot$ using data from Advanced LIGO's first observing run . No viable gravitational wave candidates were identified. We briefly describe the data analyzed and the anticipated sensitivity to sub-solar mass ultracompact objects, as well as the search that was conducted, which led to the null result. We then describe how the null result constrains the merger rate of sub-solar mass binaries in the nearby universe. We consider the merger rate constraints in the context of binary merger rate estimates most recently given by Sasaki et al [154] thereby constraining the fraction of dark matter density made up of PBHs between 0.2 $M_\odot$ and 1.0 $M_\odot$. Finally, we conclude with a discussion of future work.

4.2 Search

We report on data analyzed from Advanced LIGO's first observing run, taken from September 12, 2015 – January 19, 2016 at the LIGO Hanford and LIGO Livingston detectors. After taking into account data quality cuts [180] and detector downtime, we analyzed a total of 48.16 days of Hanford-Livingston coincident data. The data selection process was identical to that used in previous searches [181].

During Advanced LIGO's first observing run, each LIGO instrument was sensitive to sub-solar mass ultracompact binaries at extra-galactic distances. Figure 4.1 shows the maximum distance to which an equal-mass compact binary merger with given component masses would be visible at a signal-to-noise ratio of 8 in either LIGO Hanford or LIGO Livingston.

The search was conducted using standard gravitational wave analysis software [58, 148, 149, 182–184]. Our search consisted of a matched-filter stage that filtered a discrete bank of templates against the LIGO data. The peak SNR for each template for each second was identified and recorded as a trigger. Subsequently, a chi-squared test was performed that checked the consistency of the trigger with a signal [58]. The triggers from each LIGO detector and gravitational wave template were combined and searched for coincidences within 20 ms. Candidates that pass coincidence were assigned a likelihood ratio, $\mathcal{L}$, that accounts for the relative probability that the candidates are signal versus noise as a function of SNR, chi-squared, and time delay and phase offset between detectors. Larger values of $\mathcal{L}$ were deemed to be more signal-like. The rate at which noise produced candidates with a given value of $\mathcal{L}$ was computed via a Monte Carlo integral of the noise derived from non-coincident triggers, which we define as the false alarm rate of candidate signals.

Our discrete bank of 500 332 template waveforms [185] conformed to the gravitational wave emission expected from general relativity [51, 52]. We use the 3.5 post-Newtonian order TaylorF2 waveform to model the inspiral portion of the binary evolution, which is constructed under the stationary phase approximation [52]. The TaylorF2 waveform has been used in previous low-mass Advanced LIGO and Advanced Virgo searches. The bank covered component masses in the detector frame between 0.19 – 2.0 $M_\odot$ with 97% fidelity. While we restrict our analysis of the search results to the sub-solar region, we have allowed for the possibility of high mass ratio systems. Our template bank assumed that each binary component has

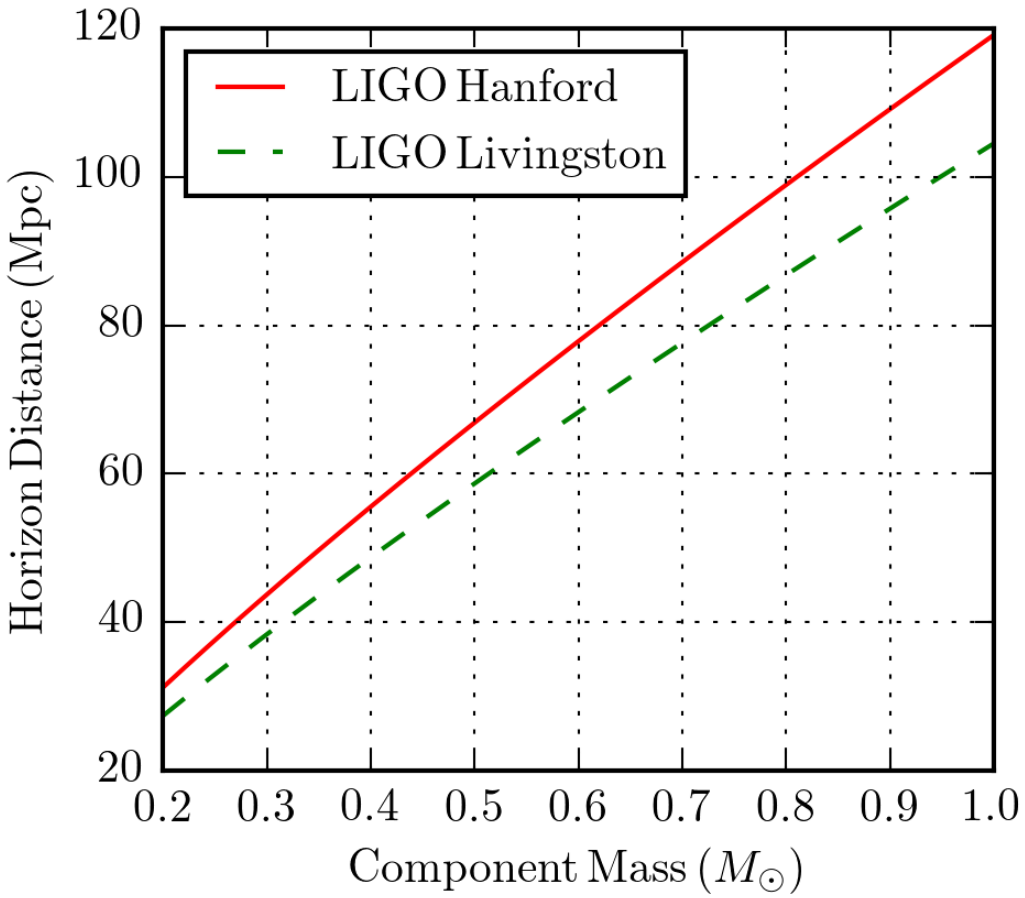

Figure 4.1: Distance to which an optimally oriented and aligned equal-mass ultracompact binary merger would produce at least SNR 8 in each of the LIGO Livingston and LIGO Hanford detectors as a function of component mass, based on the median sensitivity obtained from our analyzed data.

negligible spin. Relaxing that assumption is a direction for future work, but is a computationally challenging problem requiring resources well beyond those used for this and previous LIGO analyses. We integrated the template waveforms between 45–1024 Hz, with the longest waveform lasting about 470 seconds. Advanced LIGO is sensitive down to ~ 15 Hz, but integrating from that frequency would have been too computationally burdensome. Our choice to integrate from 45 Hz to 1024 Hz recovered 93.0% of the total possible SNR that integration over the full band would have provided. Additional details are described in [185].

No viable gravitational wave candidates were found. Our loudest gravitational wave candidate was consistent with noise and had a false alarm rate of 6.19 per year.

4.3 Constraint on binary merger rate

We constrained the binary merger rate in this mass region by considering nine monochromatic mass distributions with equal component masses and negligible spin. We constructed sets of simulated signals with component masses $m_i \in \{0.2, 0.3, \ldots, 1.0\} M_\odot$ distributed uniformly in distance and uniformly on the sky. We injected 374 480 simulated signals into the LIGO data and conducted a gravitational wave search with the same parameters as described in section 4.2. We then calculated our detection efficiency as a function of distance, $\epsilon_i(r)$. This allowed us to compute the volume-time, $\langle VT \rangle$, that was accessible for our search via,

$$\langle VT \rangle_i = T \int 4\pi r^2 \epsilon_i(r) dr, \tag{4.1}$$

where T is 48.16 days. We then used the loudest event statistic formalism [23] to compute an upper limit on the binary merger rate in each mass bin to 90% confidence,

$$\mathcal{R}_{90,i} = \frac{2.3}{\langle VT \rangle_i}. \tag{4.2}$$

We report the upper limits on the binary merger rate in Fig. 5.1. Several factors in our analysis could lead to uncertainty in $\mathcal{R}_{90}$ at the 25% level, including LIGO calibration errors and Monte Carlo errors. However, these errors are far smaller than potential systematic errors in the models we will be considering in the next section, so we do not attempt to further quantify them in this work.

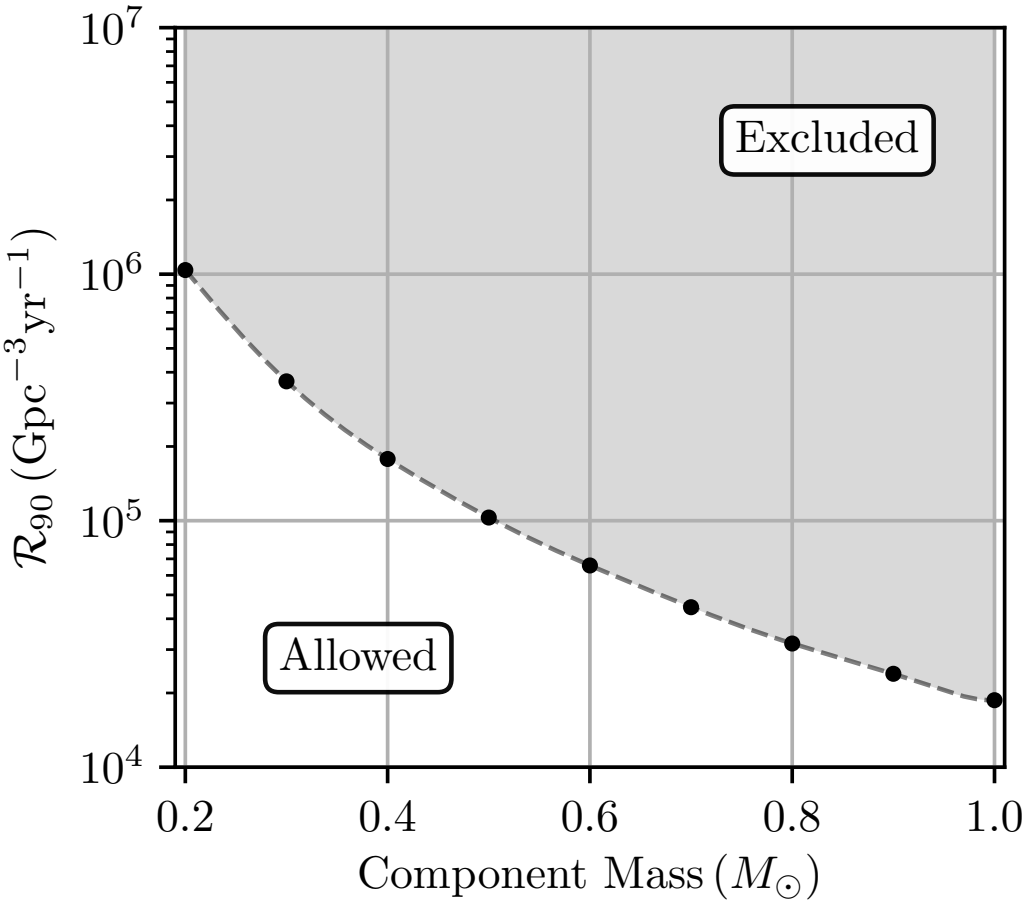

Figure 4.2: Constraints on the merger rate of equal-mass ultracompact binaries at the 9 masses considered. The gray region represents an exclusion at 90% confidence on the binary merger rate in units of Gpc^{-3} yr^{-1}. These limits are found using the loudest event statistic formalism, as described in section III and [23]. The bounds presented here are ~ 3 orders of magnitude stricter than those found in initial LIGO's search for sub-solar mass ultracompact objects [24, 25].

4.4 Constraint on primordial black holes as dark matter

For an assumed model of PBH binary formation, the constraint on the binary merger rate places bounds on the total fraction of dark matter made of primordial black holes, f. These bounds are derived from the expected event rate for a uniform

distribution of monochromatic PBHs with mass m_i as considered above. The limits on f are sensitive to the model of binary formation. Motivated by previous LIGO searches [24] we follow a method originally proposed by [152, 153] and recently used to constrain $\sim 30 M_\odot$ PBH mergers by [154].

We assume an initial, early-universe, monochromatic distribution of PBHs. As the universe expands, the energy density of a pair of black holes not too widely separated becomes larger than the background energy density. The pair decouples from the cosmic expansion and can be prevented from prompt merger by the local tidal field, determined primarily by a third black hole nearest the pair. The initial separation of the pair and the relative location of the primary perturber determine the parameters of the initial binary. From those, the coalescence time can be determined. Assuming a spatially uniform initial distribution of black holes, the distribution of coalescence times for those black holes that form binaries is

$$dP = \begin{cases} \dfrac{3\, f^{\frac{37}{8}}}{58} \left[f^{-\frac{29}{8}} \left(\dfrac{t}{t_c} \right)^{\frac{3}{37}} - \left(\dfrac{t}{t_c} \right)^{\frac{3}{8}} \right] \dfrac{dt}{t}, & t < t_c \\ \dfrac{3\, f^{\frac{37}{8}}}{58} \left[f^{-\frac{29}{8}} \left(\dfrac{t}{t_c} \right)^{-\frac{1}{7}} - \left(\dfrac{t}{t_c} \right)^{\frac{3}{8}} \right] \dfrac{dt}{t}, & t \geq t_c \end{cases} \tag{4.3}$$

where t_c is a function of the mass of the PBHs and the fraction of the dark matter they comprise:

$$t_c = \frac{3}{170} \frac{c^5}{(G m_i)^{5/3}} \frac{f^7}{(1+z_{\rm eq})^4} \left(\frac{8\pi}{3 H_0^2 \Omega_{\rm DM}} \right)^{4/3} \tag{4.4}$$

This expression is evaluated at the time today, t_0, then multiplied by $n_{\rm BH}$, the current average number density of PBHs, to get the model event rate [154]:

$$\mathcal{R}_{model} = n_{\rm BH} \left. \frac{dP}{dt} \right|_{t=t_0}. \tag{4.5}$$

Given the measured event rate, $\mathcal{R}_{90,i}$, and a particular mass, the above expression can be inverted to find a constraint on the fraction of dark matter in PBHs at that mass. The results of this calculation using the measured upper limits on the merger rate are shown in Fig. 5.2. A discussion on how some assumptions of this model may affect the constraints on f shown in Fig. 5.2, are discussed

in [185]. The non-detection of a stochastic background in the first observing run of Advanced LIGO [186] also implies an upper limit on the merger rate and therefore the PBH abundance. In particular, it is shown that the non-detection of a stochastic background yields constraints that are about a factor of two weaker than the targeted search [156, 187–189].

These results are sensitive to the model of binary formation as well as the mass distribution of PBHs. The effects of initial clustering of PBHs is a current area of research, though it appears that for the expected narrow mass distributions of PBHs this effect is small in the mass range we consider [190–192]. While the results presented here to not take into account other effects on the binary parameters [157], they provide a conservative estimate of the bounds.

4.5 Conclusion

We presented the first Advanced LIGO and Advanced Virgo search for ultracompact binary mergers with components below 1 $M_\odot$. No viable gravitational wave candidates were found. Therefore, we were able to constrain the binary merger rate for monochromatic mass functions spanning from 0.2 – 1.0 $M_\odot$. Using a well-studied model from the literature [152–154], we constrained the abundance of primordial black holes as a fraction of the total dark matter for each of our nine monochromatic mass functions considered.

This work was only the first step in constraints by LIGO on new physics involving sub-solar mass ultracompact objects. The constraints presented in Fig. 5.1 (and consequently those that arise from the model of binary formation we consider shown in Fig. 5.2) may not apply if the ultracompact binary components have non-negligible spin since the waveforms used for signal recovery were generated only for non-spinning binaries. Future work may either quantify the extent to which the present search could detect spinning components, or expand the template bank to include systems with spin. Third, we should consider more general distributions of primordial black hole masses; extended mass functions allow for the possibility of unequal mass binaries, and the effect of this imbalance on the predicted merger rate has not been quantified. We also stress that our present results do not rule out an extended mass function that peaks below 0.2 $M_\odot$ and extends all the way to LIGO's currently detected systems at or above 30 $M_\odot$. Each model would

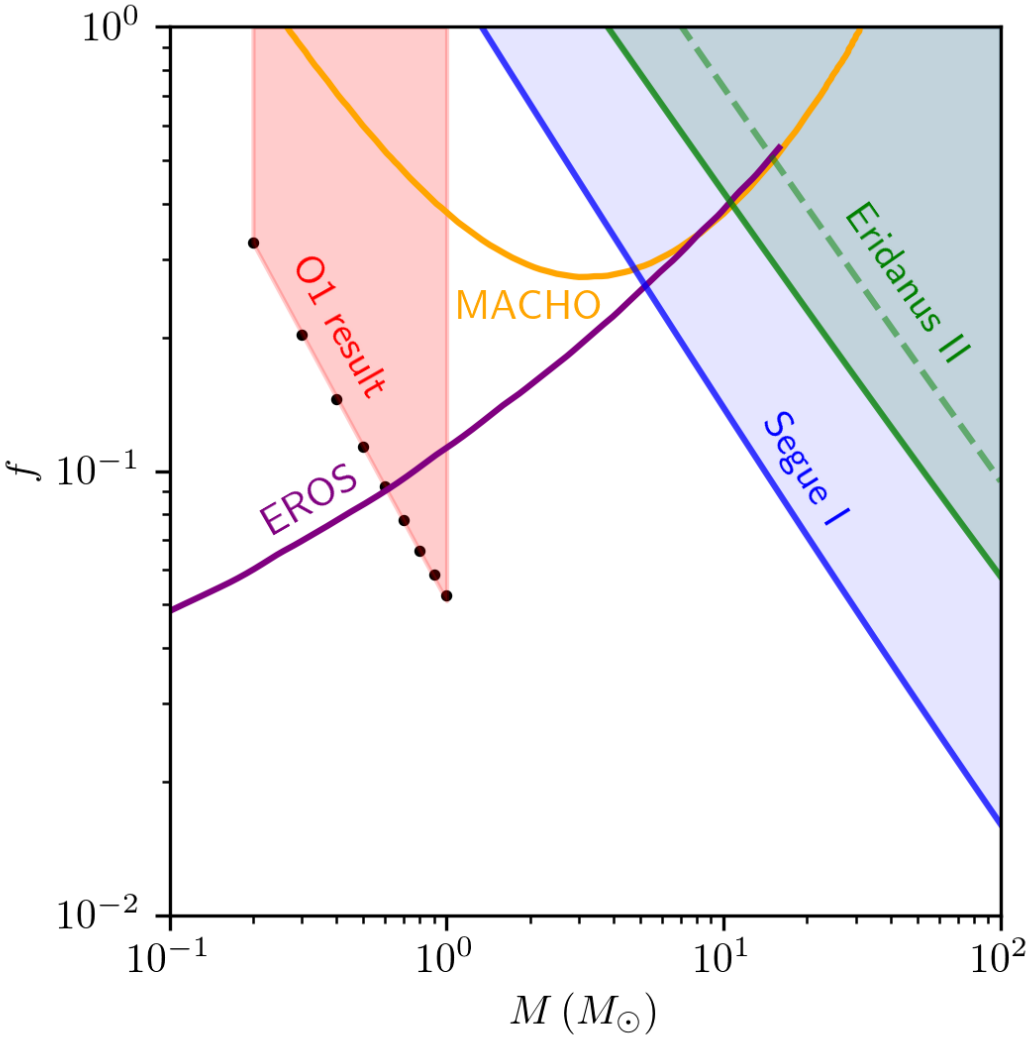

Figure 4.3: Constraints on the fraction of dark matter composed of primordial black holes for monochromatic distributions ($f = \Omega_{\rm PBH}/\Omega_{\rm DM}$). Shown in black are the results for the nine mass bins considered in this search. For this model of primordial black hole formation, LIGO finds constraints tighter than those of the MACHO collaboration [18] for all mass bins considered and tighter than the EROS collaboration [17] for $m_i \in (0.7, 1.0)M_\odot$. The limits presented here also improve upon other constraints at this mass [26]. The curves shown in this figure are digitizations of the original results from [17–20]. We use the Planck "TT,TE,EE+lowP+lensing+ext" cosmology [27].

have to be explicitly checked by producing an expected binary merger rate density that could be integrated against Advanced LIGO and Advanced Virgo search results. Extensions to more general distributions have already been considered in the literature [193].

The first two areas of future work are computational challenges. Lowering the minimum mass and including spin effects in the waveform models could easily increase the computational cost of searching for sub-solar mass ultracompact objects by an order of magnitude each, which would be beyond the capabilities of present LIGO data grid resources.

Advanced LIGO and Advanced Virgo have not reached their final design sensitivities. The distance to which Advanced LIGO will be sensitive to the mergers of ultracompact binaries in this mass range should increase by a factor of three over the next several years [47]. Furthermore, at least a factor of ten more data will be available than what was analyzed in this work. These two facts combined imply that the merger rate constraint should improve by $\gtrapprox 2$ orders of magnitude in the coming years.

4.6 Acknowledgments

The authors gratefully acknowledge the support of the United States National Science Foundation (NSF) for the construction and operation of the LIGO Laboratory and Advanced LIGO as well as the Science and Technology Facilities Council (STFC) of the United Kingdom, the Max-Planck-Society (MPS), and the State of Niedersachsen/Germany for support of the construction of Advanced LIGO and construction and operation of the GEO600 detector. Additional support for Advanced LIGO was provided by the Australian Research Council. The authors gratefully acknowledge the Italian Istituto Nazionale di Fisica Nucleare (INFN), the French Centre National de la Recherche Scientifique (CNRS) and the Foundation for Fundamental Research on Matter supported by the Netherlands Organisation for Scientific Research, for the construction and operation of the Virgo detector and the creation and support of the EGO consortium. The authors also gratefully acknowledge research support from these agencies as well as by the Council of Scientific and Industrial Research of India, the Department of Science and Technology, India, the Science & Engineering Research Board (SERB), India, the Ministry of

Human Resource Development, India, the Spanish Agencia Estatal de Investigación, the Vicepresidència i Conselleria d'Innovació, Recerca i Turisme and the Conselleria d'Educació i Universitat del Govern de les Illes Balears, the Conselleria d'Educació, Investigació, Cultura i Esport de la Generalitat Valenciana, the National Science Centre of Poland, the Swiss National Science Foundation (SNSF), the Russian Foundation for Basic Research, the Russian Science Foundation, the European Commission, the European Regional Development Funds (ERDF), the Royal Society, the Scottish Funding Council, the Scottish Universities Physics Alliance, the Hungarian Scientific Research Fund (OTKA), the Lyon Institute of Origins (LIO), the Paris Île-de-France Region, the National Research, Development and Innovation Office Hungary (NKFI), the National Research Foundation of Korea, Industry Canada and the Province of Ontario through the Ministry of Economic Development and Innovation, the Natural Science and Engineering Research Council Canada, the Canadian Institute for Advanced Research, the Brazilian Ministry of Science, Technology, Innovations, and Communications, the International Center for Theoretical Physics South American Institute for Fundamental Research (ICTP-SAIFR), the Research Grants Council of Hong Kong, the National Natural Science Foundation of China (NSFC), the Leverhulme Trust, the Research Corporation, the Ministry of Science and Technology (MOST), Taiwan and the Kavli Foundation. The authors gratefully acknowledge the support of the NSF, STFC, MPS, INFN, CNRS and the State of Niedersachsen/Germany for provision of computational resources. Funding for this project was provided by the Charles E. Kaufman Foundation of The Pittsburgh Foundation. Computing resources and personnel for this project were provided by the Pennsylvania State University. This article has been assigned the document number LIGO-P1800158-v13.

Chapter 5
Search for sub-solar mass ultracompact binaries in Advanced LIGO's second observing run

We present a search for sub-solar mass ultracompact objects in data obtained during Advanced LIGO's second observing run. In contrast to a previous search of Advanced LIGO data from the first observing run, this search includes the effects of component spin on the gravitational waveform. We identify no viable gravitational wave candidates consistent with sub-solar mass ultracompact binaries with at least one component between $0.2 - 1.0\,M_\odot$. We use the null result to constrain the binary merger rate of $(0.2\,M_\odot, 0.2\,M_\odot)$ binaries to be less than 3.7×10^5 Gpc^{-3}yr^{-1} and the binary merger rate of $(1.0\,M_\odot, 1.0\,M_\odot)$ binaries to be less than 5.2×10^3 Gpc^{-3}yr^{-1}. Sub-solar mass ultracompact objects are not expected to form via known stellar evolution channels, though it has been suggested that primordial density fluctuations or particle dark matter with cooling mechanisms and/or nuclear interactions could form black holes with sub-solar masses. Assuming a particular primordial black hole formation model, we constrain a population of merging $0.2\,M_\odot$ black holes to account for less than 16% of the dark matter density

and a population of merging $1.0\,M_\odot$ black holes to account for less than 2% of the dark matter density. We discuss how constraints on the merger rate and dark matter fraction may be extended to arbitrary black hole population models that predict sub-solar mass binaries.

5.1 Introduction

Gravitational wave and multi-messenger astronomy progressed remarkably in Advanced LIGO [45] and Advanced Virgo's [46] second observing run, which included the first observation of gravitational waves from a binary neutron star merger [9] and seven of the ten observed binary black hole mergers [135–137, 194]. These detections, as well as the candidates presented in the gravitational wave transient catalog (GWTC-1) [194], have led to a better understanding of the populations of compact binaries detectable by ground based interferometers [195]. These observations, however, represent just a portion of the parameter space that Advanced LIGO and Advanced Virgo currently search [75, 196] and are sensitive to [97]. We report on an extension of the searched parameter space in data obtained during O2 to compact binaries with component masses $< 1\,M_\odot$. To distinguish between other astrophysical compact objects (e.g. white dwarfs) that are not compact enough to form binaries that merge within LIGO's sensitive frequency band, we label our target population as *ultracompact*. This is the second search for sub-solar mass ultracompact objects in Advanced LIGO data and the fourth since initial LIGO [24, 25, 28], as well as the first search to incorporate spin effects in the modeling of the gravitational wave emission.

There is no widely accepted mechanism for the formation of ultracompact objects with masses well below a solar mass within the standard model of particle physics and the standard ΛCDM model of cosmology. Neutron stars are expected to have masses greater than the minimum Chandrasekhar mass [162] minus the gravitational binding energy. Calculations by [197] and more recently [89] found the minimum mass of a neutron star to be $1.15\,M_\odot$ and $1.17\,M_\odot$, respectively. These predictions closely agree with the lowest currently measured neutron star mass of $1.17\,M_\odot$ [166]. Similarly, black holes formed via established astrophysical collapse mechanisms are not expected to have masses below the maximum mass of a non-rotating neutron star, which recent pulsar timing observations [198] suggest

is $\sim 2\,M_\odot$. We note that there is one model that predicts that rapidly rotating collapsing cores could fission and produce a neutron star binary [199, 200], though this is not a favored astrophysical mechanism for the production of binary systems.

A detection of a sub-solar mass object in a merger would therefore be a clear signal of new physics. Indeed, there are several proposals that link sub-solar mass compact objects to proposals for the nature of dark matter, which makes up nearly 85% of the matter in the Universe. One possibility is that black holes with masses accessible to ground based interferometers could have formed deep in the radiation era from the prompt collapse of large primordial over-densities on the scale of the early time Hubble volume [103, 201]. The size and abundance of any such primordial black holes depends on the spectrum of primordial perturbations and on the equation of state of the early universe [202–205]. An alternative inflationary mechanism proposes that vacuum bubbles nucleated during inflation may result in black holes (with masses that can be around a solar mass) after inflation ends [206].

A different class of possibilities, explored more recently, is motivated by ideas for the particle nature of dark matter. For example, dark matter may have a sufficiently complex particle spectrum to support cooling mechanisms that allow dense regions to collapse into black holes at late times, in processes analogous to known astrophysical processes [150]. Alternatively, dark matter may have interactions with nuclear matter that allow it to collect inside of neutron stars and trigger their collapse to black holes [151, 207–212]. The details of when dark matter can collapse a neutron star to form a black hole or other exotic compact object are still under investigation [213], but the postulated black holes will have masses comparable to the progenitor neutron star mass, or perhaps smaller if some matter can be expelled by rapid rotation of the star during collapse.

A detection of a sub-solar mass black hole would have far-reaching implications. In the primordial black hole scenario, the mass and abundance of the black holes would constrain a combination of the spectrum of initial density perturbations on very small scales and the equation of state of the Universe at a time when the typical mass inside a Hubble volume was of the order of the black hole mass. For particle dark matter scenarios, the abundance of sub-solar mass black holes would provide a direct estimate of the cooling rate for dark matter. The black hole mass would constrain the masses of cosmologically abundant dark matter particles through, for example, the Chandrasekhar relation for fermions [150] or analogous

relations for non-interacting bosons [214, 215]. In the case that all black holes are observed to be near but not below the mass of neutron stars, the abundance of such objects would constrain the dark matter-nucleon interaction strength, as well as the dark matter self-interaction strength and mass(es) [151].

This letter reports the results of a search for gravitational waves from sub-solar mass ultracompact binaries using data from Advanced LIGO's second observing run. No significant candidates consistent with a sub-solar mass binary were identified. The null result places the tightest constraints to date on the merger rate and abundance of sub-solar mass ultracompact binaries. We describe an extension of our merger rate constraints to arbitrary populations and models under the assumption that the horizon distance controls the sensitivity of the search. We once more consider the merger rate constraints in the context of merging primordial black hole populations contributing to the dark matter [28]. We describe how to extend the dark matter fraction parameterization to other models by separating LIGO observables from model dependent quantities. Finally, we conclude with a discussion of the implications of this search.

5.2 Search

We analyze data obtained from November 30, 2016 to August 25, 2017 during Advanced LIGO's second observing run (O2).[1] Noise artifacts are linearly subtracted from the data; this includes strong sinusoidal features in both detectors due to injected calibration frequencies and the AC power grid, as well as laser beam jitter in the LIGO-Hanford detector data [216]. 117.53 days of coincident data remain after the application of data quality cuts [180, 181, 217–219]. The Advanced Virgo interferometer completed commissioning and joined Advanced LIGO in August 2017 for 15 days of triple coincident observation [194], however, we only report on the analysis of data obtained by the LIGO Hanford and LIGO Livingston interferometers.

The search was conducted using publicly available gravitational-wave analysis software [56, 58, 148, 149, 182–184]. The initial stage of the search performed a

[1]Data from Advanced LIGO's second observing run is available from the Gravitational Wave Open Science Center with and without noise sources linearly subtracted: `https://www.gw-openscience.org`

matched-filter analysis using a discrete bank of template waveforms generated using the TaylorF2 frequency-domain, post-Newtonian inspiral approximant. This waveform was chosen since negligible power is deposited in the merger and ringdown portion of the waveform for low-mass systems [220]. The template bank used for this search was designed to recover binaries with component masses of $0.19-2.0\,M_\odot$ and total masses of $0.4-4.0\,M_\odot$ in the detector frame with 97% fidelity, as in [28]. The search presented here, however, additionally includes spin effects in the modeling of the gravitational waveform. The bank is constructed to recover gravitational waves originating from binaries with component spins purely aligned or anti-aligned with the orbital angular momentum, and with dimensionless spin magnitudes of 0.1 or less. The inclusion of spin effects required denser placement of the waveforms in the template bank; the resulting bank had 992 461 templates, which is nearly twice as large as the non-spinning bank used in [28].

In order to reduce the computational burden, matched filtering was only performed for a subset of Advanced LIGO's full sensitive band [97]. The choice to only analyze the 45–1024 Hz band led to a detector averaged signal-to-noise ratio (SNR) loss of 8% when compared to the full $\sim 10-2048$Hz frequency band. This estimated SNR loss is a property of Advanced LIGO's noise curves and is independent of the templates used in the search; the discrete nature of the template bank causes an additional $\lesssim 3\%$ loss in SNR.

Gravitational-wave candidates that were found coincident in both the Hanford and Livingston detectors were ranked using the logarithm of the likelihood-ratio , $\mathcal{L}$ [56, 58, 182]. For a candidate with a likelihood-ratio of $\mathcal{L}^*$, we assign a false-alarm-rate of

$$\mathrm{FAR}(\log \mathcal{L}^*) = \frac{N}{T} P\left(\log \mathcal{L} \geq \log \mathcal{L}^* | \mathrm{noise}\right), \tag{5.1}$$

where N is the number of observed candidates, T is the total live time of the experiment, and $P\left(\log \mathcal{L} \geq \log \mathcal{L}^* | \mathrm{noise}\right)$ describes the probability that noise produces a candidate with a ranking statistic at least as high as the candidate's.

The search recovered the previously detected signal GW170817 [9], which was observed along with an electromagnetic counterpart [221]. This signal is consistent with a binary neutron star. No other viable gravitational wave candidates were identified. The next loudest candidate was identified by a template waveform with a chirp mass of $0.23\,M_\odot$ and a SNR of 9.5. The candidate was consistent with noise and assigned a FAR of 3.25 per year.

5.3 Constraint on binary merger rate

As in [28], we consider nine populations of equal mass, non-spinning binaries that are delta-function distributed in mass, i.e. $m_i \in \{0.2, 0.3, \ldots, 1.0\}$. We injected 913 931 fake signals into our data; the injections were randomly oriented and spaced uniformly in distance and isotropically across the sky. The recovered signals provide an estimate of the pipeline's detection efficiency as a function of source distance for each equal mass population. This in turn allows us to estimate the sensitive volume-time accumulated for each mass bin. We once more use the loudest event statistic formalism [23] to estimate the upper limit on the binary merger rate to 90% confidence,

$$\mathcal{R}_i = \frac{2.3}{\langle VT \rangle_i} \tag{5.2}$$

These upper limits are shown for equal mass binaries and as a function of chirp mass in Fig. 5.1. Although our template bank includes systems with total mass up to $4\,M_\odot$, we only place bounds on the merger rate of systems where both components are $\leq 1\,M_\odot$. We estimate that detector calibration uncertainties [194, 222, 223] and Monte Carlo errors lead to an uncertainty in our rate constraint of no more than 20%.

Advanced LIGO and Virgo's horizon distance scales as:

$$D_{\mathrm{horizon}} \propto \mathcal{M}^{5/6} \sqrt{\int_{f_{\mathrm{min}}}^{f_{\mathrm{max}}} \frac{f^{-7/3}}{S_n(f)}\, df} \tag{5.3}$$

where $S_n(f)$ is the noise spectra of the detector and f_{min} and f_{max} are 45 Hz and 1024 Hz, respectively.[2] For a null result, we therefore expect $\mathcal{R}(\mathcal{M}) \propto \mathcal{M}^{-15/6}$ provided the horizon distance controls the sensitivity of the search. The observed power law dependence of the rate constraint on the chirp mass is within $\sim 4\%$ of the expected $\mathcal{M}^{-15/6}$ dependence; this is well within the error bound on the rate upper limit and is strong evidence that the chirp mass is the primary parameter that dictates the sensitivity of the search. Therefore our upper limits from equal mass systems also apply to unequal mass systems within the range of mass ratios we

[2] The waveform model used to generate our template bank, TaylorF2, truncates the waveform at an upper frequency f_{ISCO}, which corresponds to radiation from the innermost stable circular orbit of a black hole binary with mass M_{total}. This frequency is above f_{max} for all non-spinning waveforms in our template bank and so does not impact D_{horizon}.

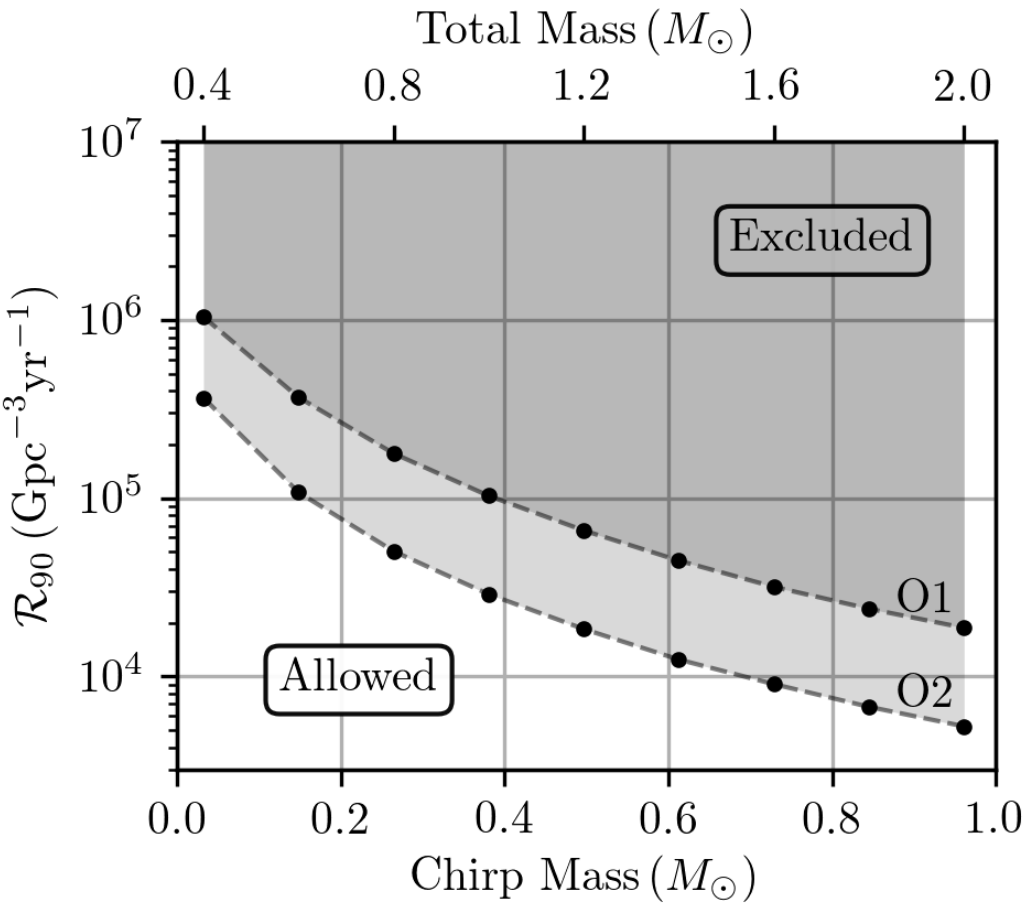

Figure 5.1: The constraint on the merger rate density for equal mass binaries as a function of total mass (top) and chirp mass (bottom). The two sets of lines show the constraints for the O1 search [28] and the O2 search presented here. The null result from O2 places bounds that are ~ 3 times tighter than the O1 results. The majority of this improvement is due to the increased coincident observing time in Advanced LIGO's second observing run (~ 118 days vs. ~ 48 days), though the improved sensitivity of the detectors led to an observed physical volume up to $\sim 50\%$ larger than in O1 for sub-solar mass ultracompact binaries.

have searched over. For verification, we performed a small injection campaign over five days of coincident data with injected component masses distributed between $0.19\,M_\odot$ and $2.0\,M_\odot$ with at least one component $< 1.0\,M_\odot$. The search sensitivity remained a function of the chirp mass; this implies that the rate constraints found from the equal mass injection sets can therefore be applied to systems with arbitrary

mass ratios provided that both component masses lie within $0.20\,M_\odot$ and $1.0\,M_\odot$ where our injection sets were performed.

The Advanced LIGO and Virgo rate upper limit can be expanded as:

$$\mathcal{R}(\mathcal{M}_1, \mathcal{M}_2) = \int_{\mathcal{M}_1}^{\mathcal{M}_2} \mathcal{R}(\mathcal{M}) \times \psi(\mathcal{M})\, \mathrm{d}\mathcal{M} \tag{5.4}$$

where $\mathcal{R}$ is the rate density as a function of chirp mass and $\psi(\mathcal{M})$ denotes the black hole population distribution in chirp mass. We ignore the effects of redshift due to the small detector range for sub-solar mass binaries. Setting $\psi(\mathcal{M}) = \delta(\mathcal{M})$ then reveals the form of the LIGO constraining rate density, $\mathcal{R}(\mathcal{M})$, which is shown in Figure 5.1. For a given model, $\psi(\mathcal{M})$, $\mathcal{R}(\mathcal{M}_1, \mathcal{M}_2)$ provides the LIGO rate constraint on that model for chirp masses between $\mathcal{M}_1$ and $\mathcal{M}_2$. The resulting rate constraints allow direct comparison of sub-solar mass ultracompact object models with LIGO observations.

5.4 General constraints on sub-solar mass black hole dark matter

We convert our limits on the merger rate of sub-solar mass ultracompact objects into a constraint on the abundance of primordial black holes using our fiducial formation model [154] first developed in [103, 152] and used previously in LIGO analyses [24,28]. We consider a population of equal mass primordial black holes that is created deep in the radiation era. We model the binary formation via three-body interactions, though others have considered the full field of tidal interactions [157]. By equating the model's predicted merger rate with the merger rate upper limit provided by Advanced LIGO and Virgo, we can numerically solve for the upper limit on the PBH abundance. These constraints are shown in Figure 5.2.[3]

This interpretation is highly model dependent; the mass distribution, binary fraction, and binary formation mechanisms all have a large effect on the expected present day merger rate and consequently the bounds on the primordial black hole

[3]The normalization of the PBH distribution used in our fiducial model [154] differs by a factor of 2 from the normalization in [103]. As such, our fiducial model (used here and in [28]) predicts a more conservative PBH merger rate and leads to less constraining limits on f_{PBH} than would be attained using the model of [103].

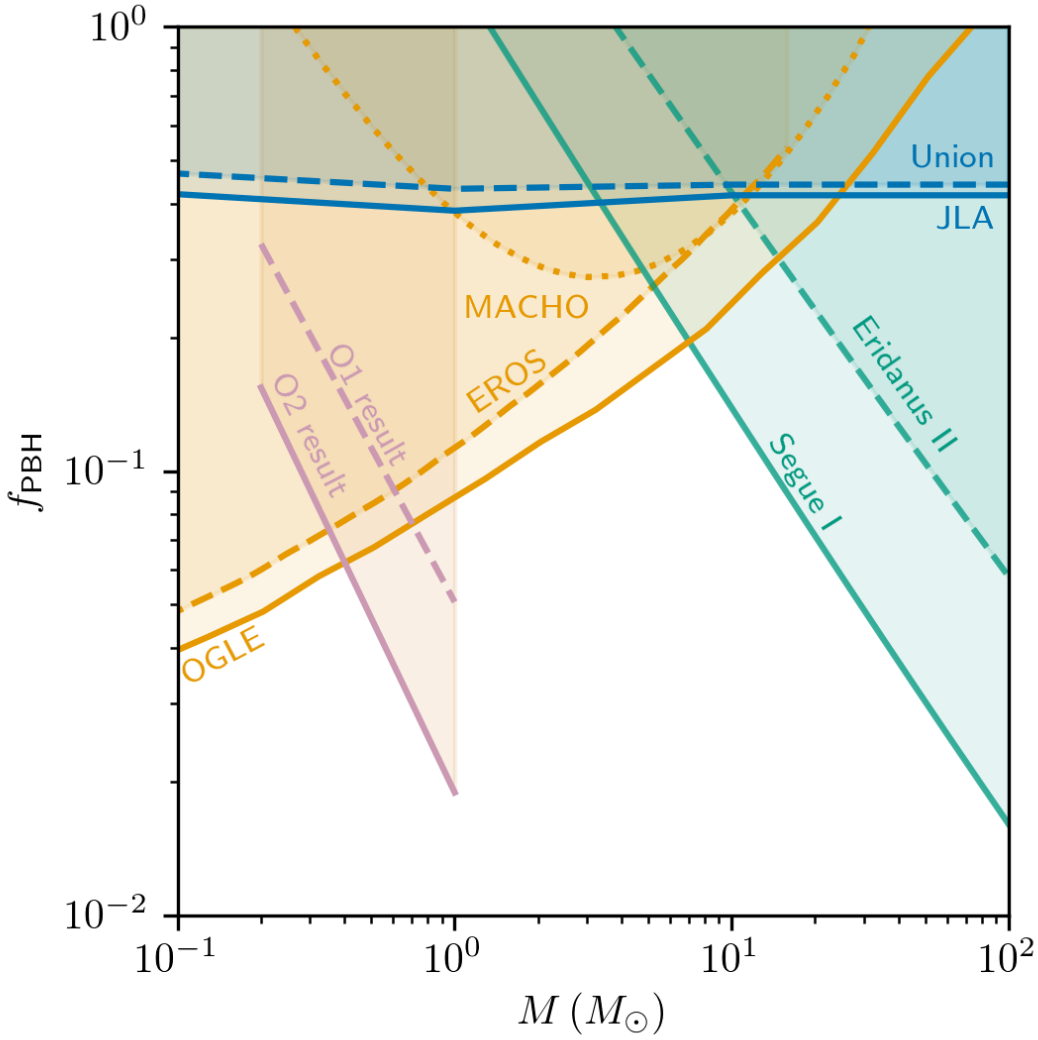

Figure 5.2: Constraints on the fraction of dark matter comprised of delta-function distributions of primordial black holes ($f_{\rm PBH} = \rho_{\rm PBH}/\rho_{\rm DM}$). Shown here are (pink) Advanced LIGO constraints from the O1 (dashed) and O2 ultracompact binary search presented here (solid), (orange) microlensing constraints provided by the OGLE (solid), EROS (dashed) [17], and MACHO (dotted) collaborations [18], (cyan) dynamical constraints from observations of Segue I (solid) [19] and Eridanus II (dashed) [20] dwarf galaxies, and (blue) supernova lensing constraints from the Joint Light-curve Analysis (solid) and Union 2.1 (dashed) datasets [26]. There is an inherent population model dependency in each of these constraints. Advanced LIGO and Advanced Virgo results carry an additional dependence on the binary fraction of the black hole population. Advanced LIGO and Advanced Virgo results use the Planck "TT,TE,EE+lowP+lensing+ext" cosmology [27].

composition of the dark matter. The Advanced LIGO and Virgo observables can be separated from the model dependent terms:

$$f_{\rm CO} = \frac{\rho_{\rm lim}}{\rho_{\rm CDM}} \times \frac{1}{f_{\rm obs}} = \frac{\mathcal{R}(M_{\rm tot})\, T_{\rm obs}\, M_{\rm tot}}{\rho_{\rm CDM}} \times \frac{1}{f_{\rm obs}}. \tag{5.5}$$

where $T_{\rm obs}$ is the duration of the observation (in the analysis presented here, 117.53 days). Here we use $f_{\rm CO}$ to refer to the dark matter fraction in ultracompact objects instead of $f_{\rm PBH}$ to emphasize that this is generally applicable to other compact object models that could contribute to the dark matter [150], and not just PBHs. The first term, $\rho_{\rm lim}/\rho_{\rm CDM}$, represents the upper limit on the fraction of the dark matter contained in presently merging sub-solar mass ultracompact binaries. In the second term, $f_{\rm obs}$ describes the fraction of sub-solar mass ultracompact objects that are observable by Advanced LIGO and Virgo for a particular model. This is set by the binary fraction and the probability density of binaries merging at present day. Note that the merger rate density must be converted from a function of chirp mass to total mass; this can be done by mapping to total mass for each mass ratio on an equal chirp mass curve.

Equation (5.5) applies to any dark matter model that predicts the formation of dark compact objects. The abundance of those dark compact objects can then be expressed as a fraction of the dark matter density.

5.5 Conclusion

We have presented the second Advanced LIGO and Advanced Virgo search for sub-solar mass ultracompact objects. No unambiguous sub-solar mass gravitational wave candidates were identified. The null result allows us to place tight constraints on the abundance of sub-solar mass ultracompact binaries.

This work represents an expansion of previous initial and Advanced LIGO and Advanced Virgo sub-solar mass searches. First, we have broadened the searched parameter space to increase sensitivity to systems with non-negligible component spins. Second, we have presented a method to extend our constraints on the binary merger rate to arbitrarily distributed populations that contain sub-solar mass ultracompact objects. Combined with the existing rate limits, this may already be enough to begin constraining collapsed particulate dark matter models [150] or

the cross section of nuclear interactions [151, 207–211]. Finally, we have provided a method to separate Advanced LIGO and Advanced Virgo observables from model dependent terms in our interpretation of the limits on primordial black hole dark matter.

Ground based interferometer searches for sub-solar mass ultracompact objects will continue to inform cosmological and particle physics scenarios. Advanced LIGO and Advanced Virgo have begun a year long observing run in early 2019, with improved sensitivities [47]. Advanced Virgo will have more coincident time with the Advanced LIGO detectors over its next observing run, which will improve network sensitivity and aid in further constraining the above scenarios.

5.6 Acknowledgments

The authors gratefully acknowledge the support of the United States National Science Foundation (NSF) for the construction and operation of the LIGO Laboratory and Advanced LIGO as well as the Science and Technology Facilities Council (STFC) of the United Kingdom, the Max-Planck-Society (MPS), and the State of Niedersachsen/Germany for support of the construction of Advanced LIGO and construction and operation of the GEO600 detector. Additional support for Advanced LIGO was provided by the Australian Research Council. The authors gratefully acknowledge the Italian Istituto Nazionale di Fisica Nucleare (INFN), the French Centre National de la Recherche Scientifique (CNRS) and the Foundation for Fundamental Research on Matter supported by the Netherlands Organisation for Scientific Research, for the construction and operation of the Virgo detector and the creation and support of the EGO consortium. The authors also gratefully acknowledge research support from these agencies as well as by the Council of Scientific and Industrial Research of India, the Department of Science and Technology, India, the Science & Engineering Research Board (SERB), India, the Ministry of Human Resource Development, India, the Spanish Agencia Estatal de Investigación, the Vicepresidència i Conselleria d'Innovació, Recerca i Turisme and the Conselleria d'Educació i Universitat del Govern de les Illes Balears, the Conselleria d'Educació, Investigació, Cultura i Esport de la Generalitat Valenciana, the National Science Centre of Poland, the Swiss National Science Foundation (SNSF), the Russian Foundation for Basic Research, the Russian Science Foundation, the European

Commission, the European Regional Development Funds (ERDF), the Royal Society, the Scottish Funding Council, the Scottish Universities Physics Alliance, the Hungarian Scientific Research Fund (OTKA), the Lyon Institute of Origins (LIO), the Paris Île-de-France Region, the National Research, Development and Innovation Office Hungary (NKFI), the National Research Foundation of Korea, Industry Canada and the Province of Ontario through the Ministry of Economic Development and Innovation, the Natural Science and Engineering Research Council Canada, the Canadian Institute for Advanced Research, the Brazilian Ministry of Science, Technology, Innovations, and Communications, the International Center for Theoretical Physics South American Institute for Fundamental Research (ICTP-SAIFR), the Research Grants Council of Hong Kong, the National Natural Science Foundation of China (NSFC), the Leverhulme Trust, the Research Corporation, the Ministry of Science and Technology (MOST), Taiwan and the Kavli Foundation. The authors gratefully acknowledge the support of the NSF, STFC, MPS, INFN, CNRS and the State of Niedersachsen/Germany for provision of computational resources. Computing resources and personnel for this project were provided by the Pennsylvania State University. This article has been assigned the document number LIGO-P1900037.

Chapter 6
Sub-threshold binary neutron star search in advanced LIGO's first observing run

6.1 Motivation

Multi-messenger astrophysics (MMA) informed by GW observations is the future of time domain astronomy. The coincident detection of messengers across distinct astrophysical channels provides a breadth of information inaccessible to independent observations. Candidate GWs especially benefit from coincidence with electromagnetic radiation, which informs the distance, location, orientation, and material composition of the source. GW170817 is a shining realization of how MMA can maximize the scientific output of GW discoveries. The coincident detection of GWs and prompt gamma ray emission placed new constraints on the speed of gravity [224], and subsequent optical measurements localized the host galaxy and provided an independent measurement of the Hubble constant [76]. Despite the

successes surrounding GW170817, it is intriguing to wonder what remains to be discovered in the ∼11 hours between gamma ray observations and those at other wavelengths [225] since the prompt emission encodes the initial conditions of the outflow and the remnant object. Early optical and ultraviolet observations are necessary to further inform our understanding of r-process nucleosynthesis [226] and shock-heated ejecta [227]. Prompt X-ray emission would reveal the final state of the system and uncover whether the remnant undergoes prompt collapse to a black hole or forms a supramassive neutron star [228–230]. This is especially important since GW analyses may remain unable to infer the remnant's state until the next generation of detectors comes online [231].

Other Advanced LIGO sources are also expected to produce electromagnetic radiation observable by current telescopes. If the neutron star in a NSBH binary can be tidally disrupted by the black hole, then a disk can form and later undergo nuclear reactions to produce electromagnetic transients. The disk formation is closely tied to the neutron star equation of state, black hole spin, and mass ratio of the system since the neutron star must not plunge directly into the black hole, and electromagnetic observations could inform our current understanding of how the remnant baryon mass affects the spectrum [232]. Additionally, although BBHs do not contain free matter, it is possible that the environment radiates near merger and produces a short gamma ray burst [233] or optical transients [234]. A gamma ray burst near the time of GW150914 inspired several searches for coincident radiation, [235–237].

One way to add to our catalog of multi-messenger discoveries is by comparing subthreshold candidates across various astrophysical messengers. Temporal and/or spatial coincidence would elevate the joint significance of the combined event. To encourage searches for quiet multi-messenger events, I led a sub-threshold search for binary neutron star systems. This work is detailed in the remainder of Chapter 6.

There are clearly tremendous scientific benefits associated with capturing prompt electromagnetic emission from GW sources, and developing technology to better inform observers is crucial. Much of the existing electromagnetic infrastructure is aging and time on the next generation of observatories, such as the Vera C. Rubin Observatory, will be highly sought after. Advanced LIGO must provide as much useful and reliable information as possible in order to command follow-up time and warrant the efforts of the electromagnetic community. I have worked to

facilitate MMA through the development of early warning detection capabilities for BNS systems. My contributions to early warning detection efforts are described in Chapter 7.

6.2 Abstract

We present a search for gravitational waves from double neutron star binaries inspirals in Advanced LIGO's first observing run. The search considers a narrow range of binary chirp masses motivated by the population of known double neutron star binaries in the nearby universe. This search differs from previously published results by providing the most sensitive published survey of neutron stars in Advanced LIGO's first observing run within this narrow mass range and including times when only one of the two LIGO detectors was in operation in the analysis. The search was sensitive to binary neutron star inspirals to an average distance of $\sim 85\,\mathrm{Mpc}$ over 93.2 days. We do not identify any unambiguous gravitational wave signals in our sample of 103 sub-threshold candidates with false-alarm-rates of less than one per day. However, given the expected binary neutron star merger rate of $\mathcal{R} \approx 100 - 4000\,\mathrm{Gpc}^{-3}\,\mathrm{yr}^{-1}$, we expect $\mathcal{O}(1)$ gravitational wave events within our candidate list. This suggests the possibility that one or more of these candidates is in fact a binary neutron star merger. Although the contamination fraction in our candidate list is $\sim 99\%$, it might be possible to correlate these events with other messengers to identify a potential multi-messenger signal. We provide an online candidate list with the times and sky locations for all events in order to enable multi-messenger searches.

6.3 Introduction

Advanced LIGO [45] conducted its first observing run (O1) from September 12, 2015 to January 19, 2016. Previous analyses of the 51.5 days of coincident LIGO Hanford and LIGO Livingston data led to three detections of binary black hole mergers [31, 134, 138, 160, 194]. No binary neutron star (BNS) or neutron-star, black-hole (NSBH) systems were observed [141] in O1. We revisit this data with a gravitational wave search targeted at binary neutron star masses and provide a list of candidate events. Searches that catalog low signal-to-noise ratio (SNR) events

probe significantly deeper into the cosmos. At low SNR it can be difficult to claim an unambiguous detection, but the multi-messenger nature of BNS systems [221] can be leveraged to identify authentic gravitational wave events. Comparisons of catalogs provide a discovery space for a host of multi-messenger signals [238, 239]. Temporal and/or spatial coincidences between candidates in distinct astrophysical channels could strongly support a multi-messenger discovery. Another potential application of this candidate list is to investigate fast radio bursts (FRB). Some FRB origin theories are based on BNS merger and thought to be associated with GWs as well [240–242]. FRBs are detected with accuracies of milliseconds, potentially allowing very tight coincidence windows in correlation studies between this catalog and arrival times of FRBs. This paper will take the lead in this future gravitational wave follow-up search.

Most LIGO analyses have required two detectors to identify candidate gravitational wave events [243]. In Advanced LIGO's first observing run, this requirement excluded nearly half of the available data[1] from analysis [138]. Previous compact binary coalescence (CBC) searches using prototype LIGO [43] and TAMA300 [42] data analyzed single detector time. In O1, the PyCBC pipeline [63, 196, 244] cataloged single detector triggers primarily for detector characterization purposes, and the search for gravitational waves associated with gamma-ray bursts [245] also analyzed times with one operating interferometer. In Advanced LIGO's second observing run, GW170817 was first identified as a LIGO Hanford trigger by the GstLAL online pipeline with an estimated false-alarm-rate of ~ 1 / 9000 years [246]. PyCBC Live also produced single detector online triggers in O2 [247]. We include single interferometer data in our search, and we assign significances to O1 single detector candidates for the first time, although we note that others have previously suggested methods to rank these candidates [58, 248, 249].

1-OGC [31] recently provided a catalog of gravitational wave candidates in O1 data obtained via the Gravitational Wave Open Science Center (GWOSC)[2] [250]. The search presented here differs in several major ways. First, we target binary neutron star systems exclusively by applying a mass model to increase sensitivity to those systems [251, 252]. Second, we use a denser grid of template waveforms to minimize signal loss caused by the discrete nature of the template bank [253].

[1]Data that passes Category 1 data quality checks. These DQ cuts eliminate $\sim 6\%$ of coincident time.

[2]`https://www.gw-openscience.org/`

Third, we include an additional 44.5 days of single detector time in our analysis to increase the analyzed time and improve the sensitivity of the search. Fourth, we include additional coincident data that was not analyzed in 1-OGC. Finally, we include all candidates with false-alarm-rates less than one per day in our list and we provide BAYESTAR [254] sky localization estimates for each candidate to encourage multi-messenger followup surveys.

6.4 Search Description

We used the GstLAL-based inspiral pipeline to conduct a matched-filter analysis [56, 58,183,184,255–257] of data provided by GWOSC and spanning September 12, 2015 to January 19, 2016. GWOSC data is only available for times that pass Category 1 data quality checks [180], leaving 48.6 days of coincident data and 44.5 days of single detector data. We exclude times known to have hardware injections from our analysis and apply no additional data quality cuts. Additional information on the data quality and hardware injections is available via GWOSC.

6.4.1 Template bank

Matched-filter based analyses correlate the data with a discrete bank of template waveforms [149, 258, 259] that model the gravitational wave emission of compact binaries [260–262]. The template bank used for this search was designed to maximize sensitivity to BNS mergers with component masses and spins motivated by double neutron star binary observations [9,263,264]. For astrophysical reasons, we consider component spins that are purely aligned or anti-aligned with the orbital angular momentum, and we limit the dimensionless spin magnitude to be ≤ 0.05 [265]. We model the component masses of our target population with a Gaussian distribution where $\bar{m} = 1.33M_{\odot}$, $\sigma = 0.05M_{\odot}$ [263]. We consider three standard deviations in mass and transform coordinates from component mass to chirp mass, $\mathcal{M} = (m_1 m_2)^{3/5}/(m_1 + m_2)^{1/5}$, as the chirp mass is the primary parameter that affects the gravitational wave signal [266]. We broaden the resulting chirp mass distribution to allow for statistical errors in our measurements and we increase the mean of the distribution to account for redshift. This results in a bank that covers detector frame chirp masses of $\mathcal{M} \in (1.04M_{\odot}, 1.36M_{\odot})$.

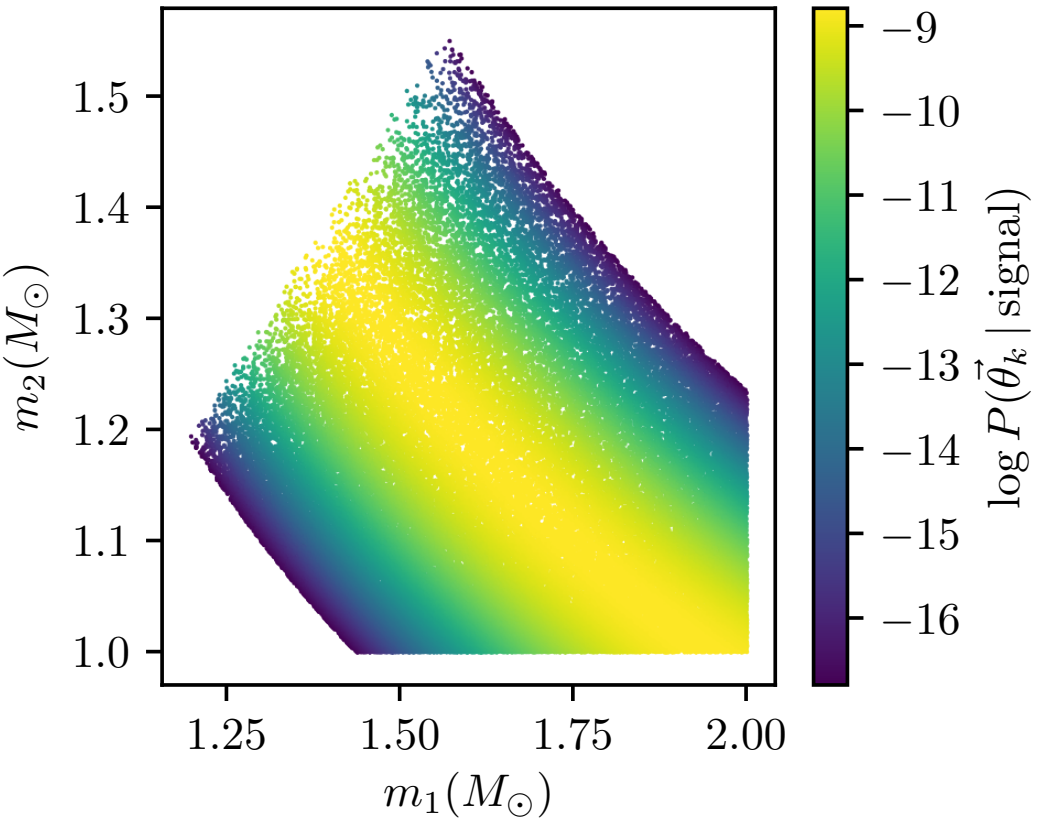

Figure 6.1: The template bank used for this search as depicted in component masses, m_1, m_2, where $m_1 > m_2$. The colors represent the logarithm of probability that a signal is recovered by a template t_k (with parameters $\vec{\theta}$); for this search, we have chosen a BNS population model with a mean mass of $\bar{m} = 1.33 M_\odot$ and a standard deviation of $\sigma = 0.05 M_\odot$. The population model considers three standard deviations in chirp mass. Although this population model neglects effects due to redshift, redshift effects are considered when we estimate the sensitivity of the search.

The final bank of 65 634 template waveforms was constructed with the `TaylorF2` approximant and a minimum match of .99, which ensures that signals with arbitrary parameters have a 99% match with at least one template in the bank. This high precision limits the loss of signals due to using a discrete template bank to $\sim 3\%$; previous searches in O1 data have used template banks that allowed signal loss up to $\lesssim 10\%$ [31, 196, 267].

6.4.2 Estimating significance of events

We use a likelihood-ratio statistic, $\mathcal{L}$, to rank candidate events by their SNR, an autocorrelation based signal consistency check, the sensitivity of each detector at the time of the candidate, and the time and phase delays between different gravitational wave observatories [56–58, 248, 251, 268, 269]. In addition we include an astrophysical prior, which provides the probability that a signal from a BNS source population is recovered by a particular template in the bank [252]. The template bank and the prior probabilities associated with each template are shown in Fig. 6.1.

Candidate events are assigned a false-alarm-rate that describes how often a candidate with a likelihood-ratio statistic at least as high as its own is expected to occur; the false-alarm-rate thus acts as a measure of how often the noise can be expected to produce a candidate with similar properties. The first gravitational wave detections had an extremely low false-alarm-rate (less than 1 / 100,000 years). Here we are interested in digging considerably deeper into the noise probing events with false-alarm-rates as high as 1 / day.

To estimate the false-alarm-rate for candidate events, we use triggers not found in temporal coincidence between the interferometers when both LIGO detectors were operating to estimate the background of noise-like events [58, 251, 270]. Single detector events also have their background estimated from the set of non-coincident triggers found when both LIGO detectors were operating, which amounts to 48.6 days of data. We estimate our background from the 48.6 days of coincident data. When a single detector candidate has a higher likelihood ratio than any candidate in the background, we bound its false-alarm-rate to 1 / 48.6 days.

6.4.3 Estimating the sensitivity of the search

The search sensitivity was estimated via Monte Carlo methods. We first generated a set of BNS signals arising from systems with parameters consistent with local populations — we chose a Gaussian distribution for component masses with $m_{\rm mean} = 1.33 M_\odot, \sigma_m = 0.05 M_\odot$ and an isotropic distribution for spin. The injected population was modeled to a redshift of $z = 0.2$, and probed a space-time volume of $0.77\,{\rm Gpc}^3\,{\rm yr}$. We rejected 17 738 506 simulated signals which had SNRs below 3 to reduce the number of compute cycles. The remaining 112 073 fake signals were

injected into the data and subsequently searched for by the detection pipeline. At a given false-alarm-rate threshold, we estimate the overall sensitivity of the search via:

$$\langle VT \rangle = \langle VT_{\text{injected}} \rangle \frac{N_{\text{recovered}}}{N_{\text{total sims}}} \tag{6.1}$$

where $N_{\text{recovered}}$ varies with the false-alarm-rate threshold. This search is approximately 30% more sensitive at the 1 / 100 year threshold than the previous BNS search presented at the end of Advanced LIGO's first observing run [141]. The inclusion of single detector time in our analysis leads to a $\sim 33\%$ improvement in our estimated $\langle VT \rangle$ at the 1 / day level.

6.5 Results

We find no unambiguous gravitational wave events, but we identify 103 candidates with false-alarm-rates less than one per day. We provide the time, SNR, and false-alarm-rate of each candidate in Table 6.1, as well as the probability that the candidate is astrophysical in origin (p_a). We compute p_a using FGMC methods [248, 271]. When the p_a assigned to single detector candidates via FGMC exceeds the estimated single detector p_a bound in [249], we substitute the lower bound. The associated source parameters and sky localization estimates obtained via BAYESTAR [254] are provided on the LIGO Document Control Center at `https://dcc.ligo.org/public/0158/P1900030/001/index.html`.

Date	FAR (yr^{-1})	SNR	p_a
2015-09-14T18:35:13.66^{H}	145.45	8.59	3.75×10^{-3}
2015-09-18T06:38:39.21	261.92	8.04	2.18×10^{-3}
2015-09-18T22:47:27.39†	193.46	8.52	2.92×10^{-3}
2015-09-19T00:05:01.08	326.71	7.63	1.78×10^{-3}
2015-09-21T10:10:02.92^{H}	7.52	8.10	6.95×10^{-2}
2015-09-22T11:26:08.35	312.67	8.61	1.86×10^{-3}
2015-09-23T13:47:35.79	165.39	8.56	3.38×10^{-3}
2015-09-24T00:53:02.68	19.68	8.45	2.29×10^{-2}
2015-09-24T05:57:35.24	107.32	8.71	4.88×10^{-3}

2015-09-25T01:24:33.74	56.59	9.15	8.73×10^{-3}
2015-09-25T21:15:15.92	38.39	8.58	1.25×10^{-2}
2015-09-26T23:51:25.50	56.05	8.39	8.81×10^{-3}
2015-09-27T14:28:55.77	243.80	8.60	2.32×10^{-3}
2015-09-29T01:46:01.42†	251.32	8.50	2.26×10^{-3}
2015-09-29T12:25:33.33	358.03	8.64	1.62×10^{-3}
2015-10-01T00:21:02.89	293.57	8.70	1.97×10^{-3}
2015-10-01T05:32:40.37	15.49	8.94	2.83×10^{-2}
2015-10-02T01:49:03.99	118.27	9.21	4.49×10^{-3}
2015-10-02T04:01:03.45	190.83	8.99	2.96×10^{-3}
2015-10-04T22:32:11.75^{H}	30.52	8.17	1.53×10^{-2}
2015-10-05T07:12:04.91	104.11	8.46	5.02×10^{-3}
2015-10-05T22:29:34.31	139.59	8.24	3.88×10^{-3}
2015-10-09T23:08:05.70	292.60	8.19	1.98×10^{-3}
2015-10-12T02:40:22.39	142.27	8.42	3.82×10^{-3}
2015-10-12T14:26:43.18	322.93	8.35	1.80×10^{-3}
2015-10-13T14:29:57.73^{H}	37.36	9.02	1.28×10^{-2}
2015-10-14T05:29:42.91†	149.36	8.75	3.68×10^{-3}
2015-10-18T19:03:46.85^{H}	7.52	8.05	0.181
2015-10-19T17:37:05.25	124.01	8.78	4.30×10^{-3}
2015-10-24T09:01:50.34^{L}	94.09	10.56	5.53×10^{-3}
2015-10-24T09:03:52.00^{L}	7.52	9.69	7.96×10^{-2}
2015-10-24T19:53:05.66	360.26	8.57	1.61×10^{-3}
2015-10-28T12:24:31.67^{H}	7.52	9.06	0.181
2015-10-28T17:03:45.19†	16.08	8.82	2.74×10^{-2}
2015-10-28T17:05:21.17†	0.78	10.63	0.289
2015-10-29T08:27:29.92	345.02	9.04	1.68×10^{-3}
2015-10-29T11:48:01.64	58.64	8.78	8.45×10^{-3}
2015-10-29T12:05:48.00	363.99	8.24	1.59×10^{-3}
2015-10-29T19:18:33.06	193.47	8.26	2.92×10^{-3}
2015-10-30T00:08:56.47	358.38	8.55	1.62×10^{-3}
2015-10-30T04:08:58.11	240.56	8.44	2.35×10^{-3}
2015-10-31T10:27:43.77	320.37	8.05	1.81×10^{-3}
2015-10-31T11:30:36.72	329.59	8.35	1.76×10^{-3}

2015-10-31T22:01:00.91^{L}	331.06	7.97	1.76×10^{-3}
2015-11-01T11:13:23.94^{L}	12.17	8.65	3.50×10^{-2}
2015-11-04T13:37:23.67†	103.50	8.43	5.05×10^{-3}
2015-11-04T15:16:09.12†	69.89	9.12	7.23×10^{-3}
2015-11-05T06:20:44.61	312.42	8.56	1.86×10^{-3}
2015-11-06T07:44:18.43	95.56	8.42	5.45×10^{-3}
2015-11-06T10:07:13.79†	172.79	8.55	3.25×10^{-3}
2015-11-06T11:05:19.24	211.28	9.18	2.67×10^{-3}
2015-11-06T22:32:34.11	190.79	8.33	2.96×10^{-3}
2015-11-10T00:32:55.28†	313.96	8.86	1.85×10^{-3}
2015-11-12T20:56:57.33	287.61	8.63	2.01×10^{-3}
2015-11-15T20:03:17.46	26.66	8.35	1.73×10^{-2}
2015-11-15T23:04:35.21	359.97	8.42	1.61×10^{-3}
2015-11-16T10:59:11.86	189.42	8.24	2.98×10^{-3}
2015-11-17T06:34:02.07^{H}	7.52	8.84	0.181
2015-11-20T21:07:08.38†	15.60	8.95	2.81×10^{-2}
2015-11-21T22:26:44.55	104.06	8.65	5.02×10^{-3}
2015-11-26T13:34:13.65	6.09	8.68	6.23×10^{-2}
2015-11-28T08:29:19.80	229.16	8.16	2.46×10^{-3}
2015-11-28T14:05:27.32	128.85	8.55	4.16×10^{-3}
2015-11-29T03:39:34.71	250.42	9.27	2.27×10^{-3}
2015-12-02T10:45:49.81	201.50	9.24	2.80×10^{-3}
2015-12-02T15:17:48.11	308.63	9.28	1.88×10^{-3}
2015-12-02T17:38:00.95†	363.08	8.14	1.60×10^{-3}
2015-12-03T20:18:18.94	110.58	8.37	4.76×10^{-3}
2015-12-04T01:53:39.14	225.02	9.09	2.50×10^{-3}
2015-12-04T21:14:59.74†	8.89	9.04	4.57×10^{-2}
2015-12-05T10:16:47.45	284.26	8.59	2.03×10^{-3}
2015-12-06T06:50:38.17^{L}	77.45	7.72	6.64×10^{-3}
2015-12-08T09:27:47.71	344.81	8.27	1.68×10^{-3}
2015-12-08T13:22:36.24	47.36	8.76	1.03×10^{-2}
2015-12-09T07:25:24.68	141.65	7.85	3.84×10^{-3}
2015-12-14T18:15:44.85	145.53	8.43	3.75×10^{-3}
2015-12-14T19:32:20.42	145.58	8.72	3.75×10^{-3}

2015-12-15T06:04:29.41	20.34	8.49	2.23×10^{-2}
2015-12-15T10:53:01.22	154.61	8.78	3.58×10^{-3}
2015-12-18T00:56:19.12	83.80	8.19	6.19×10^{-3}
2015-12-18T09:59:11.16	147.23	8.71	3.72×10^{-3}
2015-12-20T05:33:58.81	300.99	7.86	1.92×10^{-3}
2015-12-22T10:08:48.42	234.05	9.22	2.41×10^{-3}
2015-12-23T00:07:10.93	18.95	8.99	2.36×10^{-2}
2015-12-23T12:23:35.72	60.11	10.25	8.26×10^{-3}
2015-12-23T13:50:49.48	178.46	8.00	3.16×10^{-3}
2015-12-23T16:13:55.82	290.02	8.98	1.99×10^{-3}
2015-12-24T23:05:56.58	47.49	10.08	1.03×10^{-2}
2015-12-24T23:06:28.51	146.99	9.55	3.72×10^{-3}
2015-12-24T23:06:57.04	70.65	9.42	7.16×10^{-3}
2015-12-25T02:16:31.87	320.05	8.49	1.82×10^{-3}
$2015\text{-}12\text{-}28T21{:}04{:}05.90^{H}$	160.93	8.57	3.46×10^{-3}
$2015\text{-}12\text{-}29T11{:}50{:}15.09^{H}$	234.41	8.23	2.41×10^{-3}
$2015\text{-}12\text{-}31T11{:}20{:}54.32^{H}$	180.00	8.82	3.13×10^{-3}
2016-01-02T02:47:29.35	356.13	7.51	1.63×10^{-3}
2016-01-02T02:54:39.60	239.65	8.11	2.36×10^{-3}
$2016\text{-}01\text{-}03T02{:}29{:}54.78^{\dagger}$	237.44	8.56	2.38×10^{-3}
2016-01-03T17:23:13.26	208.47	8.91	2.70×10^{-3}
2016-01-08T09:21:19.61	136.59	8.89	3.95×10^{-3}
$2016\text{-}01\text{-}08T10{:}09{:}33.90^{\dagger}$	218.62	8.52	2.58×10^{-3}
2016-01-12T05:19:01.34	107.14	8.34	4.89×10^{-3}
2016-01-15T08:37:05.94	328.35	8.19	1.77×10^{-3}
$2016\text{-}01\text{-}19T05{:}40{:}13.04^{\dagger}$	228.18	8.85	2.47×10^{-3}

Table 6.1: Binary neutron star triggers from Advanced LIGO's first observing run with a false-alarm-rate (FAR) less than one per day. We provide the time of coalesence, false-alarm-rate, SNR, and astrophysical probability (p_a) for each candidate. Events marked by H, L were found as single-detector triggers in LIGO-Hanford or LIGO-Livingston, respectively. Events marked by a † occurred within 0.01 seconds of a trigger in 1-OGC [31]. We expect $\mathcal{O}(1)$ of these candidates to be gravitational waves.

Although we cannot identify any one candidate from our list as astrophysical, we

can estimate the number of true signals buried in the list from our search sensitivity and the expected binary neutron star merger rate. At a false-alarm-rate threshold of 1 / day, we estimate $\langle VT \rangle = 6.7 \times 10^5\,\mathrm{Mpc}^3\,\mathrm{yr}$. The LIGO Scientific Collaboration recently estimated the local merger rate of binary neutron star systems to be $\mathcal{R} \approx 100 - 4000\,\mathrm{Gpc}^{-3}\,\mathrm{yr}^{-1}$ at 90% confidence [194]; we adopt a nominal value of $1000\,\mathrm{Gpc}^{-3}\,\mathrm{yr}^{-1}$. We therefore expect that $\langle VT \rangle \times \mathcal{R} = 0.67^{+2.0}_{-.60}$ of the candidates presented here are gravitational wave signals from binary neutron star coalescences. We stress that although the number of expected events depends on uncertainties in both $\langle VT \rangle$ and $\mathcal{R}$, the expected number remains at most $\mathcal{O}(1)$.

A single signal in our candidate list would imply a contamination fraction of 99%. We provide the coalescence times in Table 6.1 and approximate sky localizations online to encourage multi-messenger searches that have the ability to illuminate true signals buried in the candidate list.

6.6 Discussion

We have presented a search for gravitational waves from BNS mergers. Although no gravitational wave signal was clearly identified in either single or double interferometer time, we have provided a list of candidate events with false-alarm-rates less than one per day. The parameters for this search overlap with those of gravitational wave catalogs GWTC-1 [194] and 1-OGC [31]. No shared events are found between this candidate list and GWTC-1. While the GstLAL pipeline identified a low-mass marginal candidate, 151012A, in GWTC-1, the detector frame chirp mass is not covered by the bank used here. We note that five single detector candidates meet the selection criteria for inclusion in GWTC-1 [194].

For 1-OGC, we define overlapping candidates as those that share coalescence times to a precision of two decimal places as differences between the pipelines and the template banks can account for small differences in the measured time of arrival. We find 15 BNS candidates in common with 1-OGC. This is not unexpected; 1-OGC has a trigger rate of ~ 270 per day in the overlapping region of the searched parameter space. They do not assign any of the overlapping candidates a false-alarm-rate of less than one per day. The variation in estimated false-alarm-rates can arise from differences in the pipelines, template banks, and mass models used in the searches.

In the hopes of enabling multi-messenger, sub-threshold follow-up, we have also provided the coalescence times and sky localizations of the 103 candidates with false-alarm-rates less than 1 / day. The analysis of single detector time yielded 15 of the 103 candidates presented in our list, and nearly half of the analyzed data was obtained during times at which only one detector was operating; this highlights the importance of continuing to analyze single interferometer time in future gravitational wave searches.

6.7 Acknowledgments

We thank Peter Shawhan, Thomas Dent, and Jonah Kanner for useful feedback and discussion. This work was supported by the National Science Foundation through PHY-1454389, OAC-1841480, PHY-1700765, and PHY-1607585. Computations for this research were performed on the Pennsylvania State University's Institute for CyberScience Advanced CyberInfrastructure (ICS-ACI). This research has made use of data, software and/or web tools obtained from the Gravitational Wave Open Science Center (`https://www.gw-openscience.org`), a service of LIGO Laboratory, the LIGO Scientific Collaboration and the Virgo Collaboration. LIGO is funded by the U.S. National Science Foundation. Virgo is funded by the French Centre National de Recherche Scientifique (CNRS), the Italian Istituto Nazionale della Fisica Nucleare (INFN) and the Dutch Nikhef, with contributions by Polish and Hungarian institutes. SRM thanks the LSSTC Data Science Fellowship Program, which is funded by LSSTC, NSF Cybertraining Grant-1829740, the Brinson Foundation, and the Moore Foundation. Funding for this project was provided by the Charles E. Kaufman Foundation of The Pittsburgh Foundation. SC is supported by the research programme of the Netherlands Organisation for Scientific Research (NWO). HF acknowledges support from the Natural Sciences and Engineering Research of Council of Canada (NSERC) and the Japan Society for the Promotion of Science (JSPS). This paper has been assigned the document number LIGO-P1800401.

Chapter 7
First demonstration of early warning gravitational wave alerts

The following chapter is a pre-print of an article with permission from co-authors: (https://arxiv.org/abs/2102.04555): Ryan Magee et al.

7.1 Abstract

Gravitational-wave observations became commonplace in Advanced LIGO-Virgo's recently concluded third observing run. 56 non-retracted candidates were identified and publicly announced in near real time. Gravitational waves from binary neutron star mergers, however, remain of special interest since they can be precursors to high-energy astrophysical phenomena like γ-ray bursts and kilonovae. While late-time electromagnetic emissions provide important information about the astrophysical processes within, the prompt emission along with gravitational waves uniquely reveals the extreme matter and gravity during - and in the seconds following - merger. Rapid communication of source location and properties from the gravitational-wave data is crucial to facilitate multi-messenger follow-up of such sources. This is especially enabled if the partner facilities are forewarned via an *early-warning* (pre-merger) alert. Here we describe the commissioning and performance of such a low-latency infrastructure within LIGO-Virgo. We present results from an end-to-end mock data challenge that detects binary neutron star mergers and alerts partner facilities before merger. We set expectations for these alerts in future

observing runs.

7.2 Introduction

The field of gravitational-wave astronomy has exploded in the years following the first direct observation of gravitational waves (GWs) from a binary black hole (BBH) merger [160]. Since then, LIGO-Virgo have published 49 candidate events, many of which were identified in low-latency[1]; these include 2 BNS and 2 neutron star–black hole (NSBH) candidates [2]. The detection of GWs from compact binaries, especially from BBHs, has become routine. GWs from BNS and NSBH mergers, however, remain rare. BNS and NSBH mergers are of special interest due to the possibility of counterpart electromagnetic (EM) signals. For BNS mergers in particular, it has long been hypothesized that the central engine (post-merger) can launch short gamma-ray bursts (SGRBs) [272, 273], kilonovae [274, 275], and radio waves and X-rays post merger [276, 277]. In the special case of the presence of a magnetized NS, it can also lead to GRB precursors before the merger [278].

Although the improvement in Advanced LIGO-Virgo's sensitivity was paralleled by analogous advancements in the field of time-domain astronomy, the first observed BNS merger, GW170817 [9], remains the only realization of multi-messenger astronomy (MMA) with GWs. The coincident observation of GWs followed by an SGRB, GRB 170817A, and the kilonova AT 2017gfo, [221] bore evidence to the several-decade-old hypothesis that compact object mergers were progenitors of these exotic transients. The joint observations also contributed greatly to our understanding of fundamental physics [224, 279] and astrophysical processes associated with extreme environments [226, 280]. Despite the plethora of late-time observations made starting ~ 8 hours after coalescence [221], observations of the prompt spectra were precluded by non-stationarities in the LIGO Livingston interferometer and delays in Virgo data transfer. The alert and sky localization were distributed to partner observatories ~ 40 minutes [281] and ~ 5 hours [282], respectively, after the signal arrived at the detectors; by this time, the source had set below the horizon for northern hemisphere telescopes. The circumstances surrounding this delay were unusual, but it is crucial for LIGO-Virgo to distribute alerts as quickly as possible to maximize the chance of additional multi-messenger observations.

[1] Some of the 56 have not yet appeared in a LIGO-Virgo publication.

The serendipitous discovery of GRB 170717A by Fermi and INTEGRAL show the importance of catching the prompt EM emission to our understanding of merging compact binaries. EM observatories have begun to develop capacity to perform targeted observations in response to preliminary Gamma-ray Coordinates Network (GCN) notices produced by pre-merger detections. For example, the Murchison Wide-Field Array (MWA) radio telescope has a large field of view ideally suited to searching for precursor and prompt radio emission from GW sources and an established observing plan to respond to pre-merger detections [283]. *Swift*-BAT has recently also demonstrated the potential to respond autonomously to extremely low-latency triggers in the future, with the introduction of an on-board sub-threshold trigger recovery algorithm (GUANO, [284]). By the beginning of Advanced LIGO-Virgo's fourth observing run (O4), it is expected that established missions and observatories will be joined by next generation facilities like the Rubin Observatory [285]. This greatly improves the chances of performing targeted followup observations of prompt, or even precursor [286,287], emission from compact binary mergers provided that pre-merger alerts can be issued.

LIGO-Virgo has since streamlined the alert process (see Fig. 7.3). Advanced LIGO's and Advanced Virgo's third observing run (O3) saw the dawn of autonomously distributed Preliminary GCN Notices [288][2], which allowed LIGO-Virgo to notify the world of candidate signals within 7.0^{+92}_{-4} minutes[3] of observation. To further enable EM-GW observations, we can leverage the long-lived nature of BNSs in the sensitive band of advanced ground-based GW detectors to make pre-merger detections [182, 289]. This was recently demonstrated by [290] and [291]. The early detection and communication of GWs from BNSs aims to facilitate EM follow-up efforts by further reducing the latency of alerts and improving prospects of capturing the initial spectra.

In this letter we describe the commissioning and performance of the low-latency sub-system within Advanced LIGO-Virgo that is able to provide pre-merger alerts for electromagnetically bright compact binaries. We begin by describing the end-to-end low-latency workflow in Section 7.3, from the time of data acquisition to the dissemination of public alerts. We then assess the performance of a subset of this infrastructure in a mock data challenge described in Section 7.4, with special

[2] `https://gcn.gsfc.nasa.gov/`

[3]The 95% reported here is severely impacted by several high latency events that evaded automated procedures.

emphasis placed on pre-merger alerts. We demonstrate that Preliminary GCN Notices can be distributed with true negative latencies: partner observatories receive sky localizations and source information before the binary has completed its merger. We report on the improved latencies at each step of the workflow, and set expectations for pre-merger alerts in O4 and next generation detectors in Section 7.5.

7.3 Analysis

The low-latency workflow begins with data acquisition at each interferometer. The digital signal from the output photodiode is initially calibrated by a pipeline that runs on the set of computers that directly control the interferometer. The calibrated data, while produced with near-zero latency, are not yet accurate enough for use by low-latency gravitational-wave searches. The data are broadcast to a set of computers where a GStreamer-based pipeline corrects the strain data to achieve the required level of accuracy [292]. This pipeline writes the calibrated strain data to a proprietary LIGO frame data format and then transfers them to computing sites. There, the calibrated data are ingested by the complete set of low-latency full bandwidth GW pipelines: cWB [293–297], GstLAL [56–58], MBTAOnline [59], PyCBC Live [298, 299], and SPIIR [65, 300–303]. For the first time, we also incorporate two matched-filter based pipelines focused on pre-merger detection into our workflow: GstLAL [182, 290] and SPIIR [304]. All detection pipelines analyze the data for GWs and assign significances to candidate triggers. Candidates that are assigned false alarm rates (FARs) less than one per hour[4] are uploaded to the GRAvitational-wave Candidate Event DataBase (GraceDB) [5] alongside data required downstream in the alert process.

After candidates are uploaded, the task manager GWCelery [6] interacts with low-latency searches and GraceDB to orchestrate a number of parallel and interconnected processes which, in the event of a discovery, culminates in the dissemination of GCN Notices. GWCelery provided the semi-automated infrastructure for public alerts in O3, as well as for the mock data challenge reported here. The major

[4]No trials factor is applied to the candidate upload threshold.
[5]`https://gracedb.ligo.org/`
[6]`https://gwcelery.readthedocs.io/`

subsystems include:

- The listener for LVAlert, which is a publish-subscribe system used by GraceDB to push machine-readable notifications about its state.
- The Superevent Manager, which clusters and merges related candidates into *superevents*.[7]
- The client functionality to interact with GraceDB.[8]
- The GCN listener that listens for notices from external facilities to spot coincidences with GW candidates.
- The External Trigger Manager, which correlates gravitational-wave events with GRB, neutrino, and supernova events.
- The GCN broker that disseminates GW candidate information for external consumption.
- The Orchestrator, which executes the per-(super)event annotation workflow.

After candidate events are uploaded by detection pipelines, they are localized via BAYESTAR [305], given a probability of having an electromagnetic counterpart [306], and assigned a source-category based astrophysical probability under the assumption that astrophysical and terrestrial triggers occur as independent Poisson processes [307]. Events are checked for temporal and, when possible, spatial coincidences with gamma-ray bursts or neutrino bursts using the RAVEN pipeline [308]. A joint significance is calculated to decide whether the joint candidate should be published.

BAYESTAR was optimized in order to support early warning localizations which led to a median run time of 0.5 s per event for early warning triggers and 1.1 s per event for full bandwidth triggers. The latter is a 4.2× speedup compared to usual O3 performance. The significant changes included rearrangement of loops to improve memory access patterns and make better use of x86_64 vector instructions, changes to the input data handling to distinguish properly between the merger time and the cutoff time of early warning templates, and the redesign of the reconstruction

[7] `https://emfollow.docs.ligo.org/userguide/analysis/superevents.html`
[8] `https://gracedb-sdk.readthedocs.io`

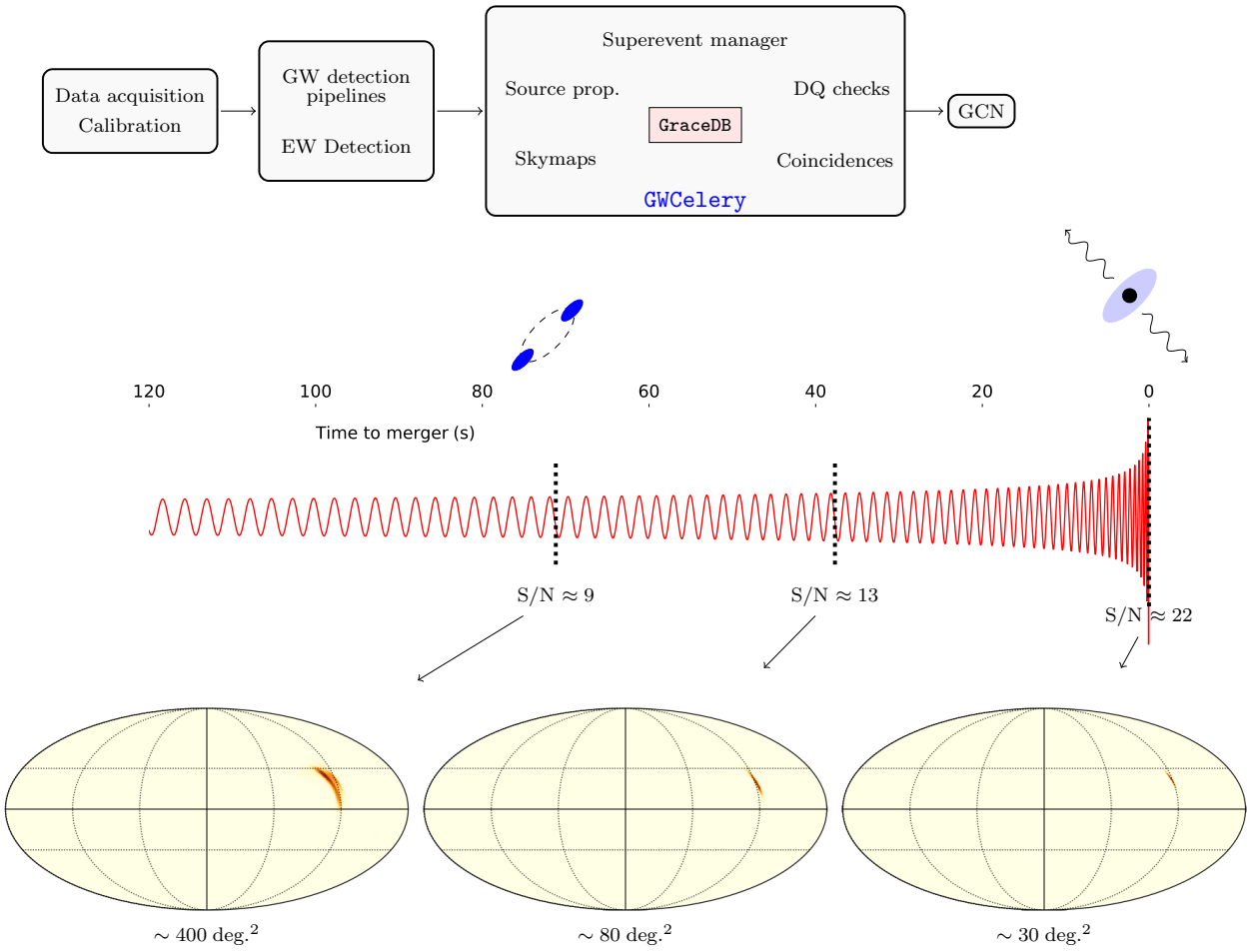

Figure 7.1: This upper half of the figure illustrates the complete pipeline and interaction of the various (sub)systems, mentioned in Sec. 7.3, responsible for disseminating early warning alerts. The waveform evolution with time is shown in the bottom half along with the dependence of the sky-localization area on the cutoff time of the early-warning templates and the accumulated S/N during the binary inspiral. The waveforms, time to merger, S/N, and localizations in this figure are qualitative.

filter that is used to sample the SNR time series for likelihood evaluation to use a lower sample rate. [9]

To mitigate the effect of noise transients, basic data quality checks are also performed for every candidate uploaded to GraceDB. In particular, specific state vectors are checked to ensure that candidate events occur during times when the

[9]The early warning templates are Nyquist critically sampled which could lead to ringing artifacts.

relevant detectors are in observing mode and to verify that there are no coincident hardware injections.

A qualitative overview of entire pipeline and the various (sub)systems mentioned above is illustrated in Fig. 7.1. A heuristic waveform evolution and the effect of different early-warning template cutoff times on the accumulated S/N and the sky-localization is also shown.

7.4 Results

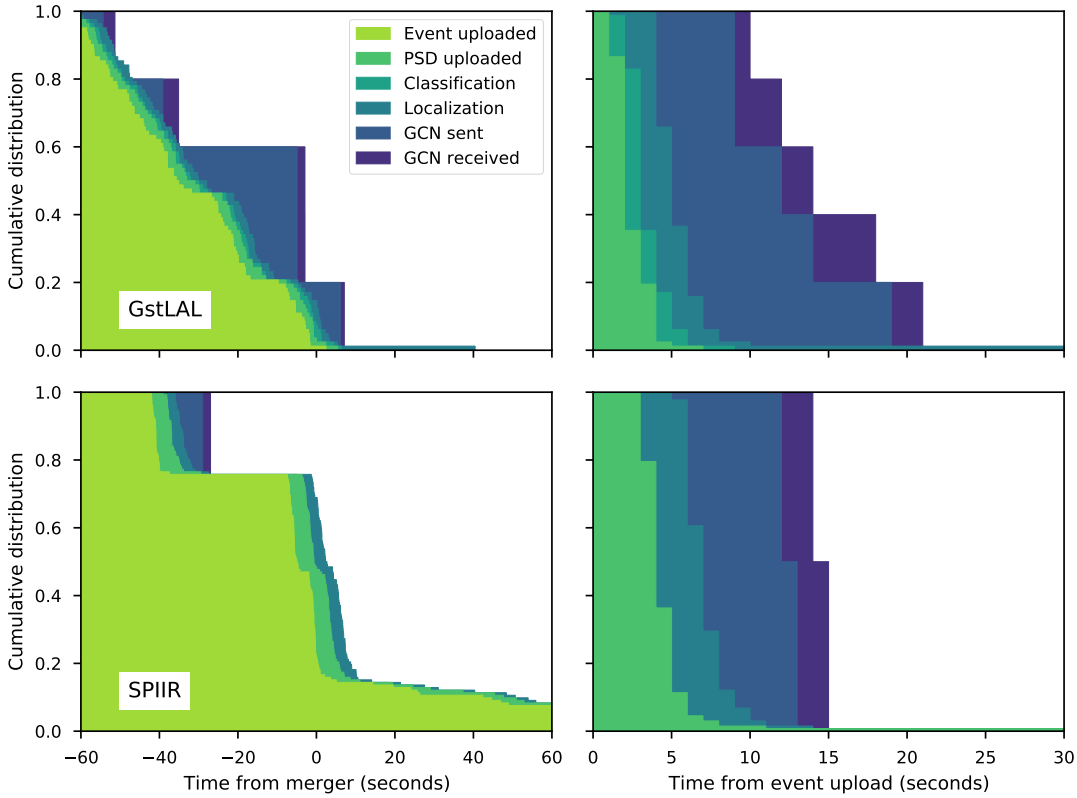

Figure 7.2: Latencies associated with early warning uploads from the GstLAL (top) and SPIIR (bottom) pipelines. Design differences between the pipelines lead to distinct distributions for the time before merger at which a candidate is identified. The left panels indicate that $\sim 85\%$ and $\sim 35\%$ of the uploaded GstLAL and SPIIR candidates, respectively, are localized prior to merger. The right panels demonstrate that despite differences in latencies associated with event identification, the scatter of the remaining processes is remarkably similar.

To demonstrate the robustness of the alert infrastructure, we describe the results of a mock data challenge carried out between 11 June 2020 1700 UTC and 19 June 2020 1700 UTC. Data previously collected during O3 were replayed as a mock low-latency analysis. We note that since the challenge relied on previously collected data, it was impossible to test the full low-latency workflow; notably, data transfer and calibration latencies are not included (~ 5 seconds). The test therefore begins with the detection pipelines, but otherwise follows a workflow identical to Advanced LIGO-Virgo observing runs.

The FAR threshold set for issuing early warning test notices was chosen to be 1 per day. Full bandwidth triggers used the same FAR threshold set throughout O3 for public alerts (1 per 2 months)[10]. At fixed FAR, the astrophysical probability [307] associated with pre-merger analyses is lower than for full bandwidth analyses. Due to this fact, combined with our chosen higher FAR threshold for early-warning alerts, we issued retraction circulars for early warning candidates that were not also identified by the full bandwidth analyses. There were no retraction criteria set for full bandwidth triggers.

During the mock data challenge, eight candidates were published via the test GCN. 3 candidates were identified by only the full bandwidth analyses and were distributed via notice and circular [309–311]. The remaining 5 public candidates were identified only by the early warning pipelines and were distributed via GCN notices to subscribers of test alerts. None of these 5 candidates were observed in the full bandwidth analyses; they were therefore subsequently retracted [312–316]. Out of the 5 retracted triggers, 4 came from the GstLAL early warning pipeline, while 1 was issued by the SPIIR early warning pipeline. An authentication issue prevented the SPIIR pipeline from issuing additional events past the FAR threshold. A summary of the 5 early warning alerts is given in Table 1.

Although only 5 pre-merger candidates passed the early warning public alert threshold, GstLAL and SPIIR uploaded 82 and 141 early warning candidate events, respectively, to GraceDB. We use the metadata associated with these uploads to produce Fig. 7.2. From the events crossing threshold we see that the maximum delivery time from event upload is 15s, independent of pipeline. This enables $\sim 85\%$ and $\sim 35\%$ of the GstLAL and SPIIR candidates, respectively, to be localized

[10]A trials factor is applied on top of this threshold to account for the two early warning and four full bandwidth matched filter pipelines

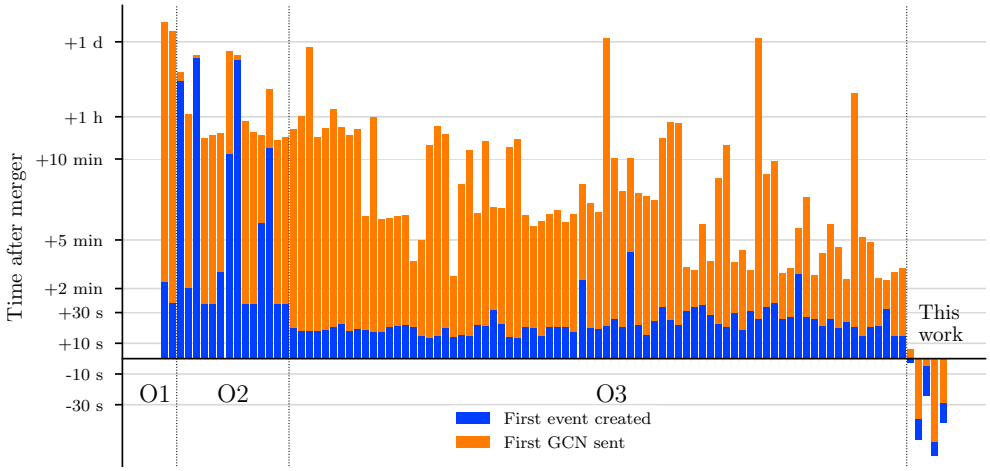

Figure 7.3: A history of end-to-end latencies across public alerts in the first three observing runs and the mock data challenge presented here [29].

before merger.

7.5 Looking ahead

Early warning alerts using real data have not yet been released by the LIGO-Virgo collaboration. Despite the steady improvement of the alert infrastructure (Figure 7.3), there remain several areas for improvement in the processing of data and production of alerts if the collaboration decides to pursue pre-merger triggers. As previously mentioned, low-latency data calibration is currently a two step process; the near-zero-latency pipeline is corrected by a secondary GStreamer-based pipeline. Work is underway to reduce this to a single calibration step to reduce latency by $\mathcal{O}$(seconds). The calibrated data are transferred from the detector sites to the computing clusters in ~ 4 seconds, and afterward at the cluster level using Kafka,[11] with an additional ~ 0.1 seconds. Another one second of latency [12] is attributed to the choice to distribute data via frame files. A number of improvements are under development to reduce this latency budget.

[11] `https://kafka.apache.org/`
[12] Four seconds for Virgo data.

Reductions to the noise budget at frequencies $\lesssim 30$ Hz will improve the possibility of detection pipelines identifying signals long before merger. We estimate that if the noise floor below 30 Hz remains unchanged from O3, the recovered S/N one minute and 30 seconds before merger will be $\sim 50\%$ and $\sim 20\%$ less, respectively, than if the detectors reach the previously projected O4 sensitivity. The effect is less severe for early warning times just before merger, but low frequency noise is a major barrier to advance alerts.

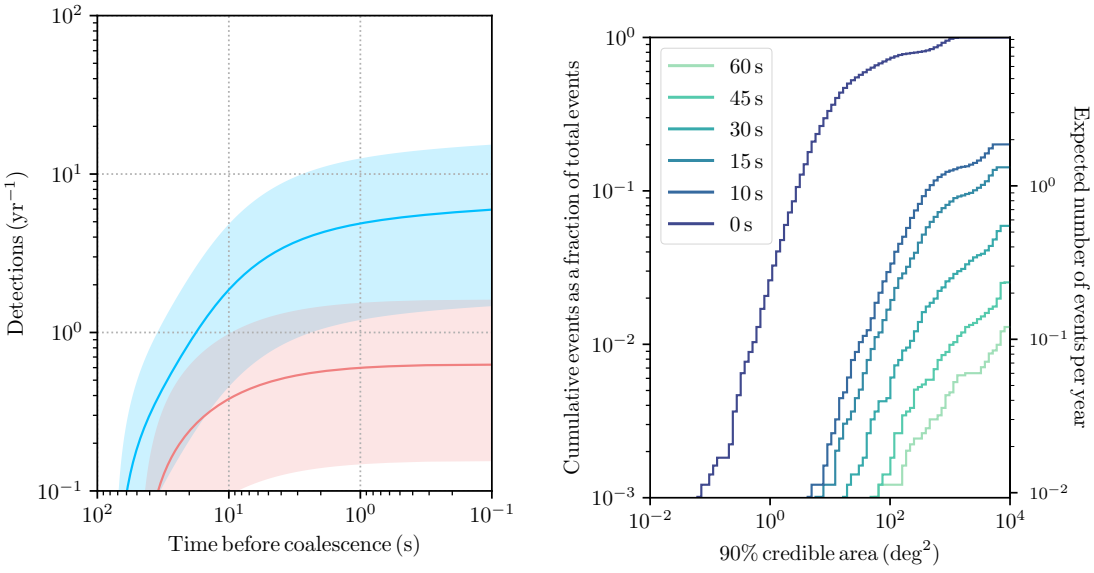

(a) (b)

Figure 7.4: (7.4a) Projected O4 early warning detection rate assuming 0 second (blue) and 25 second (red) end-to-end latencies from the GW alert system. The worst case scenario assumes 5 seconds for calibration and data transfer, 5 seconds for pipeline analysis, and 15 seconds for event upload and GCN creation. The rate of expected detections was estimated from a simulated data set assuming a 100% detector duty cycle for the 4-detector HLVK network. The uncertainty bands reflect the $(5\%, 95\%)$ confidence region for the BNS rate. Signals with network S/Ns greater than 12 are considered recovered. (7.4b) The expected localization distribution for BNS detections at six approximate early warning times. No latencies are included in this figure. The inclusion of an end-to-end latency does not shift the histogram itself; the labeled times before merger would all systematically shift instead. Both plots use the BNS rates estimated in [30].

Figures 7.2 and 7.3 demonstrate that the GW alert system is capable of providing GW alerts before merger, but they do not consider the prospects for detection from

an astrophysical source population. We generate a population of simulated BNS signals, henceforth referred to as *injections*, using the `TaylorF2` [260, 261, 317, 318] waveform model. Both source-frame component masses are drawn from a Gaussian distribution between $1.0\,M_\odot < m_1, m_2 < 2.0\,M_\odot$ with mean mass of $1.33\,M_\odot$ and standard deviation of $0.09\,M_\odot$, modeled after observations of galactic BNSs [319][13]. The neutron stars in the population are non-spinning, motivated by the low spins of BNSs expected to merge within a Hubble time [320,321]. The signals are distributed uniformly in comoving volume up to a redshift of $z = 0.2$. We consider a network of four GW detectors: LIGO-Hanford, LIGO-Livingston, Virgo, and KAGRA at their projected O4 sensitivities.[14] We simulate the results of an early warning matched-filtering pipeline by considering 6 different discrete frequency cut-offs: 29 Hz, 32 Hz, 38 Hz, 49 Hz, 56 Hz, and 1024 Hz to analyze signal recovery at (approximately) 58 s, 44 s, 28 s, 14 s, 10 s, and 0 s before merger, motivated by [290]. We calculate the network S/N of each injection at each frequency cut-off and consider the events that pass an S/N cut-off of 12.0 as 'detected'. We then calculate the sky posteriors for each of the detected signals by using BAYESTAR [305]. We use the most recent BNS local merger rate from [30] of $320^{+410}_{-240}\,\mathrm{Gpc}^{-3}\mathrm{yr}^{-1}$ to estimate the number of events detected per year in the detector network. In Figure 7.4a we see that our optimistic scenario predicts 5^{+7}_{-4} GCN will be received 1 second before merger per year, while our pessimistic scenario predicts $\mathcal{O}(1)$ GCN will be received 1 second before merger per year considering the higher end of the BNS rate. Figure 7.4b predicts that ~ 9 events will be detected per year, out of which $\sim 20\%$ ($\sim 1.3\%$) will be detected 10 s (60 s) before merger. Further, $\sim 3\%$ of the detectable events ($\sim$ 1 BNS every 3–4 years) will be detected 10 seconds prior to merger and have a localization less than 100 deg^2 at O4 sensitivities. This highlights the need for continued latency improvements in advance of O4 to maximize the potential of capturing prompt emission.

In the design sensitivity era with three detectors, [290] have shown that about half of the total detectable BNSs will be found 10 s before merger, and about 2% will be identified before merger and localized to within 100 deg^2. [290] used the GstLAL pipeline in an early warning configuration to assign FARs to simulated

[13]Note that if GW190425 is a BNS, then galactic measurements are not representative of neutron star masses.

[14] `https://dcc.ligo.org/LIGO-T2000012/public`

BNS signals to estimate these rates.[15] We extend this to include KAGRA in the detector network, but we estimate rates based on a fiducial S/N cut-off of 12. We find that our zero-latency scenario improves to ~ 2 BNS observable one minute before coalescence. Assuming 25 seconds of pipeline latency, ~ 1 BNS will be localized and disseminated one minute before merger every 2 years. The localization prospects similarly improve. At design sensitivity, ~ 3 BNS every year will be detected 10 seconds prior to merger and have localizations $\lesssim 100\text{deg}^2$, ~ 2 signals per year will be detected 15 seconds prior to merger with similar localization. The detection rates estimated by [291] are comparable to ours, considering their use of a larger BNS rate density (~ 3 times ours) and a less strict criterion for the detectability of a signal (network S/N > 10).

The next generation of ground based interferometers will offer unparalleled early warning capabilities. Using a similar S/N detection threshold (but further mandating that at least two interferometers measure S/Ns above 5.5), [322] found that the Einstein Telescope can alert observers up to 20 hours in advance for 58% of detectable BNS at 200 Mpc and 100% at 40 Mpc. The majority of these signals will be well localized. A similar study by [323] with a S/N detection threshold of 15 found that the Einstein Telescope will provide early notice for $\mathcal{O}(10^2)$ BNS mergers next decade.

7.6 Acknowledgments

We are grateful to B.S. Sathyaprakash for reviewing our manuscript and providing useful comments. We thank the LIGO Laboratory for use of its computing facility to make this work possible, and we gratefully acknowledge the support of NSF grants PHY-0757058 and PHY-0823459. C.H. gratefully acknowledges the support of NSF grant OAC-1841480. DC acknowledges NSF grant no. PHY-1700765 and PHY-1912649, and is supported by the Illinois Survey Science Fellowship of the Center for Astrophysical Surveys (CAPS) at the University of Illinois Urbana-Champaign. S.S. is supported by the Eberly Research Funds of Penn State, The Pennsylvania State University, University Park, Pennsylvania. G. M. is supported by the National Science Foundation (NSF) through award PHY-1764464 to the

[15] Note that the estimated BNS rate at the time of [290] was approximately three times larger than the updated rate presented in [30]

Superevent	Date (UTC)	FAR	Latency				GCNs
			Event	Superevent	Skymap	Notice	
MS200615h	2020-06-15 00:35:40	2.02e-06	-2.9	-1.9	0.1	7.1	27951
MS200618aq	2020-06-18 05:47:05	1.78e-07	-53.1	-52.1	-50.1	-35.1	27990
MS200618bq	2020-06-18 11:00:59	3.50e-06	-16.9	-21.9	-11.9	-2.9	27987
MS200618bx	2020-06-18 12:17:08	3.76e-06	-63.3	-62.3	-59.3	-51.3	27988
MS200619bf	2020-06-19 10:24:43	1.91e-06	-41.0	-40.0	-35.0	-27.0	27989

Table 1: A summary of the 5 early warning alert information and latencies from the mock data challenge described in Sec. 7.4. Among the 5, MS200619bf was reported by the SPIIR pipeline, while the others were reported from GstLAL. The latencies are broken down in steps of the event being uploaded into GraceDB, the superevent being created, the skymap being available for the preferred event, and the notice being acknowledged by GCN.

LIGO Laboratory. MK, QC, FP, LW, AP, AS, VO acknowledge the funding from Australian Research Council (ARC) Centre of Excellence for Gravitational Wave Discovery OzGrav under grant CE170100004.

Appendix A
GstLAL: A software framework for gravitational wave discovery

The GstLAL library, derived from Gstreamer and the LIGO Algorithm Library, supports a stream-based approach to gravitational-wave data processing. Although GstLAL was primarily designed to search for gravitational-wave signatures of merging black holes and neutron stars, it has also contributed to other gravitational-wave searches, data calibration, and detector-characterization efforts. GstLAL has played an integral role in all of the LIGO-Virgo collaboration detections, and its low-latency configuration has enabled rapid electromagnetic follow-up for dozens of compact binary candidates.

A.1 Motivation and significance

Gravitational waves were originally predicted by Einstein in 1916 [324] as a consequence of general relativity, which describes gravity as the warping of space and time caused by mass and energy [325]. Two extremely massive objects orbiting one another e.g., black holes or neutron stars, warp space dynamically and send ripples across the universe that can be observed here on Earth. As they pass by, gravitational waves stretch and squeeze the space around Earth by less than the width of an atom compared to the Earth's diameter. Due to their tiny effect on scientific instruments, gravitational waves were not observed until 100 years after

their initial prediction. Technological advances in laser interferometry led to the discovery of gravitational waves from a merging binary black hole in 2015 [160]. This watershed moment was made possible by the Advanced Laser Interferometer Gravitational-wave Observatory (LIGO) [45] and the scientists of the LIGO and Virgo Collaborations.

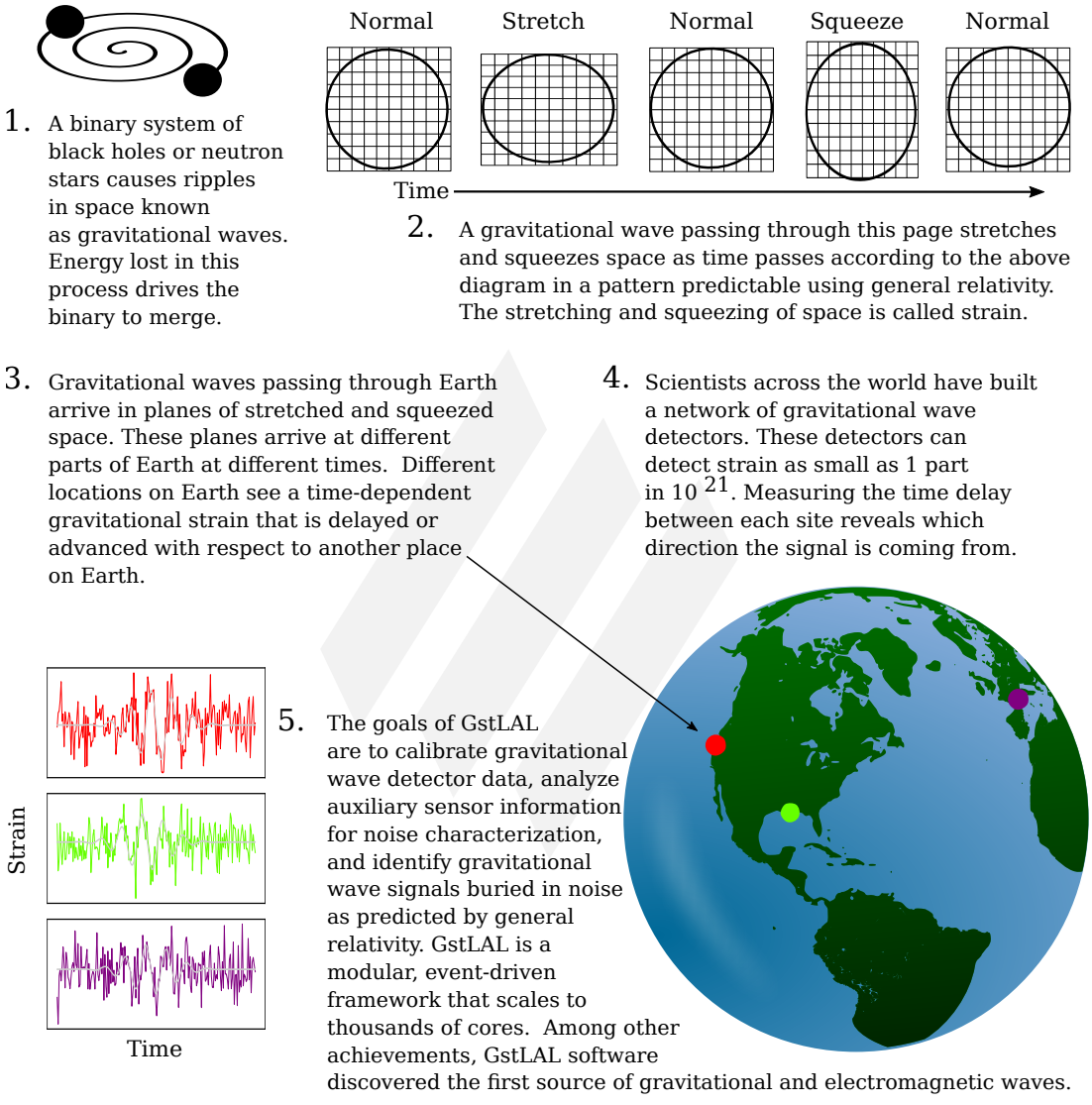

Figure A.1: Gravitational wave infographic. Gravitational wave data is time series, audio frequency data that is noise dominated. GstLAL identifies signals consistent with the predictions of general relativity as measured by multiple gravitational wave detectors and assesses the probability that these signals come from merging neutron stars and/or black holes in near real-time.

Advanced LIGO and Advanced Virgo [45, 46] are the currently operating worldwide network of kilometer-scale laser interferometric gravitational wave observatories which have measured gravitational wave signals. These detectors provide a new way to observe our Universe and enable a vast amount of new science. LIGO's observations have already deepened our understanding of the populations of compact objects such as neutron stars and black holes [194, 195], and they have also offered new tests of fundamental physics [76, 279, 326, 327]. The strong gravity regime probed by compact binary mergers is a laboratory for novel tests of general relativity, and a joint observation of gravitational waves along with electromagnetic waves [221] has taught us how matter behaves in the most extreme conditions [226, 328].

The science made possible by LIGO and Virgo is reliant on measuring miniscule changes in the arm lengths of the interferometers known as strain. The perturbations caused by incident gravitational waves manifest themselves as variations in the intensity of laser light output. *Detector calibration* aims to accurately map the intensity of the output to differential changes in the arm length through real-time signal-processing. The calibrated strain data contains the encoded properties of the astrophysical systems that produce gravitational waves. The analysis of this data is complicated by the presence of a vast array of transient noise sources. *Detector characterization* aims to quantify departures from stationary noise to identify times where instrumental issues are so severe that the data should not be analyzed or there may be a coupling between environmental sensors (such as seismometers) and the gravitational wave strain data. Once data is calibrated and assessed for quality, it is analyzed by a host of detection algorithms to identify potential gravitational wave signals. In many cases the signals are invisible to the naked-eye in raw data and discovering them requires sophisticated techniques that may involve checking millions of models against each segment of data. All three of these activities require substantial cyberinfrastructure. The GstLAL software framework [183] was initially designed to support low-latency compact binary searches to facilitate multi-messenger astronomy, but since its conception it has grown to be a key component of the software used to produce accurately calibrated strain data [223], and recently it has contributed to detector characterization efforts [329, 330]. The GstLAL framework is now contributing key cyberinfrastructure to all three of these key aspects of gravitational wave data analysis. This paper will describe how the GstLAL software is used in gravitational-wave searches [56, 58], provide examples,

and describe the history and impact of GstLAL on gravitational wave discovery.

A.2 Software description

Gravitational wave strain data quantifies how the distance between two points will change as a gravitational wave passes. The current gravitational wave observatories are sensitive to changes in strain and measure the stretching and squeezing of space as a function of time. The Advanced LIGO [45] and Advanced Virgo [46] gravitational wave detectors are most sensitive to strain frequencies between 10Hz–10kHz, which is remarkably close to the frequency range of the human ear [331]. For this reason, there is a close connection between the analysis of gravitational wave data and the analysis of audio data. Indeed, techniques such as low pass filtering, high pass filtering, channel mixing, and gating apply equally well to both audio processing and gravitational wave data processing, which provides the motivation for basing GstLAL on Gstreamer [257].

Gstreamer [257] is an open-source, cross-platform multimedia processing framework designed to execute audio and video processing graphs organized into three basic elements: sources, filters and sinks, which are provided by dynamically loaded plugins. A valid Gstreamer graph, called a pipeline, connects elements together ensuring that the capabilities of each element are satisfied. The data are passed along in *buffers* that store both the memory location of the raw data as well as rich metadata. Pipelines can be used to construct complex workflows and scale to thousands of elements. GstLAL combines standard Gstreamer signal processing elements with custom elements to analyze LIGO strain data.

The GstLAL software began development in 2008 through the exploration of novel techniques for filtering gravitational wave data [70]. It derives its name from "Gstreamer wrappings of the LIGO Algorithm Library[1] (LAL)". GstLAL began to take on its modern form by 2009 and has been since actively developed as open source software. GstLAL currently resides in the LIGO Scientific Collaboration hosted GitLab instance at `https://git.ligo.org/lscsoft/gstlal` [183].

GstLAL is primarily a mix of Python and C with contributions from 75 authors distributed across North America, Europe, Asia and Australia. The master branch currently has over 13,000 commits and 250,000 lines of code. GstLAL is released

[1] `https://git.ligo.org/lscsoft/lalsuite`

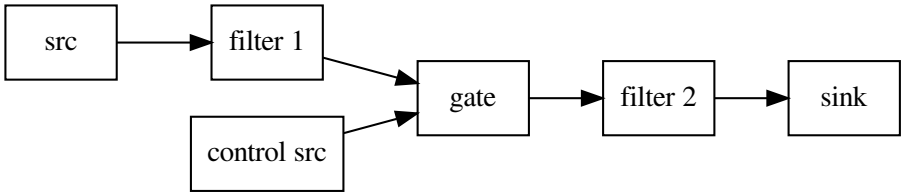

Figure A.2: A basic Gstreamer graph. Data starts at a source, “src", e.g., a file on disk or a network socket, and then is passed through a filter element, “filter 1", which transforms the data, e.g., by performing a low pass filter. A second data stream starts from “control src" and the output of filter 1 is moderated by a gate controlled by the state of “control src". The output of the gate is filtered through “filter 2" and sent to a sink which could be another file on disk or a network socket.

under the GPLv2 license with 44 distinct releases since 2011 [332]. In 2012, code solely used for gravitational wave searches for compact binaries was split off into its own package: GstLAL-Inspiral. GstLAL-Inspiral has had 45 distinct releases since then. In 2014, code used for gravitational wave burst detection was split into its own package, GstLAL-Burst, with nine distinct releases. And finally, in 2014 code used primarily for LIGO strain data calibration was split into its own package, GstLAL-Calibration, with 60 releases. In addition to tar-ball releases, RedHat and Debian compatible packages were produced for the LIGO Data Grid reference platforms [333].

At present, Docker containers with the full GstLAL/LALSuite software stack are built and distributed using the LIGO Container Registry [334]. The containers are built on top of the CentOS-based Scientific Linux 7, which currently serves as the reference operating system on the LIGO Data Grid. Binary executables are linked against Intel’s high-performance Math Kernel Library (MKL), and compiled to leverage Advanced Vector Extensions. Optimized versions of the GstLAL software stack tuned at the compiler-level to best leverage the native features of the local computing environment are often custom-built by users. Previous studies have demonstrated a $\gtrsim 2$ times increase in overall code throughput as a result of software tuning. GstLAL is also available through CondaForge [335].

A.2.1 Software Architecture

Prior to 2015, gravitational waves had not been directly observed [160]. Although analysis techniques had been studied for decades [60, 143], the character of gravitational wave data evolved with the interferometers detectors during the initial operation of LIGO and Virgo from 2002–2010 [25, 336–340]. Therefore, we aimed to make the GstLAL software modular and easy to adapt to the challenges of Advanced LIGO and Virgo data.

The joint observation of gravitational waves and electromagnetic signals, known as multi-messenger astronomy, was a significant goal for Advanced LIGO and Advanced Virgo. In this scenario, gravitational-wave observations were expected to be followed up by observations with telescopes across the electromagnetic spectrum hoping to catch a short-lived transient light source. Discovering gravitational waves quickly is critical because electromagnetic counterparts may quickly fade. GstLAL was designed to offer analysts an extremely short time-to-solution to help ensure that electromagnetic counterparts could be observed quickly.

The key design principles of GstLAL are:

Plugin-based: Libraries within GstLAL provide Gstreamer plugins to perform gravitational wave specific signal processing tasks. These are mixed together with stock Gstreamer plugins to produce gravitational wave analysis pipelines. Plugins provide elements, which are the building blocks of signal processing workflows. These elements can be ordered in multiple ways with minimal coding effort which allows for quick exploratory work and development of new methods.

Streaming: The goal of Gstreamer is to provide ultra low latency signal processing suitable for audio and video playback and editing. GstLAL pipelines typically work with streaming data buffers $\lesssim 1$ s in duration.

Event-driven: GstLAL analysis pipelines are designed to run continuously as data is collected. Each application runs an event loop which controls both application level operations as well as settings within a given plugin. This allows for the control of program behavior to be altered while the application is running. Dynamic program control is facilitated through embedding the

microservices framework Bottle [341]. Simple http APIs push information to the program, retrieve information or alter the program's behavior.

Scalable: The GstLAL framework is designed both to scale to dozens of cores on a single computer using the multi-threading provided by Gstreamer and to scale to thousands of cores across a compute cluster leveraging HTCondor directed acyclic graph (DAG) scheduling [342].

The GstLAL project is currently comprised of five distinct packages. 1) `gstlal`, 2) `gstlal-ugly`, 3) `gstlal-inspiral`, 4) `gstlal-calibration` and 5) `gstlal-burst`, all of which are described below.

A.2.2 `gstlal` package

The `gstlal` package curates a set of core plugins, functions and applications that are used by nearly every analysis workflow developed within GstLAL. The `gstlal` package is a dependency for all of the remaining packages which are described in subsequent sections. The `gstlal` package provides Gstreamer elements for Finite-Impulse-Response filtering (`lal_firbank`), $N \rightarrow M$-channel matrix operations (`lal_matrixmixer`), data whitening (`lal_whiten`), and data gating (`lal_gate`). The `gstlal` package also provides basic python APIs for building Gstreamer pipelines in the module `pipeparts`, basic data access routines in the module `datasource`, and a base class for event handling in the module `simplehandler`.

A.2.3 `gstlal-ugly` package

The `gstlal-ugly` package is an incubator package for software that is in development. Eventually all `gstlal-ugly` software is migrated to one of the other packages.

A.2.4 `gstlal-inspiral` package

The primary purpose of the `gstlal-inspiral` package is to house the GstLAL-based search for compact binaries [56, 58], which centers around the application `gstlal_inspiral`. The GstLAL-based compact binary pipeline was created to make near real-time gravitational-wave detections and aimed to one day detect electromagnetically bright systems before coalescence [182, 290].

The GstLAL-based compact binary search is a matched-filter search that incorporates efficient time-domain filtering [70, 71, 182, 343–347] of a set of template waveforms that match the gravitational wave signals of merging black holes and neutron stars [267]. LIGO and Virgo detectors are prone to bursts of nonstationary noise called glitches [348] and determining the difference between gravitational waves and glitches is well suited for many classification algorithms. GstLAL Inspiral implements a classification scheme that is a hybrid of hypothesis testing techniques with some elements coming from machine learning approaches. The classifier is an approximate likelihood ratio comprised of many terms which began as a custom implementation of Naive Bayes classification [349] applied to gravitational wave searches [350]. It was realized early in the project that two things were apparent. First, it wasn't practical to treat the classifier as entirely data driven relying purely on training sets. Training sets to adequately classify the full parameter space were too expensive to produce. Second, correlations between some parameters had to be tracked in order to classify well. The first point was addressed by developing semi-analytic models to describe parts of the data [57] and the second point was addressed by factoring the multi-dimensional likelihood ratios into groups of lower dimensional, but not one dimensional, distributions [251, 351].

The GstLAL-based compact binary search has two modes. The first is a near-real-time, "low-latency" mode that discovers and reports compact binaries within tens of seconds of the signal arriving at Earth. The second is an "offline" mode that efficiently processes data in batch jobs where time-to-solution is not as important as computational efficiency and reproducibility. Although both modes share $\gtrsim 95\%$ of the same code, their behavior and design are very different in order to address the differing concerns of real-time vs. batch processing.

The low-latency mode is a collection of typically $\mathcal{O}(1000)$ microservices that communicate (modestly) with one another asynchronously through http using python Bottle, through an Apache Kafka queue, and through a shared file system. Each one of these microservices processes a portion of the nearly 2 million models used in the current low-latency compact binary search. The low-latency workflow is designed to be fault tolerant. If a job dies, another is restarted to take its place. Since information is exchanged asynchronously and there is no guarantee of job success, the behavior in this mode is non-deterministic. In contrast, the offline mode has a fully deterministic execution which can be reproduced to floating point

precision. The determinism is imposed by organizing each job in a directed acyclic graph (DAG) using HTCondor.

A.2.5 `gstlal-burst` package

The GstLAL-based burst package is a collection of utilities intended to search for gravitational-wave sources other than compact binaries as well as non-astrophysical noise transients. One of the recent developments is a pipeline searching for cosmic strings, which are hypothetical objects considered to have formed in the early universe. The pipeline uses time-domain stream-based signal processing algorithms, along with a classification scheme using parameters specific to the search. The algorithms used are mostly in common with the `gstlal-inspiral` package, but simplified due to the smaller number of templates required for matched filtering.

In addition, `gstlal-burst` provides utilities to identify and extract features from non-Gaussian noise transients in near real-time ($O(5s)$) via the Stream-based Noise Acquisition and eXtraction, or SNAX toolkit. The SNAX toolkit also leverages time-domain signal processing, but instead utilizes a sine-Gaussian basis to identify the presence of and extract features from many types of non-Gaussian noise in strain and auxiliary data. Its main data product is multivariate time-series data containing the extracted features, including SNR and phase information as well as the waveform parameters of interest.

A.2.6 `gstlal-calibration` package

The `gstlal-calibration` package houses the unique software used for calibration of the LIGO strain data. Software in the `gstlal-calibration` package produces the only official LIGO strain data product used in all subsequent analysis. Calibration of LIGO strain data involves standard signal processing and digital filtering techniques in order to derive the differential arm motion observed in the LIGO detectors from the detector's digital readouts [223, 352, 353]. Many of the signal processing and digital filtering plugins used by the calibration pipeline `gstlal_compute_strain` are housed in the `gstlal` or `gstlal-ugly` packages. A few plugins unique to the calibration process as well as calibration-specific python APIs are housed in the `gstlal-calibration` package.

Much like the GstLAL-based compact binary pipeline, the LIGO calibration

pipeline is built to operate in two modes: a “low-latency" mode and an “offline" mode. The low-latency LIGO calibration pipeline operates on hardware located physically at the two LIGO detector sites, LIGO Hanford in Hanford, WA and LIGO Livingston in Livingston, LA. This pipeline produces calibrated LIGO data and a bit-wise state-vector that indicates the fidelity of the calibrated data within $O(5s)$ for each detector at the respective detector sites. The low-latency calibration process involves using a combination of digital filtering performed in the LIGO front-end computers, which are directly connected to the LIGO detectors and employ the CDS Real-time Code Generator (RCG) core software [354], and further digital filtering and processing performed by the GstLAL calibration software running on non-front-end hardware located at the LIGO detector sites. This two-step process takes advantage of the access the front-end computing system has to the installed detector filters and models and the advanced stream-based filtering techniques housed in the GstLAL software packages [223].

There is often a need to re-calibrate the strain data after the initial low-latency data calibration in order to improve calibration accuracy based on more sophisticated modeling or to remove systematic errors present in the low-latency calibrated strain data [223, 355, 356]. The re-calibration of LIGO data is performed using the offline mode of the `gstlal_compute_strain` pipeline. In this mode, the entire calibration process is performed by software housed in the GstLAL software packages. The offline calibrated data is processed in batch jobs using HTCondor in order to optimize computational efficiency and is completely reproducible to floating-point precision. All analyses derived from LIGO strain data use the calibrated data produced either by the low-latency GstLAL calibration pipeline or the offline GstLAL calibration pipeline.

A.3 Illustrative Examples

A.3.1 Example Gstreamer pipeline with GstLAL

The following example was run on a newly instantiated CentOS 7 64 bit virtual machine with miniconda [357] installed by doing:

```
1
```

```
wget https://repo.anaconda.com/miniconda/Miniconda3-latest-Linux-x86_64.sh
bash Miniconda3-latest-Linux-x86_64.sh
conda create -n myenv python=2.7
conda activate myenv
conda install -c conda-forge gstlal-inspiral=1.7.3
```

To verify that it works, try:

```

$ gst-inspect-1.0 gstlalinspiral | head -n4
Plugin Details:
  Name                     gstlalinspiral
  Description              Various bits of the LIGO Algorithm Library wrapped in gstreamer elements
  Filename                 <your miniconda path>/lib/gstreamer-1.0/libgstgstlalinspiral.so
```

Next we will try a very simple Gstreamer pipeline that uses two GstLAL elements: `lal_peak` and `lal_nxydump`, along with additional Gstreamer elements to construct a pipeline that generates 10 Hz Gaussian, white noise, finds the peak sample every second and streams the result to the terminal screen as ASCII text. It is possible to construct simple pipelines such as this without any code using the Gstreamer tool `gst-launch` [358]:

```

$ gst-launch-1.0 audiotestsrc wave=9 ! capsfilter caps=audio/x-raw,rate=10 ! lal_peak n=10 ! lal_nxydump ! filesink location=/dev/stdout
```

The first element, `audiotestsrc` is a Gstreamer element that can provide many test signals. The `wave=9` property sets it to be unit variance white noise. The second element, `capsfilter` specifies that we want the format of the output to be floating point audio data with a sample rate of 10 Hz. Next, `lal_peak` is the first GstLAL element. In this example it is configured to find the largest absolute value of the signal every 10 sample points. `lal_nxydump` is the second GstLAL element which converts the time-series data to two column ASCII text. Finally, `filesink` dumps the ASCII output to standard out. You should see the following output (with variations caused by the fact that the data is random):

```

```

```
$ gst-launch-1.0 audiotestsrc wave=9 ! capsfilter caps=audio/x-raw
   ,rate=10 ! lal_peak n=10 ! lal_nxydump ! filesink location=/dev
   /stdout | head -n 15
Setting pipeline to PAUSED ...
Pipeline is PREROLLING ...
Pipeline is PREROLLED ...
Setting pipeline to PLAYING ...
New clock: GstSystemClock
0.000000000     0
0.100000000     0
0.200000000     0
0.300000000     0
0.400000000     0
0.500000000     0
0.600000000     0.95523328
0.700000000     0
0.800000000     0
0.900000000     0
```

you can see that the maximum sample point was chosen in the 10 sample interval on line 13. Other values are set to 0.

`gst-launch` is useful tool for quickly testing a simple pipeline, or debugging, however it is not suitable for writing large applications with many elements or situations where program control is exposed dynamically to the user. For building applications, GstLAL relies on the Python bindings for Gstreamer and adds a substantial amount of gravitational wave specific application code written in python. An example of the pipeline above written in the style of GstLAL applications is below.

```

# boiler plate Gstreamer imports
import gi
gi.require_version('Gst', '1.0')
from gi.repository import GObject, Gst
GObject.threads_init()
Gst.init(None)

# Gstlal imports
from gstlal import datasource
from gstlal import pipeparts
from gstlal import simplehandler
```

```
13
14 # initialize an event loop, a pipeline and an event handler
15 mainloop = GObject.MainLoop()
16 pipeline = Gst.Pipeline("softwarex_demo")
17 handler = simplehandler.Handler(mainloop, pipeline)
18
19 src = pipeparts.mkaudiotestsrc(pipeline, wave = 9)
20 src = pipeparts.mkcapsfilter(pipeline, src, caps = "audio/x-raw,
       rate=10")
21 src = pipeparts.mkpeak(pipeline, src, n = 10)
22 src = pipeparts.mknxydumpsink(pipeline, src, "/dev/stdout")
23
24 if pipeline.set_state(Gst.State.PLAYING) == Gst.StateChangeReturn.
       FAILURE:
25         raise RuntimeError("pipeline failed to enter PLAYING state
       ")
26 mainloop.run()
```

We have found that, using python to procedurally build Gstreamer graphs, we can construct enormous pipelines containing tens of thousands of distinct elements. A prime example of this is our workhorse signal processing pipeline used for discovering compact binary mergers as described in the next section.

A.3.2 Compact binary searches

`Makefile.softwarex_test` provides an example of the general workflow involved in offline gravitational wave analyses, which primarily rely on the `gstlal` and `gstlal-inspiral` packages. The miniconda installation of GstLAL will run this example in ∼30 minutes on a single machine. Production level compact binary searches analyzing data from the three advanced interferometers, on the other hand, take ∼1 week when distributed over $\mathcal{O}(1000)$ core computing clusters with optimized software builds. The test Makefile is entirely self-contained; the target and dependency relationships and brief comments within describe the workflow. Although the structure presented in this test is linear in nature, full scale searches for compact binaries are heavily parallelized to take advantage of DAG scheduling. The requisite commands to run this test analysis are shown below.

```
1
2 mkdir workflow-test && cd workflow-test
```

```
export LAL_PATH=${CONDA_PREFIX} GSTLAL_FIR_WHITEN=0 TMPDIR=/tmp
wget https://dcc.ligo.org/public/0168/P2000195/004/Makefile.
    softwarex_test
make -f Makefile.softwarex_test
```

A.4 Impact

GstLAL has played an integral role in the history of gravitational wave detections, and has participated in gravitational wave searches since S5 [359]. Although GstLAL was designed specifically for near-real-time applications, the low-latency pipeline was prevented from searching for binary black holes at the start of Advanced LIGO's first observing run (O1). The pipeline was only allowed to use a template bank sensitive to electromagnetically binary neutron stars and neutron star - black hole binaries. The software was fully capable of detecting binary black holes in near-real-time. The LIGO collaboration desired blind binary black hole (BBH) analyses, and since BBH systems are not expected to produce electromagnetic radiation there was no perceived need to detect them in near-real-time. The restriction on the allowed template bank rendered GstLAL unable to detect GW150914 in low-latency, though it was one of two matched filter pipelines used to analyze archival data and validate the event [160]. GW150914 was initially detected in low-latency by the weakly-modeled burst pipeline CWB [297], which demonstrated that there could be no truly blind analysis while low-latency burst pipelines produced alerts. As a result, in late 2015 the GstLAL pipeline was approved to include BBHs with total mass $\lesssim 100 M_{\odot}$ in its low-latency configuration. GstLAL quickly demonstrated its ability to recover BBHs in low-latency; it became the first matched-filter pipeline using waveforms based on general relativity to make a near real-time detection of a compact binary with the discovery of GW151226 [134].

Development work between Advanced LIGO's first and second observing runs focused on enabling single detector discoveries and incorporating data from Virgo in the analysis. These efforts were rewarded by August 2017 as GstLAL became the first three-detector matched-filter search in the Advanced LIGO era and, more notably, the first (and to date, the only) gravitational-wave detection pipeline to observe a binary neutron star merger in low-latency [360, 361]. Although both Advanced LIGO interferometers and the Advanced Virgo interferometer

were operating at the time of GW170817, it was initially observed in a single interferometer. This marked the first single detector observation of a gravitational wave, and the autonomous identification of the candidate enabled rapid offline follow-up of the candidate within the LIGO-Virgo collaboration.

Advanced LIGO's third observing run (O3) marked the beginning of open public alerts (OPA) [288]. For the first time, candidates with false-alarm-rates below 1 per month[2] were made public at the time of discovery. Although the first public alert was distributed in error by the collaboration [362], the identification of binary black hole candidate S90408an [363] marked the successful start of the era of automated public alerts. At first only candidates appearing in two or more detectors were approved for automated release, but GW170817 had already demonstrated the importance of single detector searches. Indeed, two weeks into the third observing run GstLAL was the only pipeline to detect GW190425 in near-real-time [360, 364], further highlighting the necessity of single detector searches.

Two months into the observing run, GstLAL became the only pipeline approved to release single detector candidates as OPAs. This was a high risk, high reward endeavor. Matched filter searches have traditionally been able to suppress the background by demanding coincidence across interferometers; single detector candidates do not benefit from this effect and can therefore be more susceptible to short term noise transients. Unfortunately, this resulted in several retractions throughout O3 as the GstLAL team worked on ways to mitigate the effects of noise transients in single detectors. By the end of the second half of the observing run, pipeline tuning had reduced the rate of retractions.

GstLAL has contributed to all gravitational-wave discoveries published by the LIGO Scientific Collaboration [9, 134–137, 160, 194, 364], but it has also contributed to searches for as yet undetected sources. Sub-solar mass and intermediate mass black holes both pose problems for conventional models of stellar evolution, and GstLAL has directly contributed to searches of both [28, 96, 365, 366]. Although these searches have not yet yielded any detections, the null results have been able to place strict limits on the abundance of such objects and have also provided the tightest limit to date on a primordial black hole model of the dark matter.

[2]after applying a trials factor to account for the number of concurrently running searches.

A.5 Conclusions

The GstLAL library has significantly impacted the progress of gravitational-wave astrophysics, not only via compact binary searches, but also through contributions to detector calibration and characterization efforts. The low-latency GstLAL based inspiral pipeline was instrumental in the first multi-messenger discovery with gravitational waves, and strives to lead the march towards more remarkable observations with ground-based interferometers.

A.6 Conflict of interest

No conflict of interest exists: we wish to confirm that there are no known conflicts of interest associated with this publication and there has been no significant financial support for this work that could have influenced its outcome.

Acknowledgments

Funding for this work was provided by the National Science Foundation through awards: PHY-1454389, OAC-1642391, PHY-1700765, OAC-1841480, PHY-1607178, and PHY-1847350. Funding for this project was provided by the Charles E. Kaufman Foundation of The Pittsburgh Foundation. Computations for this research were performed on the Pennsylvania State University's Institute for Computational and Data Sciences Advanced CyberInfrastructure (ICDS-ACI) and VM hosting. We are grateful for computational resources provided by the Leonard E Parker Center for Gravitation, Cosmology and Astrophysics at the University of Wisconsin-Milwaukee. Computing support was provided by the LIGO Laboratory through National Science Foundation grant PHY-1764464. GstLAL relies on many other open source software libraries; we gratefully acknowledge the development and support of NumPy [367], SciPy [368], PyGTK [369], PyGST [370], Bottle [341], Kafka [371], Fftw3F [372], Intel MKL [373], GLib2 [374], GNU Scientific Library [375], and GWpy [376]. The authors gratefully acknowledge the LIGO-Virgo-Kagra collaboration for support, review, and valuable critiques throughout various stages of development of the GstLAL library. We are especially thankful for collaborations within the Compact Binary Coalescence working group.

Appendix B
Permissions

Kind regards,

Sophie Milne

Copyright & Permissions Team
Sophie Milne - Rights & Permissions Assistant
Sophie Brittain - Rights & Permissions Assistant
Cameron Wood - Legal & Rights Adviser
Contact Details
E-mail: permissions@ioppublishing.org

For further information about copyright and how to request permission: https://publishingsupport.iopscience.iop.org/copyright-journals/
See also: https://publishingsupport.iopscience.iop.org/
Please see our Author Rights Policy https://publishingsupport.iopscience.iop.org/author-rights-policies/
Please note: We do not provide signed permission forms as a separate attachment. Please print this email and provide it to your publisher as proof of permission. **Please note**: Any statements made by IOP Publishing to the effect that authors do not need to get permission to use any content where IOP Publishing is not the publisher is not intended to constitute any sort of legal advice. Authors must make their own decisions as to the suitability of the content they are using and whether they require permission for it to be published within their article.

[Quoted text hidden]

Ryan Magee <ry.m.magee@gmail.com> Fri, Feb 5, 2021 at 9:58 AM
To: Permissions <permissions@ioppublishing.org>

Hi,
Can I include pre-prints of published articles?
Thanks,
Ryan
[Quoted text hidden]

Permissions <permissions@ioppublishing.org> Mon, Feb 8, 2021 at 6:41 AM
To: Ryan Magee <ry.m.magee@gmail.com>

Hi Ryan,

I hope this email finds you well.

Yes, you can, our policy allows for preprints to be shared anywhere at anytime.

I hope this answers your question, please feel free to get in touch if you have any questions.

Kind Regards

American Physical Society
Reuse and Permissions License

18-Sep-2020

This license agreement between the American Physical Society ("APS") and RYAN MAGEE ("You") consists of your license details and the terms and conditions provided by the American Physical Society and SciPris.

Licensed Content Information

License Number:	**RNP/20/SEP/030837**
License date:	18-Sep-2020
DOI:	10.1103/PhysRevD.98.103024
Title:	Methods for the detection of gravitational waves from subsolar mass ultracompact binaries
Author:	Ryan Magee et al.
Publication:	Physical Review D
Publisher:	American Physical Society
Cost:	USD $ 0.00

Request Details

Does your reuse require significant modifications: No

Specify intended distribution locations:	Worldwide
Reuse Category:	Reuse in a thesis/dissertation
Requestor Type:	Author of requested content
Items for Reuse:	Whole Article
Format for Reuse:	Electronic

Information about New Publication:

University/Publisher:	Penn State University/ProQuest
Title of dissertation/thesis:	Probing the dark universe with gravitational waves from subsolar mass compact objects
Author(s):	Ryan Magee
Expected completion date:	Dec. 2020

License Requestor Information

Name:	RYAN MAGEE
Affiliation:	Individual
Email Id:	rzm50@psu.edu
Country:	United States

American Physical Society
Reuse and Permissions License

18-Sep-2020

This license agreement between the American Physical Society ("APS") and RYAN MAGEE ("You") consists of your license details and the terms and conditions provided by the American Physical Society and SciPris.

Licensed Content Information

License Number:	**RNP/20/SEP/030835**
License date:	18-Sep-2020
DOI:	10.1103/PhysRevLett.121.231103
Title:	Search for Subsolar-Mass Ultracompact Binaries in Advanced LIGO's First Observing Run
Author:	B. P. Abbott et al. (LIGO Scientific Collaboration and Virgo Collaboration)
Publication:	Physical Review Letters
Publisher:	American Physical Society
Cost:	USD $ 0.00

Request Details

Does your reuse require significant modifications: No

Specify intended distribution locations:	Worldwide
Reuse Category:	Reuse in a thesis/dissertation
Requestor Type:	Author of requested content
Items for Reuse:	Whole Article
Format for Reuse:	Electronic

Information about New Publication:

University/Publisher:	Penn State University/ProQuest
Title of dissertation/thesis:	Probing the dark universe with gravitational waves from subsolar mass compact objects
Author(s):	Ryan Magee
Expected completion date:	Dec. 2020

License Requestor Information

Name:	RYAN MAGEE
Affiliation:	Individual
Email Id:	rzm50@psu.edu
Country:	United States

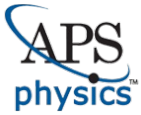

American Physical Society Reuse and Permissions License

18-Sep-2020

This license agreement between the American Physical Society ("APS") and RYAN MAGEE ("You") consists of your license details and the terms and conditions provided by the American Physical Society and SciPris.

Licensed Content Information

License Number:	**RNP/20/SEP/030836**
License date:	18-Sep-2020
DOI:	10.1103/PhysRevLett.123.161102
Title:	Search for Subsolar Mass Ultracompact Binaries in Advanced LIGO's Second Observing Run
Author:	B. P. Abbott et al. (LIGO Scientific Collaboration and the Virgo Collaboration)
Publication:	Physical Review Letters
Publisher:	American Physical Society
Cost:	USD $ 0.00

Request Details

Does your reuse require significant modifications: No

Specify intended distribution locations:	Worldwide
Reuse Category:	Reuse in a thesis/dissertation
Requestor Type:	Author of requested content
Items for Reuse:	Whole Article
Format for Reuse:	Electronic

Information about New Publication:

University/Publisher:	Penn State University/ProQuest
Title of dissertation/thesis:	Probing the dark universe with gravitational waves from subsolar mass compact objects
Author(s):	Ryan Magee
Expected completion date:	Dec. 2020

License Requestor Information

Name:	RYAN MAGEE
Affiliation:	Individual
Email Id:	rzm50@psu.edu
Country:	United States

Bibliography

[1] "LIGO's Interferometer," https://www.ligo.caltech.edu/page/ligos-ifo, accessed: 2020-10-15.

[2] Abbott, R. et al. (2020) "GWTC-2: Compact Binary Coalescences Observed by LIGO and Virgo During the First Half of the Third Observing Run," 2010.14527.

[3] Alcock, C. et al. (2000) "The MACHO project: Microlensing results from 5.7 years of LMC observations," *Astrophys. J.*, **542**, pp. 281–307, astro-ph/0001272.

[4] Allsman, R. A. et al. (2001) "MACHO project limits on black hole dark matter in the 1-30 solar mass range," *Astrophys. J.*, **550**, p. L169, astro-ph/0011506.

[5] Tisserand, P. et al. (2007) "Limits on the Macho Content of the Galactic Halo from the EROS-2 Survey of the Magellanic Clouds," *Astron. Astrophys.*, **469**, pp. 387–404, astro-ph/0607207.

[6] Koushiappas, S. M. and A. Loeb (2017) "Dynamics of Dwarf Galaxies Disfavor Stellar-Mass Black Holes as Dark Matter," *Phys. Rev. Lett.*, **119**, p. 041102.
URL https://link.aps.org/doi/10.1103/PhysRevLett.119.041102

[7] Brandt, T. D. (2016) "Constraints on MACHO Dark Matter from Compact Stellar Systems in Ultra-Faint Dwarf Galaxies," *Astrophys. J.*, **824**(2), p. L31, 1605.03665.

[8] Carr, B., F. Kühnel, and M. Sandstad (2016) "Primordial Black Holes as Dark Matter," *Phys. Rev.*, **D94**(8), p. 083504, 1607.06077.

[9] Abbott, B. P. et al. (2017) "GW170817: Observation of Gravitational Waves from a Binary Neutron Star Inspiral," *Phys. Rev. Lett.*, **119**(16), p. 161101, 1710.05832.

[10] Mei, S., J. Blakeslee, P. Cote, J. Tonry, M. J. West, L. Ferrarese, A. Jordan, E. Peng, A. Anthony, and D. Merritt (2007) "The ACS Virgo Cluster Survey. 13. SBF Distance Catalog and the Three-Dimensional Structure of the Virgo Cluster," *Astrophys. J.*, **655**, pp. 144–162, astro-ph/0702510.

[11] Pietrzyński, G. et al. (2013) "An eclipsing binary distance to the Large Magellanic Cloud accurate to 2 per cent," *Nature*, **495**, pp. 76–79, 1303.2063.

[12] Vilardell, F., I. Ribas, C. Jordi, E. L. Fitzpatrick, and E. F. Guinan (2010) "The distance to the Andromeda galaxy from eclipsing binaries," *Astronomy and Astrophysics*, **509**, A70, 0911.3391.

[13] Carter, D. et al. (2008) "The HST/ACS Coma Cluster Survey: I - Survey Objectives and Design," *Astrophys. J. Suppl.*, **176**, p. 424, 0801.3745.

[14] Gerke, J. R., C. S. Kochanek, J. L. Prieto, K. Z. Stanek, and L. M. Macri (2011) "A Study of Cepheids in M81 with the Large Binocular Telescope (Efficiently Calibrated with Hubble Space Telescope)," *Astrophysical Journal*, **743**, 176, 1103.0549.

[15] Mutabazi, T., S. L. Blyth, P. A. Woudt, J. R. Lucey, T. H. Jarrett, M. Bilicki, A. C. Schroder, and S. A. W. Moore (2014) "The Norma cluster (ACO 3627) – III. The distance and peculiar velocity via the near-infrared Ks-band Fundamental Plane," *Mon. Not. Roy. Astron. Soc.*, **439**(4), pp. 3666–3682, 1401.7478.

[16] Abbott, B. P. et al. (2016) "Sensitivity of the Advanced LIGO detectors at the beginning of gravitational wave astronomy," *Phys. Rev.*, **D93**(11), p. 112004, [Addendum: Phys. Rev.D97,no.5,059901(2018)], 1604.00439.

[17] Tisserand, P. et al. (2007) "Limits on the Macho Content of the Galactic Halo from the EROS-2 Survey of the Magellanic Clouds," *Astron. Astrophys.*, **469**, pp. 387–404, astro-ph/0607207.

[18] Allsman, R. A. et al. (2001) "MACHO project limits on black hole dark matter in the 1-30 solar mass range," *Astrophys. J.*, **550**, p. L169, astro-ph/0011506.

[19] Koushiappas, S. M. and A. Loeb (2017) "Dynamics of Dwarf Galaxies Disfavor Stellar-Mass Black Holes as Dark Matter," *Phys. Rev. Lett.*, **119**(4), p. 041102, 1704.01668.

[20] Brandt, T. D. (2016) "Constraints on MACHO Dark Matter from Compact Stellar Systems in Ultra-Faint Dwarf Galaxies," *Astrophys. J.*, **824**(2), p. L31, 1605.03665.

[21] Abbott, B. P. et al. (2018), "Search for sub-solar mass ultracompact binaries in Advanced LIGO's first observing run," ArXiv:1808.04771, 1808.04771.

[22] Abadie, J. et al. (2010) "Sensitivity to Gravitational Waves from Compact Binary Coalescences Achieved during LIGO's Fifth and Virgo's First Science Run," 1003.2481.

[23] Biswas, R., P. R. Brady, J. D. E. Creighton, and S. Fairhurst (2009) "The Loudest event statistic: General formulation, properties and applications," *Class. Quant. Grav.*, **26**, p. 175009, [Erratum: Class. Quant. Grav.30,079502(2013)], 0710.0465.

[24] Abbott, B. et al. (2005) "Search for gravitational waves from primordial black hole binary coalescences in the galactic halo," *Phys. Rev.*, **D72**, p. 082002, gr-qc/0505042.

[25] ——— (2008) "Search for gravitational waves from binary inspirals in S3 and S4 LIGO data," *Phys. Rev.*, **D77**, p. 062002, 0704.3368.

[26] Zumalacarregui, M. and U. Seljak (2017) "Limits on stellar-mass compact objects as dark matter from gravitational lensing of type Ia supernovae," 1712.02240.

[27] Ade, P. A. R. et al. (2016) "Planck 2015 results. XIII. Cosmological parameters," *Astron. Astrophys.*, **594**, p. A13, 1502.01589.

[28] Abbott, B. P. et al. (2018) "Search for Subsolar-Mass Ultracompact Binaries in Advanced LIGO's First Observing Run," *Phys. Rev. Lett.*, **121**(23), p. 231103, 1808.04771.

[29] ——— (2019) "Low-latency Gravitational-wave Alerts for Multimessenger Astronomy during the Second Advanced LIGO and Virgo Observing Run," *Astrophys. J.*, **875**(2), p. 161, 1901.03310.

[30] Abbott, R. et al. (2020) "Population Properties of Compact Objects from the Second LIGO-Virgo Gravitational-Wave Transient Catalog," 2010.14533.

[31] Nitz, A. H., C. Capano, A. B. Nielsen, S. Reyes, R. White, D. A. Brown, and B. Krishnan (2019) "1-OGC: The first open gravitational-wave catalog of binary mergers from analysis of public Advanced LIGO data," *Astrophys. J.*, **872**(2), p. 195, 1811.01921.

[32] Bredig, M. A. (1973) "The Born-Einstein Letters," *Science*, **180**(4091), pp. 1118–1118, https://science.sciencemag.org/content/180/4091/1118.3.full.pdf.
URL https://science.sciencemag.org/content/180/4091/1118.3

[33] Bondi, H. (1957) "Plane gravitational waves in general relativity," *Nature*, **179**, pp. 1072–1073.

[34] Bondi, H., F. Pirani, and I. Robinson (1959) "Gravitational waves in general relativity. 3. Exact plane waves," *Proc. Roy. Soc. Lond. A*, **251**, pp. 519–533.

[35] Robinson, I. and A. Trautman (1960) "Spherical Gravitational Waves," *Phys. Rev. Lett.*, **4**, pp. 431–432.

[36] Trautman, A. (1958) "Radiation and Boundary Conditions in the Theory of Gravitation," *Bull. Acad. Pol. Sci. Ser. Sci. Math. Astron. Phys.*, **6**(6), pp. 407–412, 1604.03145.

[37] Taylor, J. H. and J. M. Weisberg (1982) "A new test of general relativity - Gravitational radiation and the binary pulsar PSR 1913+16," *The Astrophysical Journal*, **253**, pp. 908–920.

[38] Abbott, B. P. et al. (2016) "Observation of Gravitational Waves from a Binary Black Hole Merger," *Phys. Rev. Lett.*, **116**(6), p. 061102, 1602.03837.

[39] Weber, J. (1967) "Gravitational Radiation," *Phys. Rev. Lett.*, **18**, pp. 498–501.
URL https://link.aps.org/doi/10.1103/PhysRevLett.18.498

[40] ——— (1968) "Gravitational-Wave-Detector Events," *Phys. Rev. Lett.*, **20**, pp. 1307–1308.
URL https://link.aps.org/doi/10.1103/PhysRevLett.20.1307

[41] ——— (1969) "Evidence for Discovery of Gravitational Radiation," *Phys. Rev. Lett.*, **22**, pp. 1320–1324.
URL https://link.aps.org/doi/10.1103/PhysRevLett.22.1320

[42] Tagoshi, H. et al. (2001) "The First search for gravitational waves from inspiraling compact binaries using TAMA300 data," *Phys. Rev.*, **D63**, p. 062001, gr-qc/0012010.

[43] Allen, B. et al. (1999) "Observational limit on gravitational waves from binary neutron stars in the galaxy," *Phys. Rev. Lett.*, **83**, p. 1498, gr-qc/9903108.

[44] Aasi, J. et al. (2013) "Search for gravitational waves from binary black hole inspiral, merger, and ringdown in LIGO-Virgo data from 2009–2010," *Phys. Rev. D*, **87**(2), p. 022002, 1209.6533.

[45] ——— (2015) "Advanced LIGO," *Class. Quant. Grav.*, **32**, p. 074001, 1411.4547.

[46] Acernese, F. et al. (2015) "Advanced Virgo: a second-generation interferometric gravitational wave detector," *Class. Quant. Grav.*, **32**(2), p. 024001, 1408.3978.

[47] Abbott, B. P. et al. (2018) "Prospects for Observing and Localizing Gravitational-Wave Transients with Advanced LIGO, Advanced Virgo and KAGRA," *Living Rev. Rel.*, **21**, p. 3, [Living Rev. Rel.19,1(2016)], 1304.0670.

[48] Tobin, J. J., L. W. Looney, Z.-Y. Li, S. I. Sadavoy, M. M. Dunham, D. Segura-Cox, K. Kratter, C. J. Chand ler, C. Melis, R. J. Harris, and L. Perez (2018) "The VLA/ALMA Nascent Disk and Multiplicity (VANDAM) Survey of Perseus Protostars. VI. Characterizing the Formation Mechanism for Close Multiple Systems," *The Astrophysical Journal*, **867**(1), 43, 1809.06434.

[49] Woosley, S., A. Heger, and T. Weaver (2002) "The evolution and explosion of massive stars," *Rev. Mod. Phys.*, **74**, pp. 1015–1071.

[50] Buonanno, A. and T. Damour (1999) "Effective one-body approach to general relativistic two-body dynamics," *Phys. Rev. D*, **59**, p. 084006, gr-qc/9811091.

[51] Blanchet, L., T. Damour, B. R. Iyer, C. M. Will, and A. G. Wiseman (1995) "Gravitational-Radiation Damping of Compact Binary Systems to Second Post-Newtonian Order," *Phys. Rev. Lett.*, **74**, pp. 3515–3518. URL https://link.aps.org/doi/10.1103/PhysRevLett.74.3515

[52] Buonanno, A., B. R. Iyer, E. Ochsner, Y. Pan, and B. S. Sathyaprakash (2009) "Comparison of post-Newtonian templates for compact binary inspiral signals in gravitational-wave detectors," *Physical Review D*, **80**(8), p. 084043.

[53] Pretorius, F. (2005) "Evolution of binary black hole spacetimes," *Phys. Rev. Lett.*, **95**, p. 121101, gr-qc/0507014.

[54] Campanelli, M., C. Lousto, P. Marronetti, and Y. Zlochower (2006) "Accurate evolutions of orbiting black-hole binaries without excision," *Phys. Rev. Lett.*, **96**, p. 111101, gr-qc/0511048.

[55] Baker, J. G., J. Centrella, D.-I. Choi, M. Koppitz, and J. van Meter (2006) "Gravitational wave extraction from an inspiraling configuration of merging black holes," *Phys. Rev. Lett.*, **96**, p. 111102, gr-qc/0511103.

[56] Sachdev, S. et al. (2019) "The GstLAL Search Analysis Methods for Compact Binary Mergers in Advanced LIGO's Second and Advanced Virgo's First Observing Runs," 1901.08580.

[57] Hanna, C. et al. (2019) "Fast evaluation of multi-detector consistency for real-time gravitational wave searches," 1901.02227.

[58] Messick, C. et al. (2017) "Analysis Framework for the Prompt Discovery of Compact Binary Mergers in Gravitational-wave Data," *Phys. Rev.*, **D95**(4), p. 042001, 1604.04324.

[59] Adams, T., D. Buskulic, V. Germain, G. Guidi, F. Marion, M. Montani, B. Mours, F. Piergiovanni, and G. Wang (2015) "Low-latency analysis pipeline for compact binary coalescences in the advanced gravitational wave detector era," *Classical and Quantum Gravity*, **33**.

[60] Allen, B., W. G. Anderson, P. R. Brady, D. A. Brown, and J. D. E. Creighton (2012) "FINDCHIRP: An Algorithm for detection of gravitational waves from inspiraling compact binaries," *Phys. Rev.*, **D85**, p. 122006, gr-qc/0509116.

[61] Allen, B. (2005) "χ^2 time-frequency discriminator for gravitational wave detection," *Phys. Rev.*, **D71**, p. 062001, gr-qc/0405045.

[62] Dal Canton, T. et al. (2014) "Implementing a search for aligned-spin neutron star-black hole systems with advanced ground based gravitational wave detectors," *Phys. Rev.*, **D90**(8), p. 082004, 1405.6731.

[63] Usman, S. A. et al. (2016) "The PyCBC search for gravitational waves from compact binary coalescence," *Class. Quant. Grav.*, **33**(21), p. 215004, 1508.02357.

[64] Nitz, A. H., T. Dent, T. Dal Canton, S. Fairhurst, and D. A. Brown (2017) "Detecting binary compact-object mergers with gravitational waves: Understanding and Improving the sensitivity of the PyCBC search," *Astrophys. J.*, **849**(2), p. 118, 1705.01513.

[65] Chu, Q. (2017) *Low-latency detection and localization of gravitational waves from compact binary coalescences*, Ph.D. thesis, The University of Western Australia.

[66] Damour, T. (2001) "Coalescence of two spinning black holes: an effective one-body approach," *Phys. Rev.*, **D64**, p. 124013, gr-qc/0103018.

[67] Ajith, P. et al. (2011) "Inspiral-merger-ringdown waveforms for black-hole binaries with non-precessing spins," *Phys. Rev. Lett.*, **106**, p. 241101, 0909.2867.

[68] Santamaria, L. et al. (2010) "Matching post-Newtonian and numerical relativity waveforms: systematic errors and a new phenomenological model for non-precessing black hole binaries," *Phys. Rev.*, **D82**, p. 064016, 1005.3306.

[69] Racine, E. (2008) "Analysis of spin precession in binary black hole systems including quadrupole-monopole interaction," *Phys. Rev.*, **D78**, p. 044021, 0803.1820.

[70] Cannon, K., A. Chapman, C. Hanna, D. Keppel, A. C. Searle, and A. J. Weinstein (2010) "Singular value decomposition applied to compact binary coalescence gravitational-wave signals," *Phys. Rev.*, **D82**, p. 044025, 1005.0012.

[71] Cannon, K., C. Hanna, and D. Keppel (2011) "Efficiently enclosing the compact binary parameter space by singular-value decomposition," *Phys. Rev. D*, **84**, p. 084003, 1101.4939.

[72] Abbott, R. et al. (2020) "GW190814: Gravitational Waves from the Coalescence of a 23 Solar Mass Black Hole with a 2.6 Solar Mass Compact Object," *Astrophys. J. Lett.*, **896**(2), p. L44, 2006.12611.

[73] ——— (2020) "GW190521: A Binary Black Hole Merger with a Total Mass of 150 M⊙," *Phys. Rev. Lett.*, **125**(10), p. 101102, 2009.01075.

[74] ——— (2020) "Properties and Astrophysical Implications of the 150 $M_\odot$ Binary Black Hole Merger GW190521," *Astrophys. J.*, **900**(1), p. L13, 2009.01190.

[75] Mukherjee, D., S. Caudill, R. Magee, C. Messick, S. Privitera, S. Sachdev, K. Blackburn, P. Brady, P. Brockill, K. Cannon, S. J. Chamberlin, D. Chatterjee, J. D. E. Creighton, H. Fong, P. Godwin, C. Hanna, S. Kapadia, R. N. Lang, T. G. F. Li, R. K. L. Lo, D. Meacher, A. Pace, L. Sadeghian, L. Tsukada, L. Wade, M. Wade, A. Weinstein, and L. Xiao (2018) "The GstLAL template bank for spinning compact binary mergers in the second observation run of Advanced LIGO and Virgo," *Preprint: arXiv 1812.05121*, arXiv:1812.05121, 1812.05121.

[76] Abbott, B. P. et al. (2017) "A gravitational-wave standard siren measurement of the Hubble constant," *Nature*, **551**(7678), pp. 85–88, 1710.05835.

[77] Fishbach, M. et al. (2019) "A Standard Siren Measurement of the Hubble Constant from GW170817 without the Electromagnetic Counterpart," *Astrophys. J.*, **871**(1), p. L13, 1807.05667.

[78] Riess, A. G., S. Casertano, W. Yuan, L. Macri, J. Anderson, J. W. MacKenty, J. B. Bowers, K. I. Clubb, A. V. Filippenko, D. O. Jones, et al. (2018) "New parallaxes of galactic cepheids from spatially scanning the hubble space telescope: Implications for the hubble constant," *The Astrophysical Journal*, **855**(2), p. 136.

[79] Aghanim, N. et al. (2018) "Planck 2018 results. VI. Cosmological parameters," 1807.06209.

[80] Singh, D., M. Ryan, R. Magee, T. Akhter, S. Shandera, D. Jeong, and C. Hanna (2020) "A gravitational-wave limit on the Chandrasekhar mass of dark matter," 2009.05209.

[81] Akerib, D. S. et al. (2017) "Results from a search for dark matter in the complete LUX exposure," *Phys. Rev. Lett.*, **118**(2), p. 021303, 1608.07648.

[82] Adhikari, G. et al. (2018) "An experiment to search for dark-matter interactions using sodium iodide detectors," *Nature*, **564**(7734), pp. 83–86, [erratum: Nature566,no.7742,E2(2019)], 1906.01791.

[83] Bernabei, R. et al. (2013) "Final model independent result of DAMA/LIBRA-phase1," *Eur. Phys. J.*, **C73**, p. 2648, 1308.5109.

[84] ——— (2018) "First Model Independent Results from DAMA/LIBRA–Phase2," *Universe*, **4**(11), p. 116, [Nucl. Phys. Atom. Energy19,no.4,307(2018)], 1805.10486.

[85] Khachatryan, V. et al. (2016) "Search for Resonant Production of High-Mass Photon Pairs in Proton-Proton Collisions at $\sqrt{s}$ =8 and 13 TeV," *Phys. Rev. Lett.*, **117**(5), p. 051802, 1606.04093.

[86] Aaboud, M. et al. (2016) "Search for resonances in diphoton events at $\sqrt{s}$=13 TeV with the ATLAS detector," *JHEP*, **09**, p. 001, 1606.03833.

[87] Hawkins, M. R. S. (2015) "A new look at microlensing limits on dark matter in the Galactic halo," *Astron. Astrophys.*, **575**, p. A107, 1503.01935.

[88] Bird, S., I. Cholis, J. B. Muñoz, Y. Ali-Haïmoud, M. Kamionkowski, E. D. Kovetz, A. Raccanelli, and A. G. Riess (2016) "Did LIGO detect dark matter?" *Phys. Rev. Lett.*, **116**(20), p. 201301, 1603.00464.

[89] Suwa, Y., T. Yoshida, M. Shibata, H. Umeda, and K. Takahashi (2018) "On the minimum mass of neutron stars," *Mon. Not. Roy. Astron. Soc.*, **481**(3), pp. 3305–3312, 1808.02328.

[90] Bailyn, C. D., R. K. Jain, P. Coppi, and J. A. Orosz (1998) "The Mass distribution of stellar black holes," *Astrophys. J.*, **499**, p. 367, astro-ph/9708032.

[91] Özel, F., D. Psaltis, R. Narayan, and J. E. McClintock (2010) "The Black Hole Mass Distribution in the Galaxy," *Astrophysical Journal*, **725**, pp. 1918–1927, 1006.2834.

[92] Farr, W. M., N. Sravan, A. Cantrell, L. Kreidberg, C. D. Bailyn, I. Mandel, and V. Kalogera (2011) "The Mass Distribution of Stellar-mass Black Holes," *Astrophysical Journal*, **741**, 103, 1011.1459.

[93] Belczynski, K., G. Wiktorowicz, C. L. Fryer, D. E. Holz, and V. Kalogera (2012) "Missing Black Holes Unveil the Supernova Explosion Mechanism," *The Astrophysical Journal*, **757**(1), 91, 1110.1635.

[94] Woosley, S. E. (2017) "Pulsational Pair-Instability Supernovae," *Astrophys. J.*, **836**(2), p. 244, 1608.08939.

[95] Thompson, T. A., C. S. Kochanek, K. Z. Stanek, C. Badenes, R. S. Post, T. Jayasinghe, D. W. Latham, A. Bieryla, G. A. Esquerdo, P. Berlind, M. L. Calkins, J. Tayar, L. Lindegren, J. A. Johnson, T. W.-S. Holoien, K. Auchettl, and K. Covey (2019) "A noninteracting low-mass black hole–giant star binary system," *Science*, **366**(6465), pp. 637–640, https://science.sciencemag.org/content/366/6465/637.full.pdf.
URL https://science.sciencemag.org/content/366/6465/637

[96] Abbott, B. P. et al. (2019) "Search for sub-solar mass ultracompact binaries in Advanced LIGO's second observing run," *Phys. Rev. Lett.*, **123**(16), p. 161102, 1904.08976.

[97] Magee, R., A.-S. Deutsch, P. McClincy, C. Hanna, C. Horst, D. Meacher, C. Messick, S. Shandera, and M. Wade (2018) "Methods for the detection of gravitational waves from subsolar mass ultracompact binaries," *Phys. Rev.*, **D98**(10), p. 103024, 1808.04772.

[98] Abbott, B. P. et al. (2016) "GW151226: Observation of Gravitational Waves from a 22-Solar-Mass Binary Black Hole Coalescence," *Phys. Rev. Lett.*, **116**(24), p. 241103, 1606.04855.

[99] ——— (2016) "GW150914: First results from the search for binary black hole coalescence with Advanced LIGO," *Phys. Rev.*, **D93**(12), p. 122003, 1602.03839.

[100] Abbott, B. P., R. Abbott, T. D. Abbott, F. Acernese, K. Ackley, C. Adams, T. Adams, P. Addesso, R. X. Adhikari, V. B. Adya, C. Affeldt, and Afrough (2017) "GW170104: Observation of a 50-Solar-Mass Binary Black Hole Coalescence at Redshift 0.2," *Phys. Rev. Lett.*, **118**, p. 221101.
URL https://link.aps.org/doi/10.1103/PhysRevLett.118.221101

[101] Abbott, B. P., R. Abbott, T. Abbott, M. Abernathy, F. Acernese, K. Ackley, C. Adams, T. Adams, P. Addesso, R. Adhikari, et al. (2016) "The rate of binary black hole mergers inferred from Advanced LIGO observations surrounding GW150914," *The Astrophysical Journal Letters*, **833**(1), p. L1.

[102] Abbott, B. P. et al. (2016) "Binary Black Hole Mergers in the first Advanced LIGO Observing Run," *Phys. Rev.*, **X6**(4), p. 041015, 1606.04856.

[103] Nakamura, T., M. Sasaki, T. Tanaka, and K. S. Thorne (1997) "Gravitational waves from coalescing black hole MACHO binaries," *Astrophys. J.*, **487**, pp. L139–L142, astro-ph/9708060.

[104] Zeldovich, Y. B. and I. D. Novikov (1967) "The Hypothesis of Cores Retarded during Expansion and the Hot Cosmological Model," *Soviet Astronomy*, **10**(4), pp. 602–603.

[105] Abbott, B., R. Abbott, R. Adhikari, A. Ageev, B. Allen, R. Amin, S. Anderson, W. Anderson, M. Araya, H. Armandula, et al. (2005) "Search for gravitational waves from primordial black hole binary coalescences in the galactic halo," *Physical Review D*, **72**(8), p. 082002.

[106] Abbott, B., R. Abbott, R. Adhikari, J. Agresti, P. Ajith, B. Allen, R. Amin, S. Anderson, W. Anderson, M. Arain, et al. (2008) "Search for gravitational waves from binary inspirals in S3 and S4 LIGO data," *Physical Review D*, **77**(6), p. 062002.

[107] Abbott, B., R. Abbott, T. Abbott, M. Abernathy, F. Acernese, K. Ackley, C. Adams, T. Adams, P. Addesso, R. Adhikari, et al. (2016) "GW150914: The Advanced LIGO detectors in the era of first discoveries," *Physical review letters*, **116**(13), p. 131103.

[108] Lasserre, T. (2000) "Not enough stellar mass machos in the galactic halo," *Astron. Astrophys.*, **355**, pp. L39–L42, astro-ph/0002253.

[109] Bird, S., I. Cholis, J. B. Munoz, Y. Ali-Haimoud, M. Kamionkowski, E. D. Kovetz, A. Raccanelli, and A. G. Riess (2016) "Did LIGO detect dark matter?" *Phys. Rev. Lett.*, **116**(20), p. 201301, 1603.00464.

[110] Clesse, S. and J. García-Bellido (2017) "The clustering of massive Primordial Black Holes as Dark Matter: measuring their mass distribution with Advanced LIGO," *Phys. Dark Univ.*, **15**, pp. 142–147, 1603.05234.

[111] Gaggero, D., G. Bertone, F. Calore, R. M. T. Connors, M. Lovell, S. Markoff, and E. Storm (2017) "Searching for Primordial Black Holes in the radio and X-ray sky," *Phys. Rev. Lett.*, **118**(24), p. 241101, 1612.00457.

[112] Sasaki, M., T. Suyama, T. Tanaka, and S. Yokoyama (2016) "Primordial black hole scenario for the gravitational-wave event GW150914," *Physical Review Letters*, **117**(6), p. 061101.

[113] Eroshenko, Y. N. (2016) "Formation of PBHs binaries and gravitational waves from their merge," *ArXiv e-prints*, 1604.04932.

[114] Green, A. M. (2016) "Microlensing and dynamical constraints on primordial black hole dark matter with an extended mass function," *Phys. Rev.*, **D94**(6), p. 063530, 1609.01143.

[115] Kühnel, F. and K. Freese (2017) "Constraints on Primordial Black Holes with Extended Mass Functions," *Phys. Rev.*, **D95**(8), p. 083508, 1701.07223.

[116] Alcock, C. et al. (1996) "The MACHO project first year LMC results: The Microlensing rate and the nature of the galactic dark halo," *Astrophys. J.*, **461**, p. 84, astro-ph/9506113.

[117] Wyrzykowski, L., J. Skowron, S. Kozłowski, A. Udalski, M. K. Szymański, M. Kubiak, G. Pietrzyński, I. Soszyński, O. Szewczyk, K. Ulaczyk, R. Poleski, and P. Tisserand (2011) "The OGLE view of microlensing towards the Magellanic Clouds - IV. OGLE-III SMC data and final conclusions on MACHOs," *Monthly Notices of the RAS*, **416**, pp. 2949–2961, 1106.2925.

[118] Carr, B., M. Raidal, T. Tenkanen, V. Vaskonen, and H. Veermäe (2017) "Primordial black hole constraints for extended mass functions," *Physical Review D*, **96**(2), 023514, 1705.05567.

[119] Hawkins, M. R. S. (2015) "A new look at microlensing limits on dark matter in the Galactic halo," *Astron. Astrophys.*, **575**, p. A107, 1503.01935.

[120] Paczynski, B. (1986) "Gravitational microlensing by the galactic halo," *Astrophysical Journal*, **304**, pp. 1–5.

[121] Sofue, Y. (2013) "Rotation Curve and Mass Distribution in the Galactic Center - From Black Hole to Entire Galaxy," *Publications of the ASJ*, **65**, 118, 1307.8241.

[122] Bhattacharjee, P., S. Chaudhury, and S. Kundu (2014) "Rotation Curve of the Milky Way out to $\sim$ 200 kpc," *Astrophys. J.*, **785**, p. 63, 1310.2659.

[123] Deason, A. J., V. Belokurov, N. W. Evans, and J. An (2012) "Broken degeneracies: the rotation curve and velocity anisotropy of the Milky Way halo," *Monthly Notices of the RAS*, **424**, pp. L44–L48, 1204.5189.

[124] Bratek, Ł., S. Sikora, J. Jałocha, and M. Kutschera (2014) "A lower bound on the Milky Way mass from general phase-space distribution function models," *Astronomy and Astrophysics*, **562**, A134, 1108.1629.

[125] Green, A. M. (2017) "Astrophysical uncertainties on stellar microlensing constraints on multi-Solar mass primordial black hole dark matter," *ArXiv e-prints*, 1705.10818.

[126] Alcock, C. et al. (1999) "Discovery and characterization of a caustic crossing microlensing event in the SMC," *Astrophys. J.*, **518**, p. 44, astro-ph/9807163.

[127] MACHO and C. Alcock (2000) "Binary microlensing events from the MACHO project," *Astrophys. J.*, **541**, p. 270, astro-ph/9907369.

[128] Lee, C.-H., A. Riffeser, S. Seitz, R. Bender, and J. Koppenhoefer (2015) "Microlensing events from the 11-year Observations of the Wendelstein Calar Alto Pixellensing Project," *Astrophysical Journal*, **806**, 161, 1504.07246.

[129] Lattimer, J. M. (2012) "The Nuclear Equation of State and Neutron Star Masses," *Annual Review of Nuclear and Particle Science*, **62**, pp. 485–515, 1305.3510.

[130] Littenberg, T. B., B. Farr, S. Coughlin, V. Kalogera, and D. E. Holz (2015) "Neutron stars versus black holes: probing the mass gap with LIGO/Virgo," *Astrophys. J.*, **807**(2), p. L24, 1503.03179.

[131] Chiba, T. and S. Yokoyama (2017) "Spin Distribution of Primordial Black Holes," *ArXiv e-prints*, 1704.06573.

[132] LIGO Scientific Collaboration, J. Aasi, B. P. Abbott, R. Abbott, T. Abbott, M. R. Abernathy, K. Ackley, C. Adams, T. Adams, P. Addesso, and et al. (2015) "Advanced LIGO," *Classical and Quantum Gravity*, **32**(7), 074001, 1411.4547.

[133] Acernese, F., M. Agathos, K. Agatsuma, D. Aisa, N. Allemandou, A. Allocca, J. Amarni, P. Astone, G. Balestri, G. Ballardin, and et al. (2015) "Advanced Virgo: a second-generation interferometric gravitational wave detector," *Classical and Quantum Gravity*, **32**(2), 024001, 1408.3978.

[134] Abbott, B. P. et al. (2016) "GW151226: Observation of Gravitational Waves from a 22-Solar-Mass Binary Black Hole Coalescence," *Phys. Rev. Lett.*, **116**(24), p. 241103, 1606.04855.

[135] ——— (2017) "GW170104: Observation of a 50-Solar-Mass Binary Black Hole Coalescence at Redshift 0.2," *Phys. Rev. Lett.*, **118**(22), p. 221101, 1706.01812.

[136] ——— (2017) "GW170608: Observation of a 19-solar-mass Binary Black Hole Coalescence," *Astrophys. J.*, **851**(2), p. L35, 1711.05578.

[137] ——— (2017) "GW170814: A Three-Detector Observation of Gravitational Waves from a Binary Black Hole Coalescence," *Phys. Rev. Lett.*, **119**(14), p. 141101, 1709.09660.

[138] ——— (2016) "Binary Black Hole Mergers in the first Advanced LIGO Observing Run," *Phys. Rev.*, **X6**(4), p. 041015, 1606.04856.

[139] ——— (2017) "Search for intermediate mass black hole binaries in the first observing run of Advanced LIGO," *Phys. Rev.*, **D96**(2), p. 022001, 1704.04628.

[140] Owen, B. J. and B. S. Sathyaprakash (1999) "Matched filtering of gravitational waves from inspiraling compact binaries: Computational cost and template placement," *Phys. Rev.*, **D60**, p. 022002, gr-qc/9808076.

[141] Abbott, B. P. et al. (2016) "Upper Limits on the Rates of Binary Neutron Star and Neutron Star–black Hole Mergers From Advanced Ligo's First Observing run," *Astrophys. J.*, **832**(2), p. L21, 1607.07456.

[142] Cutler, C. and E. E. Flanagan (1994) "Gravitational waves from merging compact binaries: How accurately can one extract the binary's parameters from the inspiral wave form?" *Phys. Rev.*, **D49**, pp. 2658–2697, gr-qc/9402014.

[143] Finn, L. S. and D. F. Chernoff (1993) "Observing binary inspiral in gravitational radiation: One interferometer," *Phys. Rev.*, **D47**, pp. 2198–2219, gr-qc/9301003.

[144] Abadie, J. et al. (2010) "Predictions for the Rates of Compact Binary Coalescences Observable by Ground-based Gravitational-wave Detectors," *Class. Quant. Grav.*, **27**, p. 173001, 1003.2480.

[145] Sutton, P. (2003) "S3 performance of the LIGO interferometers as measured by sensemonitor," **27**, LIGO-T030276-v1.
URL https://dcc.ligo.org/cgi-bin/private/DocDB/ShowDocument?docid=27267

[146] Chiba, T. and S. Yokoyama (2017) "Spin Distribution of Primordial Black Holes," *PTEP*, **2017**(8), p. 083E01, 1704.06573.

[147] Cho, H.-S. and C.-H. Lee (2018) "Gravitational Wave Searches for Aligned-Spin Binary Neutron Stars Using Nonspinning Templates," *J. Korean Phys. Soc.*, **72**(1), pp. 1–5, 1708.00426.

[148] Capano, C., I. Harry, S. Privitera, and A. Buonanno (2016) "Implementing a search for gravitational waves from binary black holes with nonprecessing spin," *Phys. Rev.*, **D93**(12), p. 124007, 1602.03509.

[149] Ajith, P., N. Fotopoulos, S. Privitera, A. Neunzert, and A. J. Weinstein (2014) "Effectual template bank for the detection of gravitational waves from inspiralling compact binaries with generic spins," *Phys. Rev.*, **D89**(8), p. 084041, 1210.6666.

[150] Shandera, S., D. Jeong, and H. S. G. Gebhardt (2018) "Gravitational Waves from Binary Mergers of Sub-solar Mass Dark Black Holes," 1802.08206.

[151] Kouvaris, C., P. Tinyakov, and M. H. G. Tytgat (2018) "Non-Primordial Solar Mass Black Holes," 1804.06740.

[152] Ioka, K., T. Chiba, T. Tanaka, and T. Nakamura (1998) "Black Hole Binary Formation in the Expanding Universe : Three Body Problem Approximation," *Physical Review D*, **58**(6), p. 063003, 9807018.
URL http://link.aps.org/doi/10.1103/PhysRevD.58.063003{%}5Cnhttp://arxiv.org/abs/astro-ph/9807018{%}5Cnhttp://dx.doi.org/10.1103/PhysRevD.58.063003

[153] Nakamura, T., M. Sasaki, T. Tanaka, and K. S. Thorne (1997) "Gravitational waves from coalescing black hole MACHO binaries," *Astrophys. J.*, **487**, pp. L139–L142, astro-ph/9708060.

[154] Sasaki, M., T. Suyama, T. Tanaka, and S. Yokoyama (2016) "Primordial Black Hole Scenario for the Gravitational-Wave Event GW150914," *Phys. Rev. Lett.*, **117**(6), p. 061101, 1603.08338.

[155] Eroshenko, Yu. N. (2016) "Gravitational waves from primordial black holes collisions in binary systems," 1604.04932.

[156] Wang, S., Y.-F. Wang, Q.-G. Huang, and T. G. F. Li (2018) "Constraints on the Primordial Black Hole Abundance from the First Advanced LIGO Observation Run Using the Stochastic Gravitational-Wave Background," *Phys. Rev. Lett.*, **120**(19), p. 191102, 1610.08725.

[157] Ali-Haïmoud, Y., E. D. Kovetz, and M. Kamionkowski (2017) "Merger rate of primordial black-hole binaries," *Phys. Rev.*, **D96**(12), p. 123523, 1709.06576.

[158] Wyrzykowski, L. et al. (2011) "The OGLE View of Microlensing towards the Magellanic Clouds. III. Ruling out sub-solar MACHOs with the OGLE-III LMC data," *Mon. Not. Roy. Astron. Soc.*, **413**, p. 493, 1012.1154.

[159] Green, A. M. (2017) "Astrophysical uncertainties on stellar microlensing constraints on multi-Solar mass primordial black hole dark matter," *Phys. Rev.*, **D96**(4), p. 043020, 1705.10818.

[160] Abbott, B. P. et al. (2016) "Observation of Gravitational Waves from a Binary Black Hole Merger," *Phys. Rev. Lett.*, **116**(6), p. 061102, 1602.03837.

[161] Chandrasekhar, S. (1935) "The highly collapsed configurations of a stellar mass (Second paper)," *Mon. Not. Roy. Astron. Soc.*, **95**, pp. 207–225.

[162] ——— (1931) "The maximum mass of ideal white dwarfs," *Astrophys. J.*, **74**, pp. 81–82.

[163] Glendenning, N. K. (2012) *Compact stars: Nuclear physics, particle physics and general relativity*, Springer Science & Business Media.

[164] Potekhin, A. Y., A. F. Fantina, N. Chamel, J. M. Pearson, and S. Goriely (2013) "Analytical representations of unified equations of state for neutron-star matter," *Astron. Astrophys.*, **560**, p. A48, 1310.0049.

[165] Martinez, J. G., K. Stovall, P. C. C. Freire, J. S. Deneva, T. M. Tauris, A. Ridolfi, N. Wex, F. A. Jenet, M. A. McLaughlin, and M. Bagchi (2017) "Pulsar J1411+2551: A Low-mass Double Neutron Star System," *Astrophys. J.*, **851**(2), p. L29, 1711.09804.

[166] Martinez, J. G., K. Stovall, P. C. C. Freire, J. S. Deneva, F. A. Jenet, M. A. McLaughlin, M. Bagchi, S. D. Bates, and A. Ridolfi (2015) "Pulsar J0453+1559: A Double Neutron Star System with a Large Mass Asymmetry," *Astrophys. J.*, **812**(2), p. 143, 1509.08805.

[167] Lattimer, J. M. (2012) "The Nuclear Equation of State and Neutron Star Masses," *Annual Review of Nuclear and Particle Science*, **62**(1), pp. 485–515, https://doi.org/10.1146/annurev-nucl-102711-095018.
URL https://doi.org/10.1146/annurev-nucl-102711-095018

[168] Kreidberg, L., C. D. Bailyn, W. M. Farr, and V. Kalogera (2012) "Mass Measurements of Black Holes in X-Ray Transients: Is There a Mass Gap?" *Astrophysical Journal*, **757**, 36, 1205.1805.

[169] Hawking, S. (1971) "Gravitationally Collapsed Objects of Very Low Mass," *Monthly Notices of the Royal Astronomical Society*, **152**(1), pp. 75–78.
URL https://academic.oup.com/mnras/article-lookup/doi/10.1093/mnras/152.1.75

[170] Carr, B. J. and S. W. Hawking (1974) "Black Holes in the Early Universe," *Monthly Notices of the Royal Astronomical Society*, **168**(2), pp. 399–415. URL https://academic.oup.com/mnras/article-lookup/doi/10.1093/mnras/168.2.399

[171] Mészáros, P. (1974) "The behaviour of point masses in an expanding cosmological substratum," *Astronomy and Astrophysics*, **37**, pp. 225–228. URL https://academic.oup.com/mnras/article-lookup/doi/10.1093/mnras/168.2.399

[172] Chapline, G. F. (1975) "Cosmological effects of primordial black holes," *Nature*, **253**(5489), pp. 251–252. URL http://www.nature.com/doifinder/10.1038/253251a0

[173] Clesse, S. and J. García-Bellido (2017) "The clustering of massive Primordial Black Holes as Dark Matter: measuring their mass distribution with Advanced LIGO," *Phys. Dark Univ.*, **15**, pp. 142–147, 1603.05234.

[174] Kovetz, E. D., I. Cholis, P. C. Breysse, and M. Kamionkowski (2017) "Black hole mass function from gravitational wave measurements," *Phys. Rev.*, **D95**(10), p. 103010, 1611.01157.

[175] Raccanelli, A., E. D. Kovetz, S. Bird, I. Cholis, and J. B. Munoz (2016) "Determining the progenitors of merging black-hole binaries," *Phys. Rev.*, **D94**(2), p. 023516, 1605.01405.

[176] Cholis, I., E. D. Kovetz, Y. Ali-Haïmoud, S. Bird, M. Kamionkowski, J. B. Muñoz, and A. Raccanelli (2016) "Orbital eccentricities in primordial black hole binaries," *Phys. Rev.*, **D94**(8), p. 084013, 1606.07437.

[177] Raccanelli, A. (2017) "Gravitational wave astronomy with radio galaxy surveys," *Mon. Not. Roy. Astron. Soc.*, **469**(1), pp. 656–670, 1609.09377.

[178] Koushiappas, S. M. and A. Loeb (2017) "Maximum redshift of gravitational wave merger events," *Phys. Rev. Lett.*, **119**(22), p. 221104, 1708.07380.

[179] Nishikawa, H., E. D. Kovetz, M. Kamionkowski, and J. Silk (2017) "Primordial-black-hole mergers in dark-matter spikes," 1708.08449.

[180] Abbott, B. P. et al. (2018) "Effects of data quality vetoes on a search for compact binary coalescences in Advanced LIGO's first observing run," *Class. Quant. Grav.*, **35**(6), p. 065010, 1710.02185.

[181] Abbott, B., R. Abbott, T. Abbott, M. Abernathy, F. Acernese, K. Ackley, C. Adams, T. Adams, P. Addesso, R. Adhikari, et al. (2016) "Binary black hole mergers in the first advanced LIGO observing run," *Physical Review X*, **6**(4), p. 041015.

[182] Cannon, K. et al. (2012) "Toward Early-Warning Detection of Gravitational Waves from Compact Binary Coalescence," *Astrophys. J.*, **748**, p. 136, 1107.2665.

[183] GstLAL (2020), "GstLAL software: git.ligo.org/lscsoft/gstlal," .

[184] LIGO Scientific Collaboration (2020), "LIGO Algorithm Library - LALSuite," free software (GPL).

[185] LVC (2018) "Search for sub-solar mass ultracompact binaries in Advanced LIGO's first observing run," *LIGO DCC*, **P1800158**.
URL https://dcc.ligo.org/LIGO-P1800158

[186] Abbott, B. P. et al. (2017) "Upper Limits on the Stochastic Gravitational-Wave Background from Advanced LIGO's First Observing Run," *Phys. Rev. Lett.*, **118**(12), p. 121101, [Erratum: Phys. Rev. Lett.119,no.2,029901(2017)], 1612.02029.

[187] Mandic, V., S. Bird, and I. Cholis (2016) "Stochastic Gravitational-Wave Background due to Primordial Binary Black Hole Mergers," *Physical Review Letters*, **117**(20), 201102, 1608.06699.

[188] Cholis, I. (2017) "On the gravitational wave background from black hole binaries after the first LIGO detections," *J. Cosmology Astropart. Phys.*, **6**, 037, 1609.03565.

[189] Raidal, M., V. Vaskonen, and H. Veermäe (2017) "Gravitational waves from primordial black hole mergers," *J. Cosmology Astropart. Phys.*, **9**, 037, 1707.01480.

[190] Desjacques, V. and A. Riotto (2018) "The Spatial Clustering of Primordial Black Holes," 1806.10414.

[191] Ballesteros, G., P. D. Serpico, and M. Taoso (2018) "On the merger rate of primordial black holes: effects of nearest neighbours distribution and clustering," 1807.02084.

[192] Ali-Haïmoud, Y. (2018) "Correlation function of high-threshold peaks and application to the initial (non)clustering of primordial black holes," 1805.05912.

[193] Bellomo, N., J. L. Bernal, A. Raccanelli, and L. Verde (2018) "Primordial Black Holes as Dark Matter: Converting Constraints from Monochromatic to Extended Mass Distributions," *JCAP*, **1801**(01), p. 004, 1709.07467.

[194] Abbott, B. et al. (2018) "GWTC-1: A Gravitational-Wave Transient Catalog of Compact Binary Mergers Observed by LIGO and Virgo during the First and Second Observing Runs," 1811.12907.

[195] Abbott, B. P. et al. (2018) "Binary Black Hole Population Properties Inferred from the First and Second Observing Runs of Advanced LIGO and Advanced Virgo," 1811.12940.

[196] Dal Canton, T. and I. W. Harry (2017) "Designing a template bank to observe compact binary coalescences in Advanced LIGO's second observing run," 1705.01845.

[197] Timmes, F. X., S. E. Woosley, and T. A. Weaver (1996) "The Neutron star and black hole initial mass function," *Astrophys. J.*, **457**, p. 834, astro-ph/9510136.

[198] Antoniadis, J., P. C. C. Freire, N. Wex, T. M. Tauris, R. S. Lynch, M. H. van Kerkwijk, M. Kramer, C. Bassa, V. S. Dhillon, T. Driebe, J. W. T. Hessels, V. M. Kaspi, V. I. Kondratiev, N. Langer, T. R. Marsh, M. A. McLaughlin, T. T. Pennucci, S. M. Ransom, I. H. Stairs, J. van Leeuwen, J. P. W. Verbiest, and D. G. Whelan (2013) "A Massive Pulsar in a Compact Relativistic Binary," *Science*, **340**(6131), https://science.sciencemag.org/content/340/6131/1233232.full.pdf.
URL https://science.sciencemag.org/content/340/6131/1233232

[199] Imshennik, V. S. (1992) "A possible scenario of a supernova explosion as a result of the gravitational collapse of a massive stellar core," *Soviet Astronomy Letters*, **18**, p. 194.

[200] Davies, M. B., A. King, S. Rosswog, and G. Wynn (2002) "Gamma-ray bursts, supernova kicks, and gravitational radiation," *Astrophys. J.*, **579**, pp. L63–L66, astro-ph/0204358.

[201] Carr, B. J. (1975) "The Primordial black hole mass spectrum," *Astrophys. J.*, **201**, pp. 1–19.

[202] Jedamzik, K. (1997) "Primordial black hole formation during the QCD epoch," *Phys. Rev.*, **D55**, pp. 5871–5875, astro-ph/9605152.

[203] Widerin, P. and C. Schmid (1998) "Primordial black holes from the QCD transition?" *Preprint: arXiv astro-ph/9808142*, astro-ph/9808142.

[204] Georg, J. and S. Watson (2017) "A Preferred Mass Range for Primordial Black Hole Formation and Black Holes as Dark Matter Revisited," *JHEP*, **09**, p. 138, 1703.04825.

[205] Byrnes, C. T., M. Hindmarsh, S. Young, and M. R. S. Hawkins (2018) "Primordial black holes with an accurate QCD equation of state," *JCAP*, **1808**(08), p. 041, 1801.06138.

[206] Deng, H. and A. Vilenkin (2017) "Primordial black hole formation by vacuum bubbles," *JCAP*, **1712**(12), p. 044, 1710.02865.

[207] Kouvaris, C. and P. Tinyakov (2011) "Constraining Asymmetric Dark Matter through observations of compact stars," *Phys. Rev.*, **D83**, p. 083512, 1012.2039.

[208] de Lavallaz, A. and M. Fairbairn (2010) "Neutron Stars as Dark Matter Probes," *Phys. Rev.*, **D81**, p. 123521, 1004.0629.

[209] Goldman, I. and S. Nussinov (1989) "Weakly interacting massive particles and neutron stars," *Phys. Rev. D*, **40**, pp. 3221–3230.
URL https://link.aps.org/doi/10.1103/PhysRevD.40.3221

[210] Bramante, J. and F. Elahi (2015) "Higgs portals to pulsar collapse," *Phys. Rev.*, **D91**(11), p. 115001, 1504.04019.

[211] Bramante, J. and T. Linden (2014) "Detecting Dark Matter with Imploding Pulsars in the Galactic Center," *Phys. Rev. Lett.*, **113**(19), p. 191301, 1405.1031.

[212] Bramante, J., T. Linden, and Y.-D. Tsai (2018) "Searching for dark matter with neutron star mergers and quiet kilonovae," *Phys. Rev.*, **D97**(5), p. 055016, 1706.00001.

[213] Gresham, M. I. and K. M. Zurek (2019) "Asymmetric Dark Stars and Neutron Star Stability," *Phys. Rev.*, **D99**(8), p. 083008, 1809.08254.

[214] Breit, J. D., S. Gupta, and A. Zaks (1984) "Cold Bose stars," *Physics Letters B*, **140**, pp. 329–332.

[215] Urena-Lopez, L. A., T. Matos, and R. Becerril (2002) "Inside oscillatons," *Class. Quant. Grav.*, **19**, pp. 6259–6277.

[216] Davis, D., T. Massinger, et al. (2018) "Improving the Sensitivity of Advanced LIGO Using Noise Subtraction," *Preprint: arXiv 1809.05348*, 1809.05348.

[217] Abbott, B. P. et al. (2016) "Characterization of transient noise in Advanced LIGO relevant to gravitational wave signal GW150914," *Class. Quant. Grav.*, **33**(13), 1602.03844.

[218] Nuttall, L. (2018) "Characterizing transient noise in the LIGO detectors," *Royal Society Proceedings A*, **376**(2120).

[219] Berger, B. (2018) "Identification and mitigation of Advanced LIGO noise sources," *J. Phys.: Conf. Ser.*, **957**(012004).

[220] Buonanno, A., B. R. Iyer, E. Ochsner, Y. Pan, and B. S. Sathyaprakash (2009) "Comparison of post-Newtonian templates for compact binary inspiral signals in gravitational-wave detectors," *Physical Review D*, **80**, 084043, 0907.0700.

[221] Abbott, B. P. et al. (2017) "Multi-messenger Observations of a Binary Neutron Star Merger," *Astrophys. J.*, **848**(2), p. L12, 1710.05833.

[222] Cahillane, C., J. Betzwieser, D. A. Brown, E. Goetz, E. D. Hall, K. Izumi, S. Kand hasamy, S. Karki, J. S. Kissel, G. Mendell, R. L. Savage, D. Tuyenbayev, A. Urban, A. Viets, M. Wade, and A. J. Weinstein (2017) "Calibration uncertainty for Advanced LIGO's first and second observing runs," *Physical Review D*, **96**, 102001, 1708.03023.

[223] Viets, A. et al. (2018) "Reconstructing the calibrated strain signal in the Advanced LIGO detectors," *Class. Quant. Grav.*, **35**(9), p. 095015, 1710.09973.

[224] Abbott, B. P. et al. (2017) "Gravitational Waves and Gamma-rays from a Binary Neutron Star Merger: GW170817 and GRB 170817A," *Astrophys. J.*, **848**(2), p. L13, 1710.05834.

[225] Coulter, D. A. et al. (2017) "Swope Supernova Survey 2017a (SSS17a), the Optical Counterpart to a Gravitational Wave Source," *Science*, [Science358,1556(2017)], 1710.05452.

[226] Nicholl, M. et al. (2017) "The Electromagnetic Counterpart of the Binary Neutron Star Merger LIGO/VIRGO GW170817. III. Optical and UV Spectra of a Blue Kilonova From Fast Polar Ejecta," *Astrophys. J.*, **848**(2), p. L18, 1710.05456.

[227] Metzger, B. D. (2017) "Welcome to the Multi-Messenger Era! Lessons from a Neutron Star Merger and the Landscape Ahead," *Preprint: arXiv 1710.05931*, 1710.05931.

[228] Metzger, B. D. and A. L. Piro (2014) "Optical and X-ray emission from stable millisecond magnetars formed from the merger of binary neutron stars," *Mon. Not. Roy. Astron. Soc.*, **439**, pp. 3916–3930, 1311.1519.

[229] Ciolfi, R. and D. M. Siegel (2015) "Short gamma-ray bursts in the "time-reversal" scenario," *Astrophys. J.*, **798**(2), p. L36, 1411.2015.

[230] Siegel, D. M. and R. Ciolfi (2016) "Electromagnetic emission from long-lived binary neutron star merger remnants II: lightcurves and spectra," *Astrophys. J.*, **819**(1), p. 15, 1508.07939.

[231] Abbott, B. P. et al. (2017) "Search for Post-merger Gravitational Waves from the Remnant of the Binary Neutron Star Merger GW170817," *Astrophys. J.*, **851**(1), p. L16, 1710.09320.

[232] Foucart, F., T. Hinderer, and S. Nissanke (2018) "Remnant baryon mass in neutron star-black hole mergers: Predictions for binary neutron star mimickers and rapidly spinning black holes," *Phys. Rev. D*, **98**, p. 081501. URL https://link.aps.org/doi/10.1103/PhysRevD.98.081501

[233] Perna, R., D. Lazzati, and B. Giacomazzo (2016) "Short Gamma-Ray Bursts from the Merger of Two Black Holes," *Astrophys. J.*, **821**(1), p. L18, 1602.05140.

[234] Murase, K., K. Kashiyama, P. Mészáros, I. Shoemaker, and N. Senno (2016) "Ultrafast Outflows from Black Hole Mergers with a Minidisk," *Astrophys. J.*, **822**(1), p. L9, 1602.06938.

[235] Connaughton, V. et al. (2016) "Fermi GBM Observations of LIGO Gravitational Wave event GW150914," *Astrophys. J.*, **826**(1), p. L6, 1602.03920.

[236] Savchenko, V. et al. (2016) "INTEGRAL upper limits on gamma-ray emission associated with the gravitational wave event GW150914," *Astrophys. J.*, **820**(2), p. L36, 1602.04180.

[237] Callister, T. A., M. M. Anderson, G. Hallinan, L. R. D'addario, J. Dowell, N. E. Kassim, T. J. W. Lazio, D. C. Price, and F. K. Schinzel (2019) "A First Search for Prompt Radio Emission from a Gravitational-Wave Event," *Astrophys. J.*, **877**(2), p. L39, 1903.06786.

[238] Smith, M., D. Fox, D. Cowen, P. Mészáros, G. Tešić, J. Fixelle, I. Bartos, P. Sommers, A. Ashtekar, G. J. Babu, et al. (2013) "The astrophysical multimessenger observatory network (AMON)," *Astroparticle Physics*, **45**, pp. 56–70.

[239] Burns, E. et al. (2019) "A Fermi Gamma-ray Burst Monitor Search for Electromagnetic Signals Coincident with Gravitational-Wave Candidates in Advanced LIGO's First Observing Run," *Astrophys. J.*, **871**(1), p. 90, 1810.02764.

[240] Totani, T. (2013) "Cosmological Fast Radio Bursts from Binary Neutron Star Mergers," *Pub. Astron. Soc. Jpn.*, **65**, p. L12, 1307.4985.

[241] Wang, J.-S., Y.-P. Yang, X.-F. Wu, Z.-G. Dai, and F.-Y. Wang (2016) "Fast Radio Bursts from the Inspiral of Double Neutron Stars," *Astrophys. J.*, **822**(1), p. L7, 1603.02014.

[242] Dokuchaev, V. I. and Yu. N. Eroshenko (2017) "Recurrent fast radio bursts from collisions of neutron stars in the evolved stellar clusters," 1701.02492.

[243] Babak, S., R. Biswas, P. Brady, D. A. Brown, K. Cannon, C. D. Capano, J. H. Clayton, T. Cokelaer, J. D. Creighton, T. Dent, et al. (2013) "Searching for gravitational waves from binary coalescence," *Physical Review D*, **87**(2), p. 024033.

[244] Nitz, A., I. Harry, D. Brown, C. M. Biwer, J. Willis, T. D. Canton, L. Pekowsky, C. Capano, T. Dent, A. R. Williamson, S. De, M. Cabero, B. Machenschalk, P. Kumar, S. Reyes, T. Massinger, D. Macleod, A. Lenon, S. Fairhurst, A. Nielsen, S. Khan, shasvath, F. Pannarale, L. Singer, dfinstad, M. Tápai, H. Gabbard, C. Sugar, P. Couvares, and L. M. Zertuche (2019), "gwastro/pycbc: Pre-O3 release v1," .
URL https://doi.org/10.5281/zenodo.2556644

[245] Abbott, B. P. et al. (2017) "Search for Gravitational Waves Associated with Gamma-Ray Bursts During the First Advanced LIGO Observing Run and Implications for the Origin of GRB 150906B," *Astrophys. J.*, **841**(2), p. 89, 1611.07947.

[246] Essick, R. et al. (2017) "GCN Circular 21505," .
URL https://gcn.gsfc.nasa.gov/other/G298048.gcn3

[247] Nitz, A. H., T. Dal Canton, D. Davis, and S. Reyes (2018) "Rapid detection of gravitational waves from compact binary mergers with PyCBC Live," *Phys. Rev. D*, **98**, p. 024050.
URL https://link.aps.org/doi/10.1103/PhysRevD.98.024050

[248] Cannon, K., C. Hanna, and J. Peoples (2015) "Likelihood-ratio ranking statistic for compact binary coalescence candidates with rate estimation," *arXiv preprint arXiv:1504.04632*.

[249] Callister, T. A., J. B. Kanner, T. J. Massinger, S. Dhurandhar, and A. J. Weinstein (2017) "Observing Gravitational Waves with a Single Detector," *Class. Quant. Grav.*, **34**(15), p. 155007, 1704.00818.

[250] Vallisneri, M., J. Kanner, R. Williams, A. Weinstein, and B. Stephens (2015) "The LIGO Open Science Center," *J. Phys. Conf. Ser.*, **610**(1), p. 012021, 1410.4839.

[251] Cannon, K., C. Hanna, and D. Keppel (2013) "Method to estimate the significance of coincident gravitational-wave observations from compact binary coalescence," *Phys. Rev.*, **D88**(2), p. 024025, 1209.0718.

[252] Fong, H. K. Y. (2018) *From simulation to signals: Analyzing gravitational waves from compact binary coalescences*, Ph.D. thesis, University of Toronto.

[253] Owen, B. J. (1996) "Search templates for gravitational waves from inspiraling binaries: Choice of template spacing," *Phys. Rev.*, **D53**, pp. 6749–6761, gr-qc/9511032.

[254] Singer, L. P. and L. R. Price (2016) "Rapid Bayesian position reconstruction for gravitational-wave transients," *Phys. Rev.*, **D93**(2), p. 024013, 1508.03634.

[255] Allen, B., W. G. Anderson, P. R. Brady, D. A. Brown, and J. D. Creighton (2012) "FINDCHIRP: An algorithm for detection of gravitational waves from inspiraling compact binaries," *Physical Review D*, **85**(12), p. 122006.

[256] Cannon, K., R. Cariou, A. Chapman, M. Crispin-Ortuzar, N. Fotopoulos, M. Frei, C. Hanna, E. Kara, D. Keppel, L. Liao, et al. (2012) "Toward early-warning detection of gravitational waves from compact binary coalescence," *The Astrophysical Journal*, **748**(2), p. 136.

[257] Gstreamer (2020), "Gstreamer software: https://gstreamer.freedesktop.org," .

[258] Owen, B. J. and B. S. Sathyaprakash (1999) "Matched filtering of gravitational waves from inspiraling compact binaries: Computational cost and template placement," *Physical Review D*, **60**(2), p. 022002.

[259] Harry, I. W., B. Allen, and B. Sathyaprakash (2009) "Stochastic template placement algorithm for gravitational wave data analysis," *Physical Review D*, **80**(10), p. 104014.

[260] Blanchet, L., T. Damour, B. R. Iyer, C. M. Will, and A. Wiseman (1995) "Gravitational radiation damping of compact binary systems to second postNewtonian order," *Phys. Rev. Lett.*, **74**, pp. 3515–3518, gr-qc/9501027.

[261] Buonanno, A., B. Iyer, E. Ochsner, Y. Pan, and B. S. Sathyaprakash (2009) "Comparison of post-Newtonian templates for compact binary inspiral signals in gravitational-wave detectors," *Phys. Rev.*, **D80**, p. 084043, 0907.0700.

[262] Ajith, P., S. Babak, Y. Chen, M. Hewitson, B. Krishnan, J. Whelan, B. Bruegmann, P. Diener, J. Gonzalez, M. Hannam, et al. (2007) "A phenomenological template family for black-hole coalescence waveforms," *Classical and Quantum Gravity*, **24**(19), p. S689.

[263] Ozel, F., D. Psaltis, R. Narayan, and A. S. Villarreal (2012) "On the Mass Distribution and Birth Masses of Neutron Stars," *Astrophys. J.*, **757**, p. 55, 1201.1006.

[264] Thorsett, S. E. and D. Chakrabarty (1999) "Neutron star mass measurements. I. Radio pulsars," *The Astrophysical Journal*, **512**(1), p. 288.

[265] Abbott, B. P. et al. (2016) "GW150914: First results from the search for binary black hole coalescence with Advanced LIGO," *Phys. Rev.*, **D93**(12), p. 122003, 1602.03839.

[266] Finn, L. S. and D. F. Chernoff (1993) "Observing binary inspiral in gravitational radiation: One interferometer," *Physical Review D*, **47**(6), p. 2198.

[267] Mukherjee, D. et al. (2018) "The GstLAL template bank for spinning compact binary mergers in the second observation run of Advanced LIGO and Virgo," 1812.05121.

[268] Cannon, K. C. (2008) "A Bayesian coincidence test for noise rejection in a gravitational-wave burst search," *Classical and Quantum Gravity*, **25**(10), p. 105024.

[269] Dent, T. and J. Veitch (2014) "Optimizing gravitational-wave searches for a population of coalescing binaries: Intrinsic parameters," *Phys. Rev.*, **D89**(6), p. 062002, 1311.7174.

[270] Cannon, K., C. Hanna, and J. Peoples (2015) "Likelihood-Ratio Ranking Statistic for Compact Binary Coalescence Candidates with Rate Estimation," *arXiv e-prints*, arXiv:1504.04632, 1504.04632.

[271] Farr, W. M., J. R. Gair, I. Mandel, and C. Cutler (2015) "Counting and confusion: Bayesian rate estimation with multiple populations," *Physical Review D*, **91**, 023005, 1302.5341.

[272] Lattimer, J. and D. Schramm (1976) "The tidal disruption of neutron stars by black holes in close binaries," *Astrophys. J.*, **210**, p. 549.

[273] Lee, W. H. and E. Ramirez-Ruiz (2007) "The Progenitors of Short Gamma-Ray Bursts," *New J. Phys.*, **9**, p. 17, astro-ph/0701874.

[274] Li, L.-X. and B. Paczynski (1998) "Transient events from neutron star mergers," *Astrophys. J. Lett.*, **507**, p. L59, astro-ph/9807272.

[275] Metzger, B., G. Martinez-Pinedo, S. Darbha, E. Quataert, A. Arcones, D. Kasen, R. Thomas, P. Nugent, I. Panov, and N. Zinner (2010) "Electromagnetic Counterparts of Compact Object Mergers Powered by the Radioactive Decay of R-process Nuclei," *Mon. Not. Roy. Astron. Soc.*, **406**, p. 2650, 1001.5029.

[276] Nakar, E. and T. Piran (2011) "Radio Remnants of Compact Binary Mergers - the Electromagnetic Signal that will follow the Gravitational Waves," *Nature*, **478**, pp. 82–84, 1102.1020.

[277] Metzger, B. and E. Berger (2012) "What is the Most Promising Electromagnetic Counterpart of a Neutron Star Binary Merger?" *Astrophys. J.*, **746**, p. 48, 1108.6056.

[278] Metzger, B. D. and C. Zivancev (2016) "Pair Fireball Precursors of Neutron Star Mergers," *Mon. Not. Roy. Astron. Soc.*, **461**(4), pp. 4435–4440, 1605.01060.

[279] Abbott, B. P. et al. (2019) "Tests of General Relativity with the Binary Black Hole Signals from the LIGO-Virgo Catalog GWTC-1," *Phys. Rev. D*, **100**(10), p. 104036, 1903.04467.

[280] ——— (2017) "Estimating the Contribution of Dynamical Ejecta in the Kilonova Associated withÂ GW170817," *Astrophys. J.*, **850**(2), p. L39, 1710.05836.

[281] LIGO Scientific Collaboration, V. C. (2017) *GCN*, **21505**.
URL https://gcn.gsfc.nasa.gov/gcn3/21505.gcn3

[282] ——— (2017) *GCN*, **21513**.
URL https://gcn.gsfc.nasa.gov/gcn3/21513.gcn3

[283] James, C. W., G. E. Anderson, L. Wen, J. Bosveld, Q. Chu, M. Kovalam, T. J. Slaven-Blair, and A. Williams (2019) "Using negative-latency gravitational wave alerts to detect prompt radio bursts from binary neutron star mergers with the Murchison Widefield Array," *Mon. Not. Roy. Astron. Soc.*, **489**(1), pp. L75–L79, 1908.08688.

[284] Tohuvavohu, A., J. A. Kennea, J. DeLaunay, D. M. Palmer, S. B. Cenko, and S. Barthelmy (2020) "Gamma-Ray Urgent Archiver for Novel Opportunities (GUANO): Swift/BAT Event Data Dumps on Demand to Enable Sensitive Subthreshold GRB Searches," *Astrophys. J.*, **900**(1), p. 35, 2005.01751.

[285] Ivezić, v. Z. et al. (2019) "LSST: from Science Drivers to Reference Design and Anticipated Data Products," *Astrophys. J.*, **873**(2), p. 111, 0805.2366.

[286] Troja, E., S. Rosswog, and N. Gehrels (2010) "Precursors of short gamma-ray bursts," *The Astrophysical Journal*, **723**(2), p. 1711.

[287] Tsang, D., J. S. Read, T. Hinderer, A. L. Piro, and R. Bondarescu (2012) "Resonant shattering of neutron star crusts," *Physical Review Letters*, **108**(1), p. 011102.

[288] LIGO Scientific Collaboration, V. C. (2019) *GCN*, **24045**.
URL https://gcn.gsfc.nasa.gov/gcn3/24045.gcn3

[289] Chu, Q., E. J. Howell, A. Rowlinson, H. Gao, B. Zhang, S. J. Tingay, M. Boër, and L. Wen (2016) "Capturing the electromagnetic counterparts of binary neutron star mergers through low-latency gravitational wave triggers," *Monthly Notices of the Royal Astronomical Society*, **459**(1), pp. 121–139, https://academic.oup.com/mnras/article-pdf/459/1/121/8113983/stw576.pdf.
URL https://doi.org/10.1093/mnras/stw576

[290] Sachdev, S. et al. (2020) "An early warning system for electromagnetic follow-up of gravitational-wave events," 2008.04288.

[291] Nitz, A. H., M. Schäfer, and T. Dal Canton (2020) "Gravitational-wave Merger Forecasting: Scenarios for the Early Detection and Localization of Compact-binary Mergers with Ground-based Observatories," *Astrophys. J. Lett.*, **902**, p. L29, 2009.04439.

[292] Viets, A. D., M. Wade, A. L. Urban, S. Kandhasamy, J. Betzwieser, D. A. Brown, J. Burguet-Castell, C. Cahillane, E. Goetz, K. Izumi, S. Karki, J. S. Kissel, G. Mendell, R. L. Savage, X. Siemens, D. Tuyenbayev, and A. J. Weinstein (2018) "Reconstructing the calibrated strain signal in the Advanced LIGO detectors," *Classical and Quantum Gravity*, **35**(9), p. 095015.
URL https://doi.org/10.1088%2F1361-6382%2Faab658

[293] Klimenko, S. and G. Mitselmakher (2004) "A wavelet method for detection of gravitational wave bursts," *Class. Quant. Grav.*, **21**, pp. S1819–S1830.

[294] Klimenko, S., S. Mohanty, M. Rakhmanov, and G. Mitselmakher (2005) "Constraint likelihood analysis for a network of gravitational wave detectors," *Phys. Rev. D*, **72**, p. 122002, gr-qc/0508068.

[295] ——— (2006) "Constraint likelihood method: Generalization for colored noise," *J. Phys. Conf. Ser.*, **32**, pp. 12–17.

[296] Klimenko, S., G. Vedovato, M. Drago, G. Mazzolo, G. Mitselmakher, C. Pankow, G. Prodi, V. Re, F. Salemi, and I. Yakushin (2011) "Localization of gravitational wave sources with networks of advanced detectors," *Phys. Rev. D*, **83**, p. 102001, 1101.5408.

[297] Klimenko, S. et al. (2016) "Method for detection and reconstruction of gravitational wave transients with networks of advanced detectors," *Phys. Rev.*, **D93**(4), p. 042004, 1511.05999.

[298] Nitz, A. H., T. Dal Canton, D. Davis, and S. Reyes (2018) "Rapid detection of gravitational waves from compact binary mergers with PyCBC Live," *Phys. Rev.*, **D98**(2), p. 024050, 1805.11174.

[299] Dal Canton, T., A. H. Nitz, B. Gadre, G. S. Davies, V. Villa-Ortega, T. Dent, I. Harry, and L. Xiao (2020) "Realtime search for compact binary mergers in Advanced LIGO and Virgo's third observing run using PyCBC Live," 2008.07494.

[300] Luan, J., S. Hooper, L. Wen, and Y. Chen (2012) "Towards low-latency real-time detection of gravitational waves from compact binary coalescences in the era of advanced detectors," *Physical Review D*, **85**(10), 102002, 1108.3174.

[301] Hooper, S., S. K. Chung, J. Luan, D. Blair, Y. Chen, and L. Wen (2012) "Summed parallel infinite impulse response filters for low-latency detection of chirping gravitational waves," *Physical Review D*, **86**(2), 024012, 1108.3186.

[302] Liu, Y., Z. Du, S. K. Chung, S. Hooper, D. Blair, and L. Wen (2012) "GPU-accelerated low-latency real-time searches for gravitational waves from compact binary coalescence," *Classical and Quantum Gravity*, **29**(23), 235018.

[303] Guo, X., Q. Chu, S. K. Chung, Z. Du, L. Wen, and Y. Gu (2018) "GPU-acceleration on a low-latency binary-coalescence gravitational wave search pipeline," *Computer Physics Communications*, **231**, pp. 62–71.

[304] Chu, Q. et al. (2020) "The SPIIR online coherent pipeline to search for gravitational waves from compact binary coalescences," 2011.06787.

[305] Singer, L. P. and L. R. Price (2016) "Rapid Bayesian position reconstruction for gravitational-wave transients," *Phys. Rev. D*, **93**, p. 024013. URL https://link.aps.org/doi/10.1103/PhysRevD.93.024013

[306] Chatterjee, D., S. Ghosh, P. R. Brady, S. J. Kapadia, A. L. Miller, S. Nissanke, and F. Pannarale (2020) "A Machine Learning Based Source Property Inference for Compact Binary Mergers," *Astrophys. J.*, **896**(1), p. 54, 1911.00116.

[307] Kapadia, S. J. et al. (2020) "A self-consistent method to estimate the rate of compact binary coalescences with a Poisson mixture model," *Class. Quant. Grav.*, **37**(4), p. 045007, 1903.06881.

[308] Urban, A. L. (2016) *Monsters in the Dark: High Energy Signatures of Black Hole Formation with Multimessenger Astronomy*, Ph.D. thesis, University of Wisconsin Milwaulkee.

[309] LIGO Scientific Collaboration, V. C. (2020) *GCN*, **27977**. URL https://gcn.gsfc.nasa.gov/gcn3/27977.gcn3

[310] ——— (2020) *GCN*, **27965**. URL https://gcn.gsfc.nasa.gov/gcn3/27965.gcn3

[311] ——— (2020) *GCN*, **27963**. URL https://gcn.gsfc.nasa.gov/gcn3/27963.gcn3

[312] ——— (2020) *GCN*, **27951**. URL https://gcn.gsfc.nasa.gov/gcn3/27951.gcn3

[313] ——— (2020) *GCN*, **27987**. URL https://gcn.gsfc.nasa.gov/gcn3/27987.gcn3

[314] ——— (2020) *GCN*, **27988**. URL https://gcn.gsfc.nasa.gov/gcn3/27988.gcn3

[315] ——— (2020) *GCN*, **27989**. URL https://gcn.gsfc.nasa.gov/gcn3/27989.gcn3

[316] ——— (2020) *GCN*, **27990**. URL https://gcn.gsfc.nasa.gov/gcn3/27990.gcn3

[317] Sathyaprakash, B. S. and S. V. Dhurandhar (1991) "Choice of filters for the detection of gravitational waves from coalescing binaries," *Phys. Rev.*, **D44**, pp. 3819–3834.

[318] Blanchet, L., T. Damour, G. Esposito-Farese, and B. R. Iyer (2005) "Dimensional regularization of the third post-Newtonian gravitational wave generation from two point masses," *Phys. Rev.*, **D71**, p. 124004, gr-qc/0503044.

[319] Özel, F. and P. Freire (2016) "Masses, Radii, and the Equation of State of Neutron Stars," *Ann. Rev. Astron. Astrophys.*, **54**, pp. 401–440, 1603.02698.

[320] Burgay, M. et al. (2003) "An Increased estimate of the merger rate of double neutron stars from observations of a highly relativistic system," *Nature*, **426**, pp. 531–533, astro-ph/0312071.

[321] Zhu, X., E. Thrane, S. Oslowski, Y. Levin, and P. D. Lasky (2018) "Inferring the population properties of binary neutron stars with gravitational-wave measurements of spin," *Phys. Rev.*, **D98**, p. 043002, 1711.09226.

[322] Chan, M. L., C. Messenger, I. S. Heng, and M. Hendry (2018) "Binary Neutron Star Mergers and Third Generation Detectors: Localization and Early Warning," *Phys. Rev. D*, **97**(12), p. 123014, 1803.09680.

[323] Akcay, S. (2019) "Forecasting Gamma-Ray Bursts Using Gravitational Waves," *Annalen Phys.*, **531**(1), p. 1800365, 1808.10057.

[324] Einstein, A. (1916) "Approximative Integration of the Field Equations of Gravitation," *Sitzungsber. Preuss. Akad. Wiss. Berlin (Math. Phys.)*, **1916**, pp. 688–696.

[325] ——— (1915) "The Field Equations of Gravitation," *Sitzungsber. Preuss. Akad. Wiss. Berlin (Math. Phys.)*, **1915**, pp. 844–847.

[326] Abbott, B. P. et al. (2019) "Tests of General Relativity with GW170817," *Phys. Rev. Lett.*, **123**(1), p. 011102, 1811.00364.

[327] Abbott, B., R. Abbott, T. Abbott, S. Abraham, F. Acernese, K. Ackley, C. Adams, R. Adhikari, V. Adya, C. Affeldt, et al. (2019) "A gravitational-wave measurement of the Hubble constant following the second observing run of Advanced LIGO and Virgo," *arXiv preprint arXiv:1908.06060*.

[328] Abbott, B. P. et al. (2018) "GW170817: Measurements of neutron star radii and equation of state," *Phys. Rev. Lett.*, **121**(16), p. 161101, 1805.11581.

[329] Essick, R., P. Godwin, C. Hanna, E. Katsavounidis, R. Vaulin, and L. Blackburn "iDQ: Statistical Inference for Non-Gaussian Noise with Auxiliary Degrees of Freedom in Gravitational-Wave Detectors," *In preparation*.

[330] Godwin, P., C. Hanna, and R. Essick ",” *In preparation.*

[331] Olson, H. (1967) *Music, Physics and Engineering*, Dover Books, Dover Publications.
URL https://books.google.com/books?id=RUDTFBbb7jAC

[332] "LIGO Software: http://software.ligo.org," .

[333] "LIGO Packages: http://software.igwn.org/lscsoft/," .

[334] "Container Registry - lscsoft/gstlal: https://git.ligo.org/lscsoft/gstlal/container_registry," .

[335] "Gstlal Inspiral :: Anaconda Cloud: https://anaconda.org/conda-forge/gstlal-inspiral," .

[336] Abbott, B. et al. (2004) "Analysis of LIGO data for gravitational waves from binary neutron stars," *Phys. Rev. D*, **69**, p. 122001, gr-qc/0308069.

[337] ——— (2005) "Search for gravitational waves from galactic and extra-galactic binary neutron stars," *Phys. Rev. D*, **72**, p. 082001, gr-qc/0505041.

[338] Abbott, B. P. et al. (2009) "Search for Gravitational Waves from Low Mass Binary Coalescences in the First Year of LIGO's S5 Data," *Phys. Rev. D*, **79**, p. 122001, 0901.0302.

[339] ——— (2009) "Search for Gravitational Waves from Low Mass Compact Binary Coalescence in 186 Days of LIGO's fifth Science Run," *Phys. Rev. D*, **80**, p. 047101, 0905.3710.

[340] Abadie, J. et al. (2012) "Search for Gravitational Waves from Low Mass Compact Binary Coalescence in LIGO's Sixth Science Run and Virgo's Science Runs 2 and 3," *Phys. Rev. D*, **85**, p. 082002, 1111.7314.

[341] "Bottle: Python Web Framework: https://bottlepy.org/docs/dev/," .

[342] "HTCondor High Throughput Computing: https://research.cs.wisc.edu/htcondor/," .

[343] Cannon, K., C. Hanna, D. Keppel, and A. C. Searle (2011) "Composite gravitational-wave detection of compact binary coalescence," *Phys. Rev. D*, **83**, p. 084053, 1101.0584.

[344] Cannon, K., C. Hanna, and D. Keppel (2012) "Interpolating compact binary waveforms using the singular value decomposition," *Phys. Rev. D*, **85**, p. 081504, 1108.5618.

[345] Cannon, K., J. Emberson, C. Hanna, D. Keppel, and H. Pfeiffer (2013) "Interpolation in waveform space: enhancing the accuracy of gravitational waveform families using numerical relativity," *Phys. Rev. D*, **87**(4), p. 044008, 1211.7095.

[346] Smith, R., K. Cannon, C. Hanna, D. Keppel, and I. Mandel (2013) "Towards Rapid Parameter Estimation on Gravitational Waves from Compact Binaries using Interpolated Waveforms," *Phys. Rev. D*, **87**(12), p. 122002, 1211.1254.

[347] Tsukada, L., K. Cannon, C. Hanna, D. Keppel, D. Meacher, and C. Messick (2018) "Application of a Zero-latency Whitening Filter to Compact Binary Coalescence Gravitational-wave Searches," *Phys. Rev. D*, **97**(10), p. 103009, 1708.04125.

[348] Abbott, B. P. et al. (2016) "Characterization of transient noise in Advanced LIGO relevant to gravitational wave signal GW150914," *Class. Quant. Grav.*, **33**(13), p. 134001, 1602.03844.

[349] Zhang, H. (2004) "The optimality of naive Bayes," *AA*, **1**(2), p. 3.

[350] Cannon, K. C. (2008) "A Bayesian coincidence test for noise rejection in a gravitational-wave burst search," *Class. Quant. Grav.*, **25**, p. 105024.

[351] Cannon, K., C. Hanna, and J. Peoples (2015) "Likelihood-Ratio Ranking Statistic for Compact Binary Coalescence Candidates with Rate Estimation," 1504.04632.

[352] Abbott, B. P. et al. (2017) "Calibration of the Advanced LIGO detectors for the discovery of the binary black-hole merger GW150914," *Phys. Rev. D*, **95**(6), p. 062003, 1602.03845.

[353] Tuyenbayev, D., S. Karki, J. Betzwieser, C. Cahillane, E. Goetz, K. Izumi, S. Kandhasamy, J. S. Kissel, G. Mendell, M. Wade, A. J. Weinstein, and R. L. Savage (2016) "Improving LIGO calibration accuracy by tracking and compensating for slow temporal variations," *Classical and Quantum Gravity*, **34**(1), p. 015002.
URL https://doi.org/10.1088%2F0264-9381%2F34%2F1%2F015002

[354] Bork, R., K. Thorne, D. Barker, and J. Hanks (2016) "Real-Time Code Generator (RCG) Version 3.0 Release Notes," *LIGO DCC*, **T1600055**.

[355] Cahillane, C., J. Betzwieser, D. A. Brown, E. Goetz, E. D. Hall, K. Izumi, S. Kandhasamy, S. Karki, J. S. Kissel, G. Mendell, R. L. Savage, D. Tuyenbayev, A. Urban, A. Viets, M. Wade, and A. J.

Weinstein (2017) "Calibration uncertainty for Advanced LIGO's first and second observing runs," *Phys. Rev. D*, **96**, p. 102001.
URL https://link.aps.org/doi/10.1103/PhysRevD.96.102001

[356] Sun, L., E. Goetz, J. S. Kissel, J. Betzwieser, S. Karki, A. Viets, M. Wade, D. Bhattacharjee, V. Bossilkov, P. B. Covas, L. E. H. Datrier, R. Gray, S. Kand hasamy, Y. K. Lecoeuche, G. Mendell, T. Mistry, E. Payne, R. L. Savage, A. J. Weinstein, S. Aston, A. Buikema, C. Cahillane, J. C. Driggers, S. E. Dwyer, R. Kumar, and A. Urban (2020) "Characterization of systematic error in Advanced LIGO calibration," *arXiv e-prints*, arXiv:2005.02531, 2005.02531.

[357] "Miniconda: https://docs.conda.io/en/latest/miniconda.html," .

[358] "gst-launch-1.0: https://gstreamer.freedesktop.org/documentation/tools/gst-launch.html?gi-language=c," .

[359] Wade, M. (2015) *Gravitational-wave Science with the Laser Interferometer Gravitational-wave Observatory*, Ph.D. thesis, University of Wisconsin-Milwaukee, LIGO-P1500068.
URL https://dcc.ligo.org/LIGO-P1500068/public

[360] LIGO Scientific Collaboration, V. C. (2019) *GCN*, **24168**.
URL https://gcn.gsfc.nasa.gov/gcn3/24168.gcn3

[361] ——— (2017) *GCN*, **G298048**.
URL https://gcn.gsfc.nasa.gov/other/G298048.gcn3

[362] ——— (2019) *GCN*, **24109**.
URL https://gcn.gsfc.nasa.gov/gcn3/24109.gcn3

[363] ——— (2019) *GCN*, **24069**.
URL https://gcn.gsfc.nasa.gov/gcn3/24069.gcn3

[364] Abbott, B. P. et al. (2020) "GW190425: Observation of a Compact Binary Coalescence with Total Mass $\sim 3.4 M_{\odot}$," 2001.01761.

[365] ——— (2019) "Search for intermediate mass black hole binaries in the first and second observing runs of the Advanced LIGO and Virgo network," *Phys. Rev. D*, **100**(6), p. 064064, 1906.08000.

[366] ——— (2019) "All-Sky Search for Short Gravitational-Wave Bursts in the Second Advanced LIGO and Advanced Virgo Run," *Phys. Rev. D*, **100**(2), p. 024017, 1905.03457.

[367] Oliphant, T. (2006–), "NumPy: A guide to NumPy," USA: Trelgol Publishing, [Online; accessed <today>].
URL http://www.numpy.org/

[368] Virtanen, P., R. Gommers, T. E. Oliphant, M. Haberland, T. Reddy, D. Cournapeau, E. Burovski, P. Peterson, W. Weckesser, J. Bright, S. J. van der Walt, M. Brett, J. Wilson, K. Jarrod Millman, N. Mayorov, A. R. J. Nelson, E. Jones, R. Kern, E. Larson, C. Carey, İ. Polat, Y. Feng, E. W. Moore, J. Vand erPlas, D. Laxalde, J. Perktold, R. Cimrman, I. Henriksen, E. A. Quintero, C. R. Harris, A. M. Archibald, A. H. Ribeiro, F. Pedregosa, P. van Mulbregt, and S. . . Contributors (2020) "SciPy 1.0: Fundamental Algorithms for Scientific Computing in Python," *Nature Methods*, **17**, pp. 261–272.

[369] "PyGtk software: https://wiki.python.org/moin/PyGtk," .

[370] Erik, L. Saldyt, Rob, J. Gross, tjproct, kmrudin, T. L. Scholten, msarovar, kevincyoung, R. Blume-Kohout, pyIonControl, and D. Nadlinger (2020), "pyGSTio/pyGSTi: Version 0.9.9.1," .
URL https://doi.org/10.5281/zenodo.3675466

[371] "Apache Kafka software: https://kafka.apache.org/," .

[372] Frigo, M. and S. G. Johnson (2005) "The Design and Implementation of FFTW3," *Proceedings of the IEEE*, **93**(2), pp. 216–231.

[373] "Intel Math Kernel Library: https://software.intel.com/content/www/us/en/develop/tools/math-kernel-library.html," .

[374] "GLib2 software: https://github.com/GNOME/glib," .

[375] Galassi, M., J. Davies, J. Theiler, B. Gough, and G. Jungman (2009) *GNU Scientific Library - Reference Manual, Third Edition, for GSL Version 1.12 (3. ed.)*.

[376] Macleod, D., A. L. Urban, S. Coughlin, T. Massinger, M. Pitkin, paulaltin, J. Areeda, E. Quintero, T. G. Badger, L. Singer, and K. Leinweber (2020), "gwpy/gwpy: 1.0.1," .
URL https://doi.org/10.5281/zenodo.3598469

Vita

Ryan Magee

Education

The Pennsylvania State University, Ph.D. Physics	2020
Washington State University, M.Sc Physics	2014
Duke University, B.Sc Physics	2012

Selected publications

Abbott, R., et al. "GWTC-2: Compact Binary Coalescences Observed by LIGO and Virgo During the First Half of the Third Observing Run"
Abbott, R., et al. "Population Properties of Compact Objects from the Second LIGO-Virgo Gravitational-Wave Transient Catalog"
Sachdev, Surabhi and Magee, Ryan, et al. "An early warning system for electromagnetic follow-up of gravitational-wave events."
Abbott, B. P. et al. "Search for subsolar mass ultracompact binaries in Advanced LIGO's second observing run."
Magee, Ryan, et al. "Sub-threshold binary neutron star search in Advanced LIGO's first observing run."
Abbott, B. P. et al. "Search for subsolar mass ultracompact binaries in Advanced LIGO's first observing run."
Magee, Ryan, et al. "Methods for the detection of gravitational waves from subsolar mass ultracompact binaries."
Magee, Ryan and Hanna, Chad "Disentangling the potential dark matter origin of LIGO's black holes."

Selected awards and fellowships

Edward A. and Rosemary A. Mebus Graduate Fellowship in Physics	2019
Downsbrough Department Head's Chair in Physics Award	2018
David C. Duncan Graduate Fellowship in Physics	2017
The Nellie H. and Oscar L. Roberts Scholarship Fund	2017
Special Breakthrough Prize in Fundamental Physics	2016
Verne M. Willaman Distinguished Graduate Fellowship in Science	2016